UNIVERSITY OF THE
FREE STATE
UNIVERSITEIT VAN DIE
VRYSTAAT
YUNIVESITHI YA
FREISTATA

UFS
UV

An investigation into the inflammatory properties of tenofovir in $HepG_2$ human liver cells

by

SONGEZO VAZI

Submitted in fulfilment of the requirements for the degree of

Master of Medical Science (Physiology)

in the

Department of Basic Medical Sciences

School of Biomedical Sciences

Faculty of Health Sciences

University of the Free State

2023

Supervisor: Dr C Tiloke

Co-supervisor: Dr S Van Zyl

Co-supervisor: Dr Vorster-de Wet

DECLARATION

I hereby declare that this work, submitted for the degree Master of Medical Science with specialisation in Physiology at the University of the Free State, is my original work and has not previously been submitted to any other institution of higher learning for degree purposes or otherwise. I further declare that all sources cited or quoted are indicated and acknowledged through a comprehensive list of references. Copyright hereby cedes to the University of the Free State.

24 July 2023

---------- ----------

Name and Surname Date

DEDICATION

I dedicate this thesis

to my family

Nokwandisa Vazi, Zimkhatha Vazi, Kwakhanya Vazi

and

Liyema Vazi

I appreciate your continuous motivation, words of encouragement, and prayers.

ACKNOWLEDGEMENTS

SUPERVISORY TEAM

Dr Charlette Tiloke, Dr Sanet van Zyl and Dr Roné Vorster-de Wet, I appreciate your guidance and advice throughout the study. The study would not have been possible without your valuable suggestions and constructive feedback. I am also grateful for the skills that you have given me to develop into a better researcher. Your valuable time spent with us in the laboratory after hours, during the weekends and holidays is much appreciated. I am blessed to be supervised by you. Thank you for your endless inspiration, motivation and dedication in sharing your knowledge. Thank you for all your efforts in developing me. Thank you for your assistance in the manuscript preparations. I thank you for your presence throughout my master's degree journey.

MY FRIENDS

Mr Bopape Abel Matlola, Miss Saki Mbasakazi and Miss Moremane Malebogo, thank you for your unwavering support, assistance and teamwork. I am grateful to have classmates like you. Thank you for your friendship.

BASIC MEDICAL SCIENCES DEPARTMENT STAFF

Dr Claudia Matlakala Ntsapi and Dr Abrahams Beynon, and the rest of the staff, thank you for your support and assistance throughout this thesis. I am so grateful to have met such kind, motivating, hardworking individuals.

MY FAMILY

Thank you for your love, support and encouragement. To my parents, this project would not have been possible without you. Thank you for your financial support. It's greatly appreciated. I thank you so much for all the sacrifices you have made to help me reach this goal**.**

FUNDING

I thank the University of the Free State tuition bursary for the master's partial funding opportunity. The Avacare bursary from Farmovs also supported the study. Thank you for recognising the importance of research.

PUBLICATIONS

1) Vazi, S., van Zyl, S., Vorster-de Wet., R, Tiloke, C. 2023. A review into the inflammatory properties of tenofovir in $HepG_2$ human liver cells. Health Sciences Review 8(2023): 100114.

PRESENTATIONS

The study titled: An investigation into the inflammatory properties of tenofovir in $HepG_2$ human liver cells by Vazi, S., van Zyl, S., De Wet., P.C., Tiloke, C was presented to the Evaluation Committee (Oral):

1. Department of Basic Medical Sciences 10 August, University of the Free State, Bloemfontein, South Africa, 2021

The study titled: An investigation into the inflammatory properties of tenofovir in $HepG_2$ human liver cells by Vazi, S., van Zyl, S., De Wet., P.C., Tiloke, C was presented at the Departmental Journal Club (Oral):

1. Department of Basic Medical Sciences 21 September, University of the Free State, Bloemfontein, South Africa, 2022

The study titled: An investigation into the inflammatory properties of tenofovir in $HepG_2$ human liver cells by Vazi, S., van Zyl, S., De Wet., P.C., Tiloke, C was presented at the Health Sciences Faculty meetings (Oral):

1. Department of Haematology 14 March, University of the Free State, Bloemfontein, South Africa, 2023

The study titled: An investigation into the inflammatory properties of tenofovir in $HepG_2$ human liver cells by Vazi, S., van Zyl, S., De Wet., P.C., Tiloke, C will be presented at a local conference (Oral):

1. Faculty of Health Sciences Research Forum 22-25 August, University of the Free State, Bloemfontein, South Africa, 2023

PREFACE

ARRANGEMENT OF THE THESIS

The following outline provides the reader with an overview of the arrangement of the thesis:

Chapter 1: This chapter briefly explored the global and local burden of HIV, introducing the background and problem statement of the study, followed by the research rationale, aims, research questions and objectives of the study. The chapter concluded with the significance, the value of the study and the arrangement of the thesis.

Chapter 2: This chapter provides an overview of existing literature on HIV/AIDS, antiretroviral drugs, inflammation and tenofovir's properties.

Chapter 3: Outlines the material and methods used in the research study, followed by a detailed description of the study design, techniques and procedures used during the research project.

Chapter 4: This chapter presents the core findings of this study derived from methods.

Chapter 5: The discussion provides the interpretation and description of the significance of the research findings considering what is already known about tenofovir and its mechanism in liver inflammation.

Chapter 6: Finally, chapter 6 presents the study conclusions and recommendations for future research areas. This chapter also includes limitations for the study.

Lastly, references and appendices are incorporated at the end of the thesis.

TABLE OF CONTENTS

LIST OF FIGURES

LIST OF TABLES

LIST OF APPENDICES

LIST OF ABBREVIATIONS

3TC	Lamivudine
3TC-TP	Lamivudine triphosphate
AIDS	Acquired Immunodeficiency Syndrome
ART	Antiretroviral therapy
ARV	Antiretroviral
APC	Antigen-presenting cell
APP	Acute phase proteins
AZT	Zidovudine
CHB	Chronic hepatitis B
CRP	C-reactive proteins
CYP450	Cytochrome p450
dATP	Deoxyadenosine-5'-triphosphate
DC	Dendritic cells
DM	Diabetes mellitus
DMSO	Dimethyl sulfoxide
DTG	Dolutegravir
ER	Endoplasmic reticulum
FDA	Food and Drug Administration
FOHS	Faculty of Health Sciences
GAPDH	Glyceraldehyde 3-phosphate dehydrogenase
GM-CSF	Granulocyte-macrophage colony-stimulating factor
GP120	Glycoprotein 120
HAART	Highly active antiretroviral therapy
HBV	Hepatitis B viruses
HCV	Hepatitis C viruses

$HepG_2$	Human hepatoma cells
HIV	Human immunodeficiency virus
HR1	Heptad repeat 1
HR2	Heptad repeat 2
HRP	Horse-radish peroxidase
HSREC	Health Sciences Research Ethics Committee
IKK	IκB kinase
IL	Interleukin
Kg	Kilograms
mtDNA	Mitochondrial DNA
MtROS	Mitochondrial reactive oxygen species
NASH	Nonalcoholic steatohepatitis
NIAID	National Institute of Allergy and Infectious Diseases
NK	Natural killer cells
NF-KB	Nuclear factor-kappa b
NNRTIs	Non-nucleoside reverse transcriptase inhibitors
NRTIS	Nucleoside reverse transcriptase inhibitors
O_2	Oxygen
OD	Optical density
PAMP	Pathogen-associated molecular pattern
PBMCS	Peripheral blood mononuclear cells
PIs	Protease inhibitors
PRR	Pattern recognition receptors
Pol-γ	Polymerase gamma
qPCR	Quantitative polymerase chain reaction
ROS	Reactive oxygen species

RT	Reverse transcriptase
SA	South Africa
SAHPRA	South African Health Products Regulatory Authority
TCR	T-cell receptor
TDF	Tenofovir disoproxil fumarate
TLD	Tenofovir, lamivudine, and dolutegravir
TLE	Tenofovir-lamivudine-efavirenz
TLRS	Toll-like receptors
TLR4	Toll-like receptor 4
TNF-α	Tumour necrosis factor-alpha
UFS	University of the Free State
UNAIDS	United Nations Programme on HIV/AIDS
USA	United States of America
WHO	World Health Organization

ABSTRACT

INTRODUCTION: Since the introduction of antiretroviral (ARV) drugs in 1996, the life expectancy of HIV-infected individuals has been nearly comparable to that of HIV-uninfected individuals. However, increasing evidence shows that antiretroviral therapy (ART) is associated with increased metabolic disorders, systemic inflammation, and hepatotoxicity. Tenofovir induces oxidative stress via mitochondrial DNA polymerase inhibition in $HepG_2$ cells at chronic exposure. Although *in vitro* and *in vivo* studies have been performed to determine the effect of tenofovir on the inflammatory response, the inflammatory effect of this antiretroviral drug in liver cells still needs elucidation.

AIM: This study aimed to investigate tenofovir's potential pro- and anti-inflammatory properties in $HepG_2$ human liver cells at different time frames.

METHODOLOGY: $HepG_2$ cells were treated with tenofovir (1.2 µM) over 24h and 120h; pro- and anti-inflammatory cytokines levels were assessed using a SimpleStep human ELISA kit specific to each analyte (IL-6, IL-1β, TNF-α, IL-10). Protein expression of p-NF-κBp65, NF-κBp65, p-IκBα, and IκBα was determined with Western blotting. A quantitative polymerase chain reaction assessed the mRNA expression of *NF-κBp65* and *IkBα*.

RESULTS: Tenofovir significantly increased IL-6 and 10 levels, *NF-κBp65* mRNA expression and NF-κBp65, p-NF-κBp65 and p-IκBα protein expression. Additionally, a significant decrease in IL-1β levels and *IκBα* mRNA expression at 24h were observed. After 120h, tenofovir-treated cells showed increased p-NF-κBp65 and IκBα protein expression. Furthermore, a significant decrease in IL-6 and IL-10 levels, *NF-κBp65* and *IκBα* mRNA expression and NF-κBp65 and p-IκBα protein expression were observed.

CONCLUSION: The study demonstrated that tenofovir elevated the anti-inflammatory cytokines at acute exposure. Tenofovir increased pro-inflammatory cytokines and downregulated anti-inflammatory cytokines at chronic exposure of tenofovir in $HepG_2$ human liver cells. The knowledge

obtained from tenofovir-induced inflammatory changes can provide valuable information regarding tenofovir's clinical use.

KEYWORDS: Tenofovir, $HepG_2$ cell line, ART, HIV/AIDS, inflammatory properties

CHAPTER 1: ORIENTATION OF THE STUDY

1.1 INTRODUCTION

Globally, the Human Immunodeficiency Virus (HIV) had a sustained negative impact on health since the report of the first cases in 1981 (Pant and Singh, 2018; Bosh et al.,2021). HIV can lead to Acquired Immunodeficiency Syndrome (AIDS), occurring at a later stage of infection (Stevenson et al., 2020). The immune system is affected by viral infections, increasing the risk of other diseases and infections, such as renal dysfunction, liver disease, and cardiovascular disease (Mahy et al., 2019). In 2020, an estimated 37.7 million individuals lived with HIV worldwide. This includes children, with 1.5 million newly infected people and a mortality rate of 680 000 from AIDS-related causes worldwide (WHO, 2021). The global HIV prevalence in adults is 0.8%, with approximately 7.1 million individuals unaware of their HIV-positive status (UNAIDS, 2020).

South Africa (SA) is largely affected by HIV/AIDS (UNAIDS, 2020). In 2020, approximately 7.7 million people were HIV-positive, with a prevalence rate of up to 20.4% (UNAIDS, 2020). This prevalence increases among gay men, transgender women, sex workers, and drug addicts (Stevenson et al., 2020). Figure 1.1 illustrates the number of new HIV infections and deaths in SA (Marcus and MacDonell, 2020). The graph illustrates a declining trend of HIV infections since 1996. The decrease was followed by a sharp decline in HIV death observed from 2005. Subsequently, the number of HIV deaths is lower than HIV new infections, meaning more people living with HIV. This resulted from introducing antiretroviral therapy in 1996 and its wide use starting in 2005 (Trickey et al., 2017).

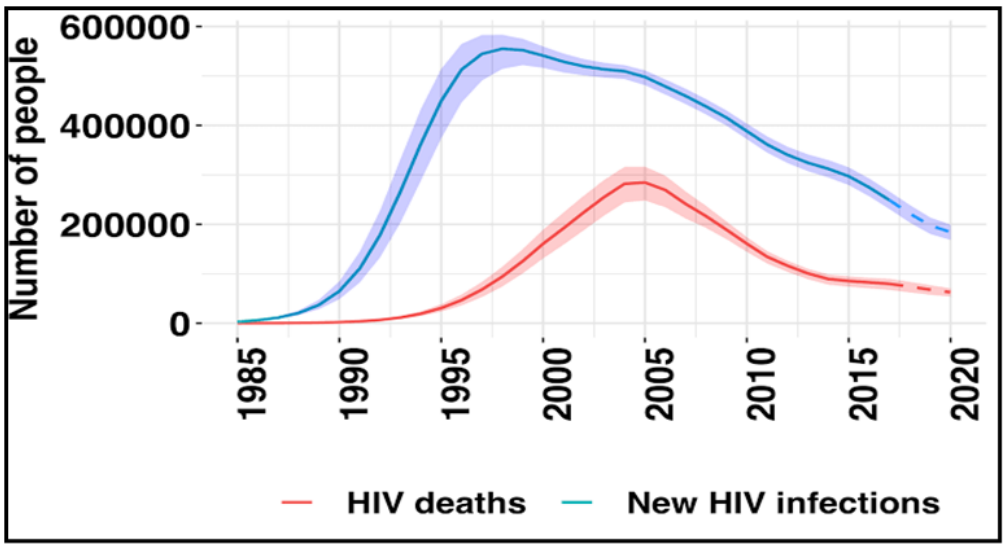

Figure 1.1: Line graph showing new HIV infections and related deaths in the South African population (Marcus and MacDonell, 2020)

The introduction of antiretroviral (ARV) drugs is one of the most noticeable signs of progress in HIV/AIDS control (Schwetz and Fauci, 2019). In the 1980s, an AIDS diagnosis typically resulted in a 1-year life expectancy (NIAID, 2020). Today, with the combination of antiretroviral drug treatments, HIV-positive individuals can have a normal life expectancy (Smiley et al., 2021). However, long-term usage of antiretroviral drugs is associated with many adverse effects, such as mitochondrial toxicity, hepatotoxicity, and lactic acidosis (Calza et al., 2017). According to UNAIDS (2021), the affordability of a high generic combination of drugs such as tenofovir/lamivudine/dolutegravir (TLD) can help achieve the 95-95-95 strategy. This strategy was introduced in 2014 to diagnose 95% of HIV-positive people and aimed to suppress viral load, with 95% of patients receiving antiretroviral drugs by 2030. Today, 84% of HIV-positive people have been diagnosed, and only 90% are virally suppressed (UNAIDS, 2021).

Among HIV-infected patients, liver disease is the most common non-AIDS-related cause of death (Morrison et al., 2019). The liver is the primary site of antiretroviral drug metabolism through the cytochrome P450 system (McMillan et al., 2018). Chronic use of antiretroviral drugs is associated with mitochondrial toxicity causing liver damage (Margolis et al., 2014; van Welzen et al., 2019).

Nucleotide reverse transcriptase inhibitors (NRTIs) cause mitochondrial toxicity by inhibiting mitochondrial DNA polymerase gamma (Pol-γ) (Smith et al., 2017). This inhibition reduces oxidative phosphorylation in the electron transport chain resulting in oxidative stress (Ganta and Chaubey, 2019).

Tenofovir is a NRTI drug used with lamivudine and dolutegravir (Venter et al., 2019). A study by Nagiah and colleagues in 2015 has shown that tenofovir induces oxidative stress in human hepatoma ($HepG_2$) liver cells, compared to other regimens (Nagiah et al., 2015). Lingappan (2018) found that oxidative stress affects NF-κB-related activities. NF-κB is a transcription factor activated in response to external stimuli, regulating pro-inflammatory genes (Liu et al., 2017).

Antiretroviral therapy causes liver toxicity as one of its most serious side effects (Bordes et al., 2020). Several studies have been performed to determine tenofovir's cytotoxic effect; however, inflammatory response in liver cells still needs to be fully elucidated (Nagiah et al., 2015; Zhang et al.,15; Vidal et al., 2006). Therefore, in the present study, tenofovir's inflammatory properties were investigated at different time exposures by assessing pro- and anti-inflammatory markers in $HepG_2$ human liver cells. This study also focused on the role of oxidative stress on inflammatory mediators of the NF- κB signalling pathway.

1.2 PROBLEM STATEMENT

A major problem linked to the successful application of antiretroviral therapy in HIV-positive people is liver disease (Ganesan et al., 2018). Tenofovir is one of the ARV drugs used as a first-line regimen known to suppress HIV viral load successfully. However, its clinical application is limited by a lack of understanding of its inflammatory response in human liver cells. Liver toxicity has been linked to long-term use of highly active antiretroviral therapy (HAART) (Baynes et al., 2017); thus, the need for antiretroviral agents that are safer and more effective.

South Africa has 84.6% of HIV-positive people, with 70.7% on ART (Marinda et al., 2020). Chronic antiretroviral therapy is linked to increased metabolic disorders such as metabolic syndrome, dyslipidemia, and systemic inflammation (Calza et al., 2017). Furthermore, a study by Bakasis and Androutsakos (2021). identified liver dysfunction, which is usually related to the inflammatory mechanism and pharmacological impact of ART (Bakasis and Androutsakos., 2021). While these complications are common in the general population, the sub-Saharan Africa population has a prevalence rate of deaths related to liver disease of 2.5 (Spearman, 2023).

Tenofovir is the preferred drug in the NRTI class. It is deemed a safer alternative to treat HIV/AIDS and hepatitis B. On the other hand, tenofovir has been shown to cause mitochondrial structural changes and dysfunction while retaining mtDNA levels in the kidneys, resulting in nephropathy (Zanger and Schwab, 2013) and, in the liver, elevating mitochondrial reactive oxygen species (MtROS) induction resulting in hepatotoxicity (Abraham et al., 2013).

1.3 RESEARCH RATIONALE

The Southern African HIV Clinicians Society guidelines recommend the combination of tenofovir with dolutegravir and lamivudine as a first-line regimen (SAHCS, 2012). Tenofovir is regarded as a potent drug for HIV treatment; however, recently, it has been associated with many adverse effects, such as lactic acidosis, hepatic steatosis, and liver cirrhosis (Wassner et al., 2020). According to Nagiah et al. (2015), tenofovir induces oxidative stress via mitochondrial DNA polymerase inhibition in $HepG_2$ cells. Enhanced generation of reactive oxygen species can activate the NF-κB signalling pathway through the IκB kinase (IKK) complex system (Adebayo et al., 2020). NF-κB is an important pro-inflammatory transcription factor that plays a significant role in oxidative stress-induced inflammation. Following its activation, it can increase the transcription of various genes and subsequently regulate inflammation. Based on the above information, tenofovir exhibits its cytotoxic effect via induced mitochondrial dysfunction; however, its effect on liver inflammation is yet to be determined. Therefore, the overall goal of this study was to broaden the understanding of the inflammatory properties of tenofovir by investigating its effect on $HepG_2$ cells. Investigating the inflammatory properties of tenofovir in acute and chronic exposure can provide physiologically relevant insight, supplement available information on tenofovir and inform targeted therapeutic intervention.

1.4. AIM OF THE STUDY

The study aimed to determine tenofovir's potential pro- and anti-inflammatory properties in $HepG_2$ human liver cells at different time exposures.

1.5 RESEARCH QUESTIONS

This study aimed to answer the following research questions:

1.5.1 How does tenofovir affect pro- and anti-inflammatory cytokines in $HepG_2$ cells?

1.5.2 Which inflammatory proteins will be expressed after exposure to tenofovir in $HepG_2$ cells?

1.5.3 Will the NF-κB signalling pathway be induced after exposure to tenofovir in $HepG_2$ cells?

1.6. OBJECTIVES OF THE STUDY

From the research questions, the following objectives were identified:

1.6.1 To quantify pro- and anti-inflammatory cytokine levels (IL-6, IL-1β, TNF-α, IL-10) after exposure to tenofovir in $HepG_2$ human liver cells.

1.6.2 To measure inflammatory mRNA (*NF-κBp65* and *IκBα*) following exposure to tenofovir in $HepG_2$ human liver cells.

1.6.3 To determine the protein expression of the NF-κB signalling pathway (p-NF-κBp65, NF-κB-p65, p-IκBα, and IκBα) after exposure to tenofovir in $HepG_2$ human liver cells.

1.7. METHODOLOGY

This study followed an experimental research design. An *in vitro* assessment of pro- and anti-inflammatory markers was done after exposure of $HepG_2$ cells to tenofovir. Treatment with tenofovir and untreated controls was conducted over two time periods, acute (24h) and chronic (120h) exposure. Pro- and anti-inflammatory cytokines were assessed using a SimpleStep human ELISA kit specific to each analyte (IL-6, IL-1β, TNF-α, IL-10). Protein expression of the NF-κB signalling pathway was determined with Western Blot. A quantitative polymerase chain reaction assessed the mRNA expression of *NF-κBp65* and *IκBα*. The knowledge obtained from tenofovir-induced inflammatory changes can provide valuable information regarding tenofovir's clinical use.

1.8. SIGNIFICANCE AND VALUE OF THE STUDY

1.8.1 Significance

This study contributes to scientific knowledge by elucidating tenofovir's effect on the human liver cell inflammatory response. Understanding tenofovir's inflammatory properties might lead to advanced tools to gain insight into pro- and anti-inflammatory cytokines profiles. Comprehension of tenofovir's possible effect on inflammatory cytokines and transcription factors elucidates this drug's acute and chronic response mechanism.

1.8.2 Value

The value of this study is to provide a scientific basis for treatment management, reducing the chances of developing liver inflammation. The lack of information contributing to understanding the effects of tenofovir on inflammation justifies the initiation of the present study. This study aims to broaden the understanding of the inflammatory properties of tenofovir in $HepG_2$ cells. Therefore, allowing proactive measures to be taken in the prevention of liver inflammation.

1.10 CONCLUSION

Chapter 1 provided an orientation to this study entitled: An investigation into the inflammatory properties of tenofovir in $HepG_2$ human liver cells. It briefly introduced the problem statement, research rationale and aims, research questions and objectives of the study. It also provided a brief overview of the significance and value of the study.

CHAPTER 2: LITERATURE REVIEW

2.1 INTRODUCTION

Chapter 2 provides an overview of existing literature on HIV/AIDS, antiretroviral drugs, tenofovir's properties, its association with inflammation and its effect on the liver. Furthermore, available literature regarding antiretroviral effects on $HepG_2$ human liver cell models will be discussed.

In this study, literature searches were conducted using several search engines such as Google Scholar, PubMed, Science direct, UFS electronic journals, EBSCO web and Google Chrome.

2.2 HUMAN IMMUNODEFICIENCY VIRUS / ACQUIRED IMMUNODEFICIENCY SYNDROME

2.2.1 BACKGROUND

Acquired Immunodeficiency Syndrome (AIDS) was first described in 1981 (CDC 1982; Greene 2007). After several years, the causative lentivirus that emerged as the Human Immunodeficiency Virus-1 (HIV-1) was identified. However, HIV-1 and HIV-2 originated from the Simian Immunodeficiency Viruses (SIVs) of primates (Sharp and Hahn, 2011). Thus, HIV-1 and HIV-2 had a zoonotic derivation but are currently spread from human to human (Sharp and Hahn, 2011). The transmission of the SIVs to humans remains a mystery. Still, it is suspected that it may have occurred during the hunting of the primates by indigenous people from Central and Western Africa (Schneider, 2021). Medical specialists apprehend that HIV has become a worldwide pathogen capable of manifesting in almost every organ, causing severe illnesses, especially in the advanced stage of the disease (Alonzo and Reynolds, 1995).

2.2.2 Classification of Human Immunodeficiency Virus

The two main types of HIV viruses, HIV-1 and HIV-2, belong to the family of Retroviruses in the genus of Lentiviruses (Sharp and Hahn, 2011). However, the disease appearances are similar (Castro-Nallar et al., 2012). Retroviruses are associated with autoimmune diseases, malignancies, and immunodeficiency syndromes (Blattner, 1989).

HIV-1 has been classified into four subtypes: major (M), new (N), outlier (O), and putative (P); each subtype represents an independent transmission of SIV into humans (Sharp et al., 2001). However, the major (M) group is the predominant subtype of HIV, with more than 90% of HIV/AIDS cases resultant from HIV-1 (Spira et al., 2003). HIV-2 shows molecular heterogeneity with five subtypes, A to E, with Subtype A and B viruses considered epidemic (Gao et al., 1994). The HIV-1 strain is observed globally and has high virulence, while the HIV-2 strain is confined to areas of West Africa and has inadequate virulence (Serra et al., 2021).

2.2.3 Transmission of HIV/AIDS

HIV can be transmitted in two ways, namely, horizontal and vertical transmission (Taqaddas, 2020). In horizontal transmission, the virus is transmitted from one individual to another via unprotected sex, contaminated blood, and sharing of needles (Shamsi, 2019). Vertical transmission refers to mother-to-child transmission through childbirth and breastfeeding (Edwards et al., 2006).

2.2.4 The HIV replication cycle and the immune response

The HIV genome comprises two identical single-stranded RNA molecules encased within the inner core of the virus (Figure 2.1). The outer phospholipid bilayer consists of constituents that are significant for the virus's infection and disease development. The viral envelope glycoprotein 120 (gp120) is visible on the surface of HIV. This envelope, gp120, interacts with the host cell receptors on normal healthy cells such as CD4+ lymphocytes, macrophages, and monocytes (Paoletti et al.,

2019). Glycoprotein 120 is equivalent to gp41, the envelope transmembrane viral protein necessary for viral-cell membrane fusion (Finzi et al., 2010).

Glycoprotein 120 interact with the CD4+ receptors through chemokine receptor CCR5 (macrophage-trophic) and CXCR4 (T-cell-trophic); these co-receptors allow cell binding and entry of the virus (Shearer, 1998). HIV viral infection impairs cellular functions, characterised by a decline in CD4+ cell count. This decline increases susceptibility to opportunistic, viral, bacterial, protozoa and fungal infections (Sadiq et al., 2018). This immune deficiency is known as AIDS (Gallo and Montagnier, 2003). Figure 2.1 below illustrates the structure of HIV and its essential parts for viral replication.

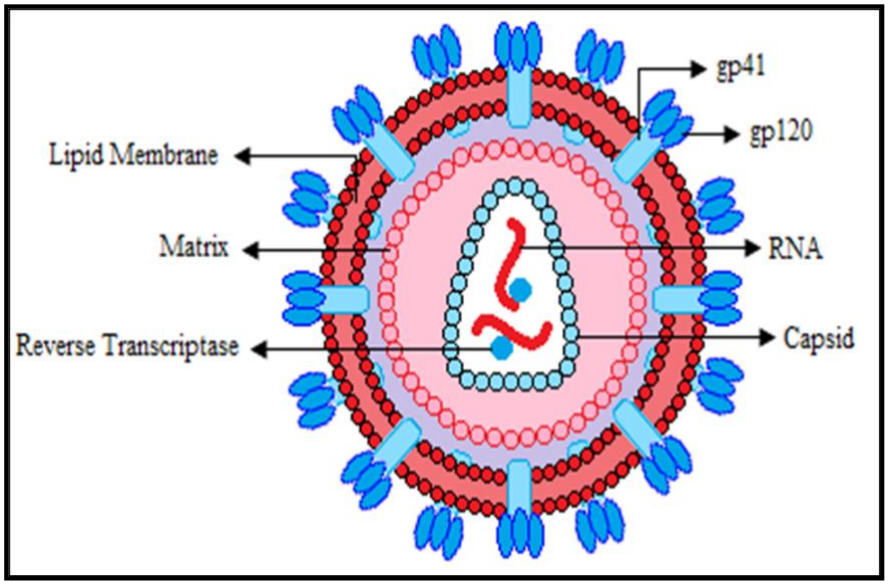

Figure 2.1: Structure of the Human Immunodeficiency Virus (HIV) (Dawany, 2010)

The HIV replication cycle can be divided into six stages, summarised in Figure 2.2 and discussed below:

1. Binding and Fusion: The initial stage of the replication cycle begins with virus particles adhering to a CD4+ receptor and with co-receptors on the surface of a CD4+ T-lymphocyte. The virus merges with the host cells releasing its RNA into the host cell cytoplasm (Sperber, 2021).

2. Reverse Transcription: The enzyme reverse transcriptase is crucial for converting the single-stranded RNA to double-stranded DNA. This conversion of RNA to DNA allows HIV to combine with the cell's genetic material (Shcherbatova et al., 2020).

3. Integration: The integrase enzyme integrates newly formed viral DNA into the host cell's nucleus, forming a provirus that can be activated to produce viral proteins (Anderson and Maldarelli, 2018).

4. Transcription: The process of copying information from a DNA strand into a new shorter strand of RNA called messenger RNA (mRNA). The mRNA is utilised as a blueprint to synthesise long chains of HIV proteins (Sperber, 2021).

5. Assembly: The newly produced HIV proteins and RNA translocates into the cell's surface and assemble into immature HIV (Shcherbatova et al., 2020).

6. Budding: The newly assembled immature HIV pushes itself out of the host CD4+ cell. The protease enzyme breaks up long protein chains in the immature virus creating the mature infectious virus. The new copies of HIV can now infect other CD4+ cells (Shcherbatova et al., 2020).

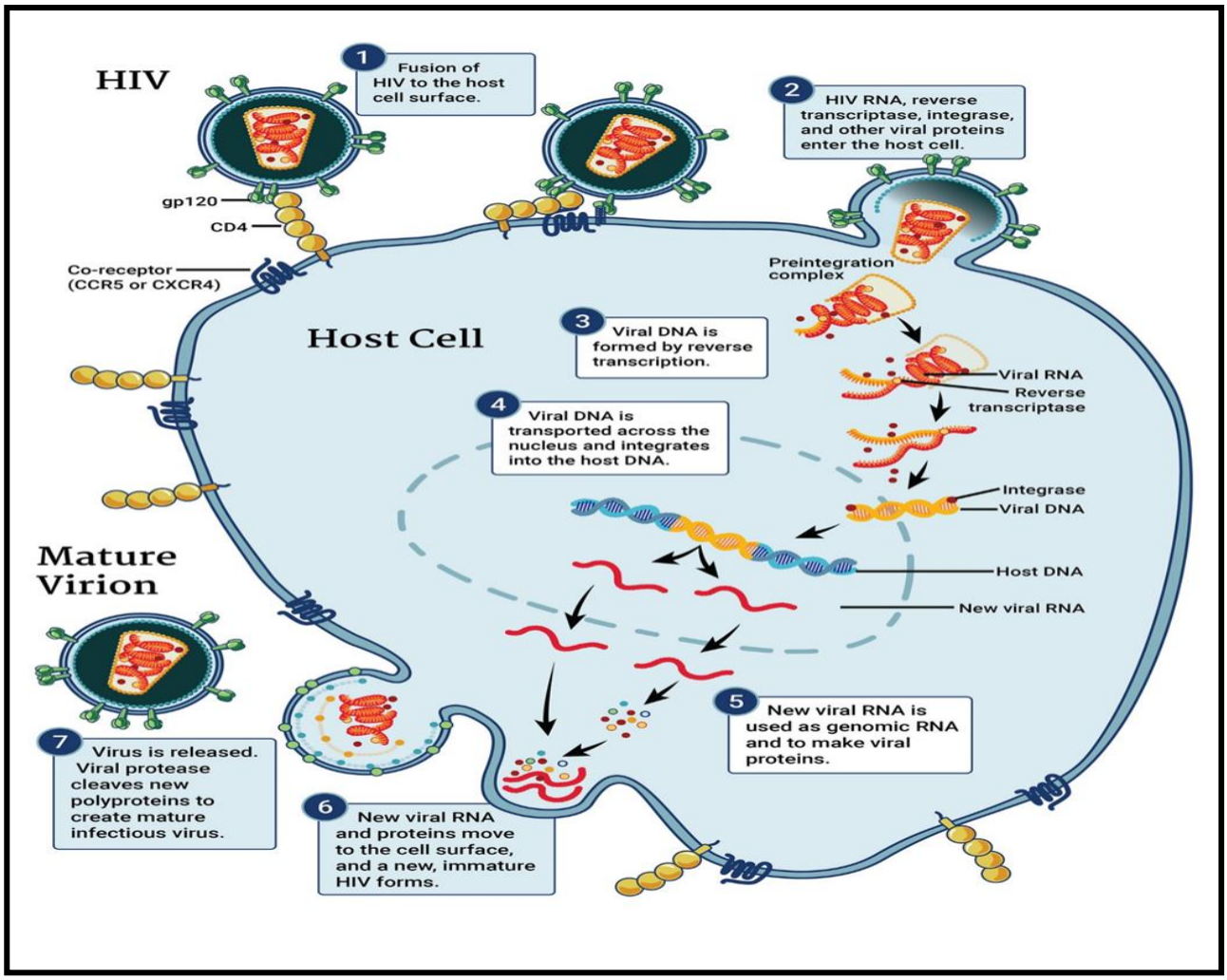

Figure 2.2: The HIV replication cycle (NIAID, 2018)

2.2.5 Management techniques for HIV/AIDS

Medical scientists and clinical practitioners continue searching for an HIV vaccine, treatment, and cure (Pitman et al., 2018). Treatment with antiretroviral drugs can control HIV, but there is no cure for it. Developing new medications and treatment strategies has greatly improved HIV infection management over the past decade (Tseng et al., 2015). The use of combination antiretroviral therapy (cART) generally resulted in effective control of HIV viremia. It maintained the increase in CD4+ T-cell numbers. Both HIV-1 and HIV-2 lead to AIDS in affected individuals; therefore, disease monitoring includes CD4+ cell count, while treatment includes antiretroviral drugs (Volberding et al., 2004).

According to Chibawara et al. (2019): *"HIV/AIDS has struck regions, countries, and populations in unusual ways. With the introduction of antiretroviral drugs, people living with HIV (PLHIV) have a much better prognosis."*

In the 1980s, HIV/AIDS mortality rose steadily and peaked in 1995 (Taqaddas, 2020). This disease weakens the body's immune system making it vulnerable to other infections. However, after investigating the HIV mechanisms of action and its replication cycle, antiretroviral therapy was introduced in 1996, giving HIV-positive individuals a better prognosis.

2.3 ANTIRETROVIRAL DRUGS

Antiretroviral (ARV) drugs are used to treat HIV (WHO, 2014). Antiretroviral therapy (ART) has reduced HIV-associated morbidity and mortality (Calza et al., 2017). The primary aim of ARV drugs is to provide a better quality of life for HIV-positive individuals by restoring immunologic functions and viral suppression. These ARV drugs inhibit different phases of the HIV replication cycle; thus, they are classified into six classes.

2.3.1 Classes of antiretroviral drug therapy

Over 30 treatment regimens (Table 2.1) are classified into six different classes according to their molecular mechanisms and resistance profiles (Lu et al., 2018). The mechanism of action of each drug type differs (Table 2.1). Generally, drugs from two or sometimes three classes are combined to ensure the necessary efficacy (Calza et al., 2017). However, the antiretroviral drug classes share a common goal: to prevent the virus from replicating and allow the immune system to produce more CD4+ T cells (Calza et al., 2017). Table 2.1 below summarises classes of HIV treatment regimens.

Table 2.1: HIV treatment regimens (compiled by the researcher, S Vazi)

Class of Antiretroviral drugs	Antiretroviral drugs	Mechanism of action	References
Nucleoside reverse transcriptase inhibitors (NRTIs)	- Tenofovir - Lamivudine - Stavudine	Reverse transcriptase Inhibition	Gulick, 2003
Non-nucleoside reverse transcriptase inhibitors (NNRTIs)	- Efavirenz - Nevirapine - Etravirine	Reverse transcriptase Inhibition	De Clercq, 1995
Protease inhibitors (PIs)	- Saquinavir - Tipranavir	Protease inhibition	De Clercq, 1995
Fusion inhibitors (FIs)	- Aplaviroc - Ibalizumab	Fusion inhibition of HIV to CD4+ T cells	Gulick, 2003
Co-receptor inhibitors (CRIs)	- Maraviroc - Vicriviroc	Block the virus from binding to the co-receptor	De Clercq, 1995
Integrase inhibitors (INIs)	- Dolutegravir - Raltegravir	Inhibit viral DNA strand transfer	Lataillade and Kozal, 2006

HIV treatment regimens, as mentioned in Table 2.1, have different mechanisms of action. After the drug has been introduced into viral DNA, nucleoside reverse transcriptase inhibitors (ARVs that induce viral DNA termination are classified as class 1) block reverse transcription by inducing chain termination (Table 2.1) (Sahin, 2020). When reverse transcriptase joins viral DNA, the NRTIs that lack the 3'-OH group function as chain terminators (Edagwa et al., 2017). NRTIs are activated intracellularly by phosphotransferases and nucleoside kinases into an active form (Holec et al., 2017). Drugs commonly used in this class include tenofovir, which is used in combination with lamivudine (3TC) and dolutegravir (DTG) to suppress HIV effectively (Pau and George, 2014).

The shape of the catalytic site of reverse transcriptase is altered by non-nucleoside reverse transcriptase inhibitors (ARVs that directly target enzyme reverse transcriptase classified as Class 2

drugs) through direct inhibition (Table 2.1) (Edagwa et al., 2017). Two subunits (p66 and p51) form a heterodimer called HIV reverse transcriptase (Sahin, 2020). NNRTIs bind the p66 subunit in a hydrophobic pocket away from the enzyme's active site (Fletcher et al., 2020). Due to the non-competitive binding, the enzyme undergoes a conformational change, altering the active site and restricting its activity (Edagwa et al., 2017).

The Class 3 drugs (ARVs targeting protease enzyme), Protease inhibitors (PIs), are the most effective anti-HIV drugs but are associated with many adverse effects such as gastrointestinal (diarrhoea and vomiting) and metabolic complications (dyslipidemia and insulin resistance) (Nagiah et al., 2015). PIs are intended to suppress viral proteases at the later stage of viral replication and maturation. During viral maturation, protease separates Gag and Gag-Pol polypeptide precursors (Pau and George, 2014). The inhibition of the enzyme prohibits a mature infectious virus from developing (Pau and George, 2014).

For Class 4 drugs (ARVs that target glycoprotein 41), the fusion process of the viral life cycle is dependent on the communication of two areas of the gp41 transmembrane protein heptad repeat 1 and 2 (HR1 and HR2) (Mzoughi et al., 2019). Combining these two motifs results in a hairpin structure that pushes the cell membrane toward the viral membrane (Mzoughi et al., 2019). Fusion inhibitors imitate one of these domains and stop intramolecular interaction from occurring. Fortunately, these drugs also make the virus more susceptible to anti-gp41 antibodies by prolonging the virus's exposure during fusion (Nagiah et al., 2015).

Co-receptor inhibitors (ARVs that target glycoprotein 120 are classified as Class 5 drugs) act as allosteric viral entry inhibitors (Shamsabadi, 2014). A co-receptor, CCR5, is activated by gp120 during viral replication to initiate fusion (Nagiah et al., 2015). CCR5 antagonists are small molecules that bind to the hydrophobic pockets between the receptors (Shamsabadi, 2014). These small molecules alter the CCR5 receptor's conformation, rendering it unrecognisable to the virus (Hashemi, 2019).

Class 6 drugs (ARVs that target an enzyme integrase), Integrase inhibitors (IN) process the 3' end of viral DNA and aid in the viral DNA strand joining to host DNA (Nagiah et al., 2015). Integrase inhibitors are the most recent advancement in ARV therapy (Cames et al., 2018). Integrase inhibitors bind to the complex formed by viral RNA and Integrase to prevent viral DNA strand transfer (Nagiah et al., 2015). Integrase inhibitors have a metal-binding pharmacophore, allowing them to interact with magnesium ion cofactors, which is essential for Integrase function (Sahin, 2020).

A few regimens with appropriate antiretroviral strength are currently available, consisting of three or four antiretroviral drugs (Eggleton and Nagalli, 2020). In 2018, the combination of tenofovir-lamivudine-efavirenz (TLE) was introduced as the first-line regimen for HIV-1 treatment (Kouanfack et al., 2019). Nevertheless, TLE has a low genetic barrier to drug resistance (Raffi et al., 2014). Therefore, the South African National Department of Health replaced TLE with tenofovir–lamivudine–dolutegravir (TLD), a fixed-dose combination (Mendelsohn and Ritchwood, 2020).

2.3.2 Tenofovir–lamivudine–dolutegravir, a fixed-dose combination therapy

Tenofovir–lamivudine–dolutegravir (TLD) is a fixed-dose combination of antiretroviral medication used to treat HIV/AIDS (Mendelsohn and Ritchwood, 2020). It is a combination of two NRTIs (tenofovir and lamivudine) and one PI (dolutegravir) (Eggleton and Nagalli, 2020). In October 2019, the South African National Department of Health introduced TLD (Mendelsohn and Ritchwood, 2020). The TLD treatment is proven to provide effective viral suppression and a high genetic barrier to resistance compared to other combination therapy (Umar et al., 2020). Detailed information on each drug is given below.

2.3.2.1 Lamivudine

Lamivudine belongs to NRTIs class, inhibiting viral DNA synthesis through DNA chain termination (Max and Sherer, 2000). Inactive 3TC is phosphorylated by nucleoside kinase into active lamivudine triphosphate (3TC-TP) (Taylor et al., 2020). The 3TC-TP competes for the viral binding site with endogenous triphosphate. Lamivudine is well-tolerated in combination with other antiretroviral drugs in HIV-infected individuals (Dumitrescu et al., 2020). Figure 2.3 below illustrates the chemical structure of lamivudine.

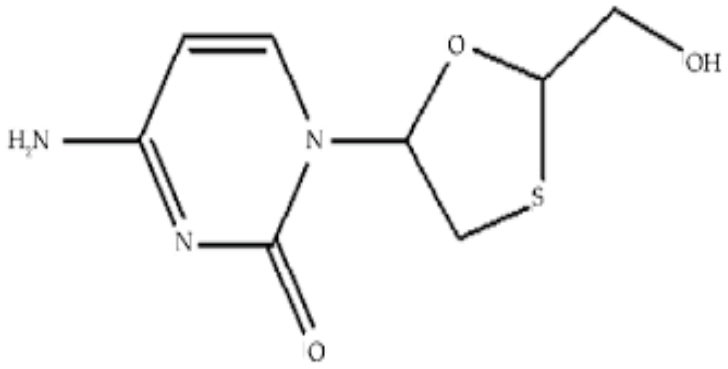

Figure 2.3: Chemical structure of lamivudine (Matta et al., 2012)

Lamivudine is a monothioacetal that consists of cytosine having a (2R,5S)-2-(hydroxymethyl)-1,3-oxathiolan-5-yl moiety in the first carbon (Sohrabi and Zarkesh, 2014; Reis et al., 2020). The 3TC-TP inhibit HIV-1 and HIV-2 reverse transcriptase enzyme activity; therefore, it is essential for HIV/AIDS and hepatitis B treatment (Taylor et al., 2020).

2.3.2.2 Dolutegravir

Dolutegravir (DTG) is an orally bioavailable integrase strand transfer inhibitor (Mohan et al., 2021). DTG hinders the activity of the integrase enzyme by binding to its active site. The integrase enzyme catalyses the integration of viral DNA into chromosomal DNA, resulting in viral replication (Kandel and Walmsley, 2015). DTG is metabolised in the liver by uridine 5'-diphospho-glucuronosyltransferase and cytochrome P450. DTG is a well-tolerated ARV drug which has fewer side effects when compared to Efavirenz and other ARV drugs (Fantauzzi and Mezzaroma, 2014). Figure 2.4 depicts the chemical structure of dolutegravir.

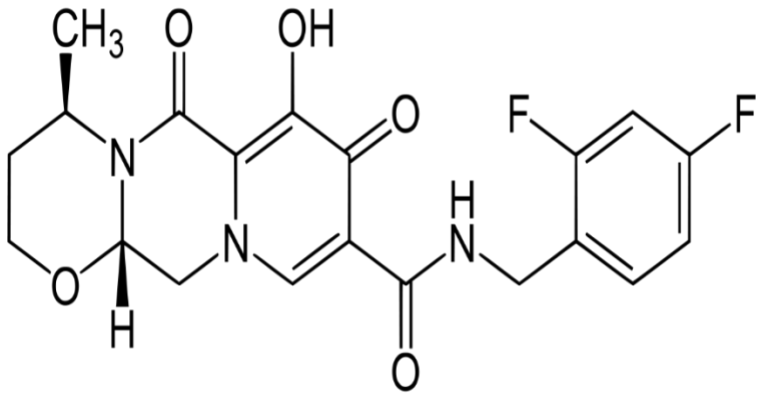

Figure 2.4: Chemical structure of dolutegravir (Han et al., 2020)

Dolutegravir is a monocarboxylic acid amide and an organic heterocyclic compound with a sodium moiety (Zamora et al., 2019). DTG inhibits the active site of the integrase enzyme, which catalyses the integration of viral DNA into chromosomal DNA, inducing viral replication (Kandel and Walmsley, 2015).

2.3.2.3 Tenofovir

Tenofovir is an adenosine acyclic nucleotide analogue used along with other HIV therapeutic agents (Hoofnagle, 2013). Tenofovir blocks reverse transcriptase, an enzyme needed for viral replication (Holec et al., 2017). The reduced viral replication impacts the HIV viral load. In 2001, tenofovir was approved in the United States of America (USA) (Ustianowski and Arends, 2015), followed by SA in 2004 (Williams et al., 2011).

Tenofovir must be phosphorylated to become pharmacologically active in two steps (Fletcher et al., 2020). First, tenofovir is phosphorylated into tenofovir monophosphate by an enzyme adenylate kinase and then phosphorylated to active tenofovir-diphosphate (Hamlin et al., 2019). In competition with the natural substrate 5′-triphosphate, tenofovir diphosphate inhibits the action of HIV-1 reverse transcriptase and terminates the DNA chain after its incorporation into the DNA strand (Holec et al., 2017). Although tenofovir has been demonstrated to be effective in treating HIV, there is still more to be understood regarding its inflammatory properties. Figure 2.5 illustrates the chemical structure of tenofovir.

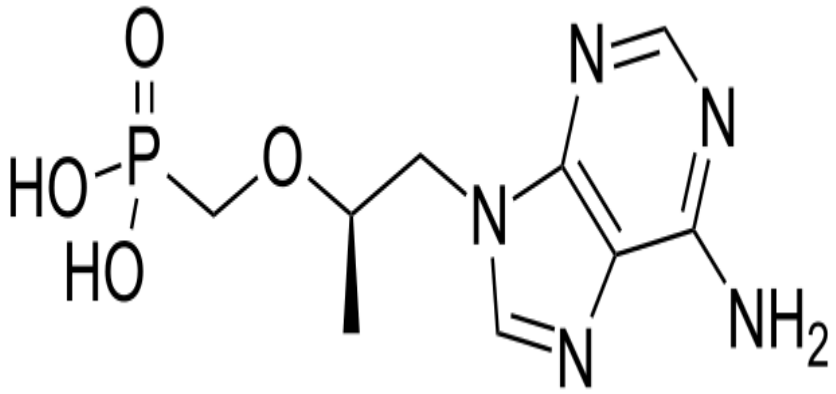

Figure 2.5: Chemical structure of tenofovir (Grigsby et al., 2010)

As illustrated in Figure 2.5, tenofovir is a methyl phosphonic acid having the methyl hydrogen substituted by a [(2R)-1-(6-amino-9H-purin-9-yl) propan-2-yl] oxy group (Grigsby et al., 2010). Tenofovir inhibit HIV-1 and HIV-2 reverse transcriptase enzyme activity; therefore, it is important

for HIV/AIDS treatment (Holec et al., 2017). Several studies assessed tenofovir's toxicity in $HepG_2$ cells and found mitochondrial DNA (mtDNA) depletion, which causes mitochondrial toxicity and possible inflammation (Nagiah et al., 2015).

2.3.3. The effect of tenofovir on inflammation

Hoofnagle recommended antiretroviral treatment with nucleoside analogue tenofovir to patients with hepatitis to reduce liver disease progression (Hoofnagle, 2013). Tenofovir suppresses the synthesis of interleukin (IL)-8, an inflammatory cytokine, during cellular stress or damage in HIV patients with liver disease (Deng et al., 2018). Interleukin (IL)-8 is a potent chemoattractant for neutrophils and contributes to acute hepatitis (Kaspar and Sterling, 2017). In addition, the drug raises the levels of IL-12, thus responding to other infectious pathogens, and maintaining low levels of IL-10, preventing the body from inhibiting the immune response (Dayakar et al., 2019).

Different studies have been carried out in different models, such as peripheral blood mononuclear cells (PBMCs) and mouse cells, investigating the inflammatory properties of tenofovir (Figure 2.6) (Olojede et al., 2022; Castillo-Mancilla et al., 2015; Biswas et al., 2014: Melchjorsen et al., 2011). These studies formulated the same conclusion that tenofovir upregulates pro-inflammatory cytokines and downregulate anti-inflammatory cytokines in acute and chronic exposure. However, tenofovir's mechanism of action is not fully understood in human liver cells. Figure 2.6 indicates tenofovir's effects on inflammatory properties.

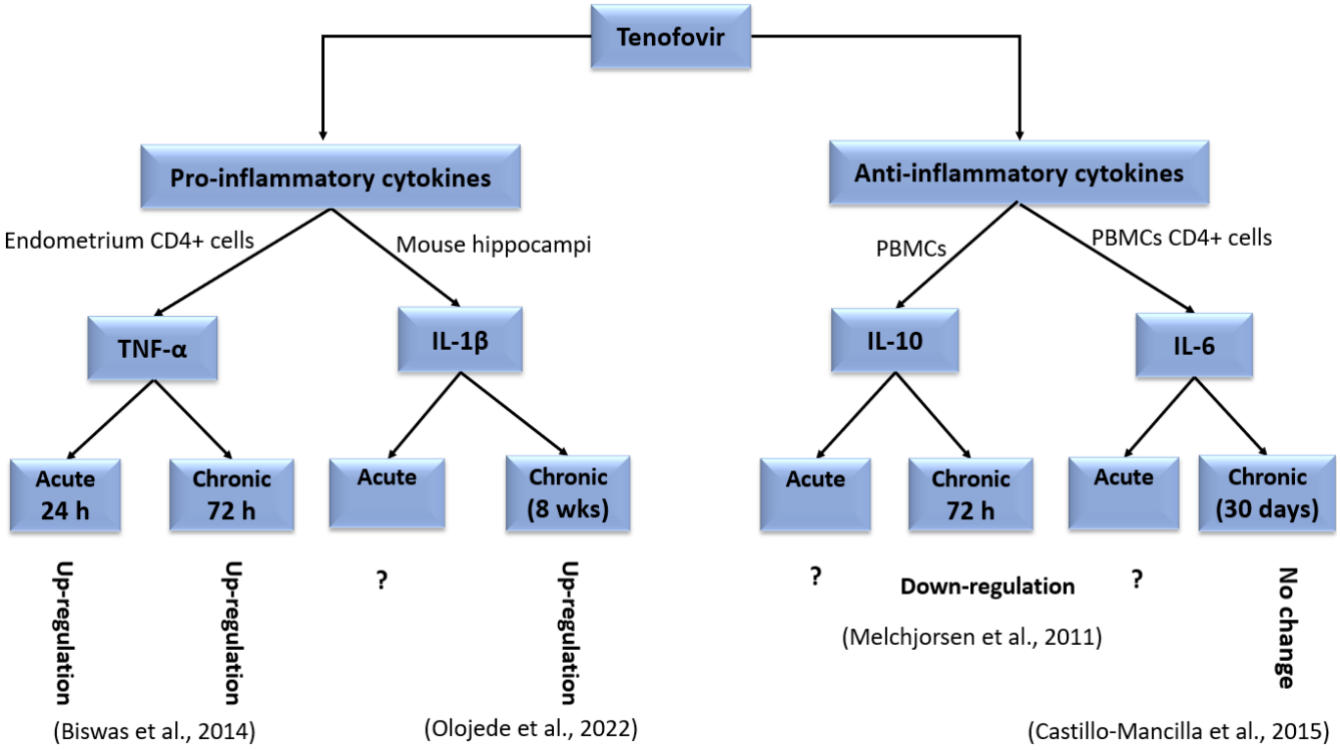

Figure 2.6: Tenofovir's effects on inflammatory markers at different time exposures (compiled by the researcher, S Vazi)

2.3.4 Effect of antiretroviral drugs

The prevalence of opportunistic infections due to immune suppression has declined in HIV-positive patients on HAART, remarkably reducing mortality. However, the chronic nature of the anti-HIV treatment has seen the emergence of long-term side effects ranging from low intolerance to life-threatening effects (Edagwa et al., 2017), with NRTI-associated mitochondrial dysfunction resulting in lactic acidosis, pancreatitis, peripheral neuropathies, and liver toxicity (Holec et al., 2017).

A study by Macías and colleagues found that long-term usage of HAART is associated with hepatic steatosis (Macías et al., 2017). Nassir et al. (2015) further explained hepatic steatosis as a disorder in which the liver forms triacylglycerol-containing vacuoles due to excessive lipid retention and disrupted lipid metabolism (Nassir et al., 2015). Consistently, several researchers found that NRTIs induce hepatic steatosis through mitochondrial toxicity, disrupting lipid metabolism and promoting inflammation (Macías et al., 2017; Nagiah et al., 2015; Nassir et al., 2015).

Overall, effective antiretroviral therapy is the most significant intervention in averting opportunistic infections in an HIV-positive patient. However, antiretroviral drugs are associated with several side effects arising during their metabolism (Thet and Siritientong, 2020). The liver is a key organ required for the normal homeostasis and metabolism of drugs (Zanger and Schwab, 2013).

2.4 ANATOMY AND PHYSIOLOGY OF THE LIVER

The liver weighs approximately 1.36 to 1.59 kilograms, which makes it one of the largest internal solid organs (Zhang et al., 2020). The human liver is positioned in the right upper quadrant of the abdomen, receiving oxygenated blood from the heart via the hepatic artery (Yang, 2021). Furthermore, the liver receives deoxygenated blood from the hepatic portal vein containing newly absorbed nutrients, drugs, and toxins from the gastrointestinal tract (Yang, 2021). The most significant role of the liver is the detoxification of harmful substances, chemicals, and metabolic waste products (Hall and AC, 2015). Additionally, the liver functions as an exocrine and endocrine organ. In exocrine function, the liver secretes bile, which contains waste products, cholesterol, and bile acids essential for intestinal absorption and digestion. The endocrine function entails large amounts of secreted serum factors, including albumin and protein components of lipoproteins (Zhang et al., 2020).

Approximately 80% of the liver comprises hepatocytes, which perform the main roles of the liver. Hepatocytes are organised into plates and are parted by sinusoids (Kuntz and Kuntz, 2006). The sinusoids are connected by endothelial cells and macrophages called Kupffer cells and separated from hepatocytes by the space of Disse responsible for vitamin A storage (Abdulrasool and Briggs, 2018). The thin layer between sinusoids and the basal surface of the hepatocyte aids in the exchange of substances between the blood and the liver cells (Szafranska et al., 2021). The hepatic portal vein and hepatic artery supply the liver with blood, while the hepatic vein drains the liver. Through this arrangement, the liver can control blood flow from the gastrointestinal tract and pancreas to the rest of the body (Abdulrasool and Briggs, 2018).

The liver is an essential organ with many functions, including the metabolism of key nutrients such as carbohydrates, proteins, and lipids (Zhang et al., 2020). Additionally, it is responsible for the detoxification of harmful substances such as drugs and toxins (Costanzo, 2018). Figure 2.7 illustrates both the anterior and posterior view of the human liver.

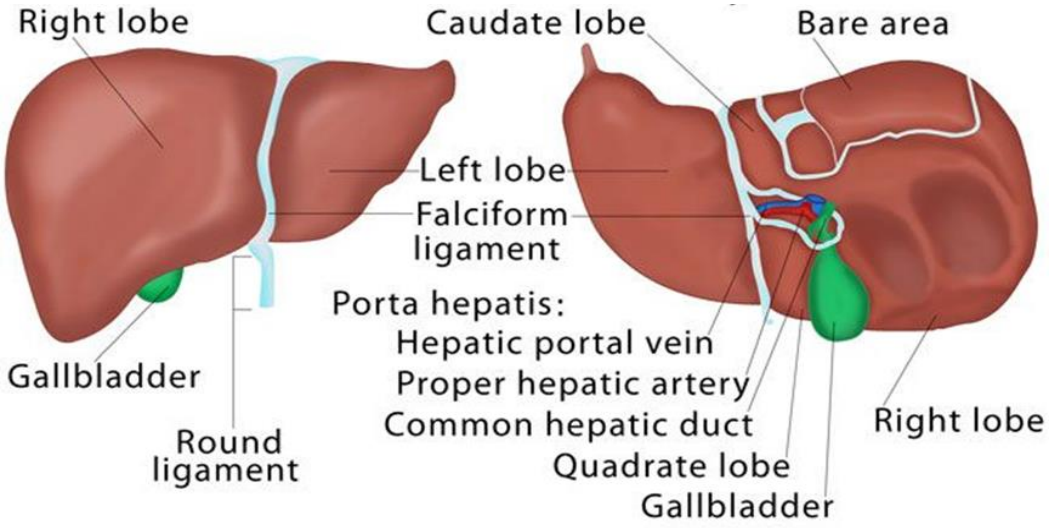

Figure 2.7: Anatomy of the human liver (Mahadevan, 2020)

2.4.1 Metabolism of tenofovir

In the liver, drugs are metabolised primarily (Almazroo et al., 2017), which occurs via the cytochrome P450 (CYP450) enzyme located in the endoplasmic reticulum (ER) (Zanger and Schwab, 2013). However, tenofovir is not metabolised through the CYP450 system (Chittick et al., 2006). Tenofovir is commercially accessible as a pro-drug, tenofovir disoproxil fumarate (TDF) (Fletcher et al., 2020). After oral intake, TDF is quickly converted to tenofovir in the intestinal walls entering the cell through its transporters (Cressey et al., 2020).

Intracellularly, tenofovir is phosphorylated by adenylate kinases and subsequently phosphorylated by nucleoside diphosphate kinases into its active form, tenofovir-diphosphate (Hamlin et al., 2019). Tenofovir-diphosphate is an analogue of deoxyadenosine-5’-triphosphate (dATP), a regular substrate for DNA polymerase (Holec et al., 2017). Tenofovir diphosphate terminates the viral DNA chain

elongation by competing with dATP to be incorporated into viral DNA (Fernandez-Fernandez et al., 2011). Tenofovir is excreted by the kidneys via glomerular filtration and tubular secretion (James et al., 2012).

2.4.2 Antiretroviral drugs effect on the liver

In treating HIV-positive patients, NRTI's long-term usage is associated with hepatic toxicity (Fletcher et al., 2020). Findings from preclinical and clinical-based studies have also linked ART with hepatotoxicity, which is influenced by oxidative stress (Elias et al., 2013). Hepatotoxicity is function impairment triggered by exposure to drugs, alcohol and environmental toxicants (Paniagua and Amariles, 2017).

The tenofovir drug has been associated with severe lactic acidosis and hepatic steatosis (Wassner et al., 2020). The possible mechanism behind tenofovir causing the latter complications is the inhibition of mitochondrial DNA (mtDNA) polymerase gamma (γ) (Chhatwani et al., 2016).

2.4.3 ART-induced mitochondrial toxicity

Nucleoside reverse transcriptase inhibitors are frequently used antiretroviral drugs as a backbone for first-line treatment regimens (Edagwa et al., 2017). A study by Sahin in 2020 suggests that NRTIs' interaction with DNA Polymerase gamma (Pol-γ) results in evident mitochondrial dysfunction. Most NRTIs can act as substrates for Pol-γ disturbing mtDNA synthesis, diminishing mtDNA content, oxidative phosphorylation, and ROS overproduction (Ahmed et al., 2018). These modifications result in changes in nucleotide phosphorylation and mitochondrial toxic effects on mitochondrial respiration (Blas-García et al., 2010). Tenofovir has been proven to inhibit the mitochondrial adenylate kinase and adenosine nucleotide translocator in isolated mitochondria. This inhibition results in mitochondrial dysfunction through ROS overproduction and inhibition of the electron transport chain (Ahmed et al., 2018; Feeney et al., 2012).

In 2019, Zhang and colleagues determined that mitochondrial dysfunction results in damage and depletion of mtDNA and the release of mtDNA (Zhang et al., 2019). The mtDNA molecule encodes 13 polypeptides of the oxidative phosphorylation system (Mustafa et al., 2020). MtDNA lesions could aggravate mitochondrial oxidative stress, damaging hepatocytes (Zhang et al., 2019). Due to the damage of hepatocytes, mtDNA leaves the confines of mitochondria to the cytoplasm. The circulating mtDNA act as damage-associated molecular patterns (DAMPs) to stimulate the Toll-like receptor 9 (TLR9) and inflammasomes, promoting inflammation (Xuan et al., 2020).

Antiretroviral drugs are generally metabolised through cytochrome P450 enzyme activity except for tenofovir. The tenofovir is metabolised by intracellular enzymes adenylate kinases and nucleoside diphosphate kinases into active tenofovir diphosphate. However, tenofovir is associated with hepatotoxicity by inhibiting mtDNA polymerase gamma (γ), resulting in mtROS. The mtROS damages the hepatocyte, releasing mtDNA, which promotes inflammation.

2.5. INFLAMMATION

According to Lonardo et al. (2021), liver inflammation substantially negatively impacts HIV-positive patients receiving ART. Chen et al. (2018) defined liver inflammation as a reaction that occurs when a foreign substance attacks the liver cell. Liver inflammation results from hepatotoxicity through exposure to substances such as dietary supplements, toxic chemicals, and drugs (Singh et al., 2016). ART-induced hepatotoxicity aggravates liver disease by activating an inflammatory response (Ganesan et al., 2018).

2.5.1 Liver inflammation linked to tenofovir

The liver highly depends on mitochondria to produce Adenosine 5′-triphosphate (ATP), which is crucial for biosynthetic pathways (Spinelli and Haigis, 2018). Various studies that assessed tenofovir's mitochondrial toxicity found that tenofovir induces mtROS resulting in hepatocyte damage through mtDNA depletion (Nagiah et al., 2015; Abraham et al., 2013). The damaged

hepatocytes release mtDNA into the extracellular environment and circulation (Zhang et al., 2019). As mentioned in the previous section, cytosolic mtDNA acts as DAMP, activating TLR9 and inflammasomes resulting in liver inflammation (Xuan et al., 2020). Due to variations in the duration of inflammatory processes, inflammation has two categories (Deng et al., 2018). Inflammation is acute or chronic (Deng et al., 2018), and acute inflammation is the first rapid response to a dangerous stimulus (Kany et al., 2019). Chronic inflammation refers to long-term tissue damage and repair, often associated with fibrosis. Cell regeneration is achieved by releasing inflammatory cytokines such as interleukin-1β and tumour necrosis factor-alpha (TNF-α) (Kany et al., 2019).

2.5.2. Regulation of the inflammatory response

The inflammation process involves a series of reactions which protect the host from infections and tissue damage (Zhang and Sun, 2015). These reactions include recruiting immune cells and plasma proteins to the inflammation site (Liu et al., 2017). Generally, inflammation is beneficial to the host and can be resolved promptly; however, deregulated inflammation is linked with chronic tissue damage, resulting in acute or chronic inflammatory diseases (Kany et al., 2019). The NF-κB pathway induces pro-inflammatory gene expression (Liu et al., 2017).

2.5.3. NF-κB signalling pathway

NF-κB is a significant transcription factor regulating immune and inflammatory responses (Liu et al., 2017). The NF-κB family comprises five members: p50, p52, p65 (RelA), and c-Rel and RelB proteins, which facilitate the transcription of specific genes (Nagel et al., 2014). The p65 is a REL-associated protein involved in NF-κB heterodimer formation and nuclear translocation and is typically activated during the inflammatory response (Ghosh and Hayden, 2012).

Mitochondrial ROS generation occurs at the electron transport chain during oxidative phosphorylation (Zhao et al., 2019). The generated ROS can activate the NF-κB signalling pathway (Figure 2.8). NF-κB is a transcription factor that regulates the function of the innate and adaptive

immune system, which mediates the inflammatory response by expression of proinflammatory genes (Giuliani et al., 2018; Liu et al., 2017). In addition, NF-κB expresses inflammatory cytokines that are key components in immune response regulations (Liu et al., 2017).

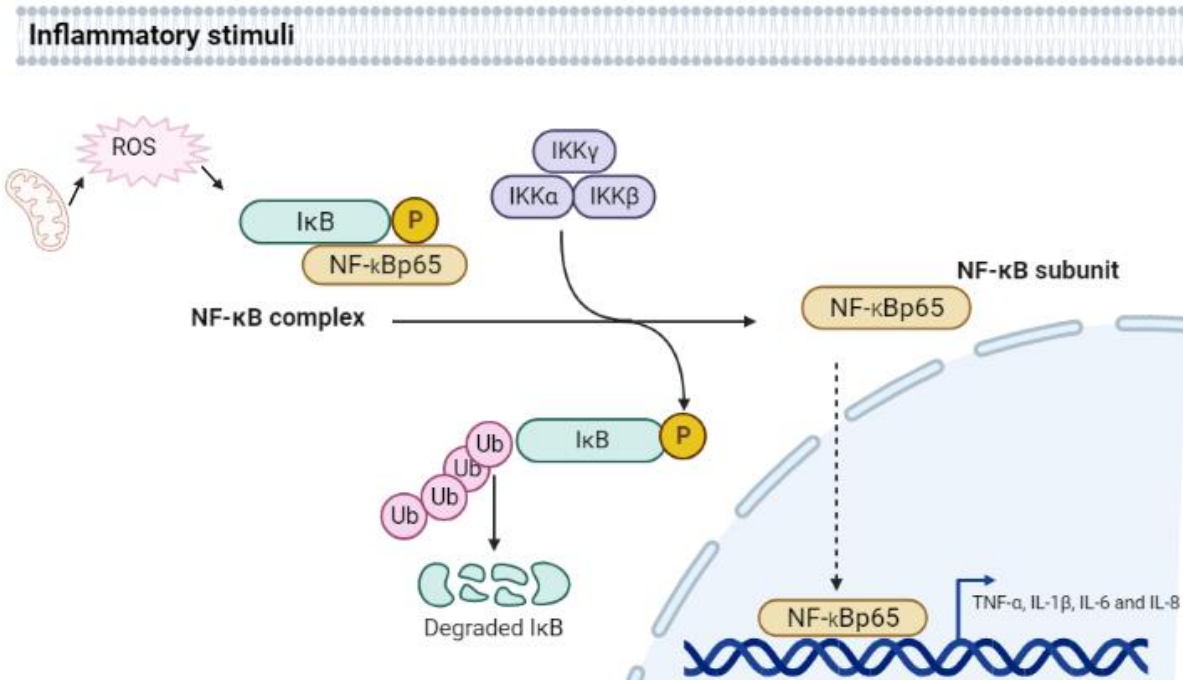

Figure 2.8: NF-κB signalling and inflammation (adapted from Morgan and Liu, 2011)

As illustrated in Figure 2.8, increased generation of ROS acts as an inflammatory stimulus. The increase in ROS leads to the phosphorylation of the IκB kinase (IKK) complex. This phosphorylation results in the dissociation of IκB from NF-κB. The NF-κB translocates into the nucleus, activating specific genes for pro-inflammatory cytokines. Elevated pro-inflammatory cytokines are necessary for acute inflammation and the retention of chronic inflammatory responses. These pro-inflammatory cytokines also mediate inflammation as a response to infection and injury. Furthermore, pro-inflammatory cytokines IL-1β and TNF-α trigger NF-κB and form a forward feed loop in response to the activation of NF-κB. The transcription factor, NF-κB, regulates the expression of several pro-inflammatory genes and helps to coordinate an inflammatory response (Dorrington and Fraser, 2019).

2.5.4. Inflammatory cytokines

Cytokines are proteins that are important in controlling other immune system cells and blood cells (Zhang and Bansal, 2020). Inflammatory cytokines play a role in introducing the inflammatory response and controlling the host defence against pathogens mediating the innate immune response (Chen et al., 2018). Two categories of inflammatory cytokines (Table 2.2) exist: pro-inflammatory cytokines and anti-inflammatory cytokines. Pro-inflammatory cytokines are involved in initiating the inflammatory response. In contrast, anti-inflammatory cytokines regulate the pro-inflammatory cytokine response. Table 2.2 below categorises inflammatory cytokines that are quantified in this study.

Table 2.2: Examples of pro- and anti-inflammatory cytokines (compiled by the researcher, S Vazi)

Pro-inflammatory cytokines	**Anti-inflammatory cytokines**
Interleukin 1-β	Interleukin 10
Tumour necrosis factor-alpha	Interleukin 6

Inflammatory cytokines regulate the host's defence against pathogens mediating the innate immune response (Gulati et al., 2016). As a result, the levels of inflammatory cytokines naturally produced by CD4+ T cells during HIV infection are expected to decrease. Inflammatory mechanisms are present in acute and chronic liver diseases, with increased expression of various pro- and anti-inflammatory cytokines in the liver (Hernaez et al., 2017).

Kupffer cells are essential to the immune response by releasing inflammatory cytokines (Zhang and Bansal, 2020). Inflammatory cytokines play a significant role in triggering the inflammatory response and controlling host defence against pathogens through the innate immune system (Chen et al., 2018).

In antiretroviral-treated HIV infection, cytokines play a role in chemical signalling pathways that control cell growth, tissue repair, immune response, and inflammation (Kany et al., 2019).

2.6. Antiretroviral drug investigations in $HepG_2$ liver cell model

$HepG_2$ cells, a human hepatoma, is commonly used in liver metabolism studies and toxicity of drugs (Xuan et al., 2016). Scientists have conducted numerous studies on antiretroviral drugs using $HepG_2$ cells and found that tenofovir, lamivudine, and dolutegravir fixed-dose combination exhibited the lowest cytotoxic effect compared to other NRTIs (WHO, 2018). In 2017, Paemanee and colleagues found that mitochondrial dysfunction is linked to the induction of apoptosis of $HepG_2$ cells treated with Nevirapine (Paemanee et al., 2017). Tunicamycin and thapsigargin, both oxidative stress inducers, caused a significant increase in Fibroblast growth factor 21 (FGF21) protein release in $HepG_2$ cells treated with ART (Moure et al., 2018). In human hepatic cell lines, NNRTIs and PI groups have been identified for the first time as causing disturbances in the FGF21/KLB system (Moure et al., 2018). Nagiah et al. (2015) found that tenofovir, stavudine, and zidovudine exhibited mitochondrial toxicity and oxidative stress, especially at chronic (5 days) exposure in $HepG_2$ cells. Tenofovir caused mitochondrial dysfunction without lowering the levels of mitochondrial DNA.

In conclusion, tenofovir is scientifically proven to inhibit HIV-1 and HIV-2 reverse transcriptase enzyme activity. However, it is associated with many adverse effects, such as lactic acidosis, hepatic steatosis and mitochondrial toxicity (Wassner et al., 2020). Tenofovir is found to exhibit mitochondrial toxicity and induce oxidative stress. Oxidative stress indirectly induces inflammation through the activation of the NF-κB signalling pathway. Currently, there are limited reports on tenofovir's inflammatory activity in human $HepG_2$ human liver cells.

2.7. CONCLUSION

This chapter aimed to summarise the literature and recent finding on antiretroviral therapy, specifically tenofovir, the drug of interest and its possible influence on liver inflammation. The review explored the research gap in tenofovir's properties. The existing literature stipulated that tenofovir induces ROS, which activates the NF-κB signalling pathway. This study also investigated tenofovir's influence on pro- and anti-inflammatory markers.

CHAPTER 3: MATERIALS AND METHODS

3.1 INTRODUCTION

This chapter presents the research design, materials, and methods used in the study. A quantitative research design (Figure 3.1) was followed to address the research questions mentioned in Chapter 1. Furthermore, this chapter provides an in-depth description and justification of the methods used.

3.2 RESEARCH DESIGN

This study followed an *in vitro* experimental research design. The researcher created an experimental and a control group. This study treated the experimental group with tenofovir and the control group with regular complete culture media (CCM) for 24h and 120h. After that, pro- and anti-inflammatory markers were quantified. The Enzyme-linked Immunosorbent Assay (ELISA), quantitative polymerase chain reaction (qPCR) and Western blot techniques were employed. The experimental techniques were carried out in the Department of Basic Medical Sciences and Human Molecular Biology Unit laboratories. Figure 3.1 represents a schematic overview of the research design and methodology that was followed.

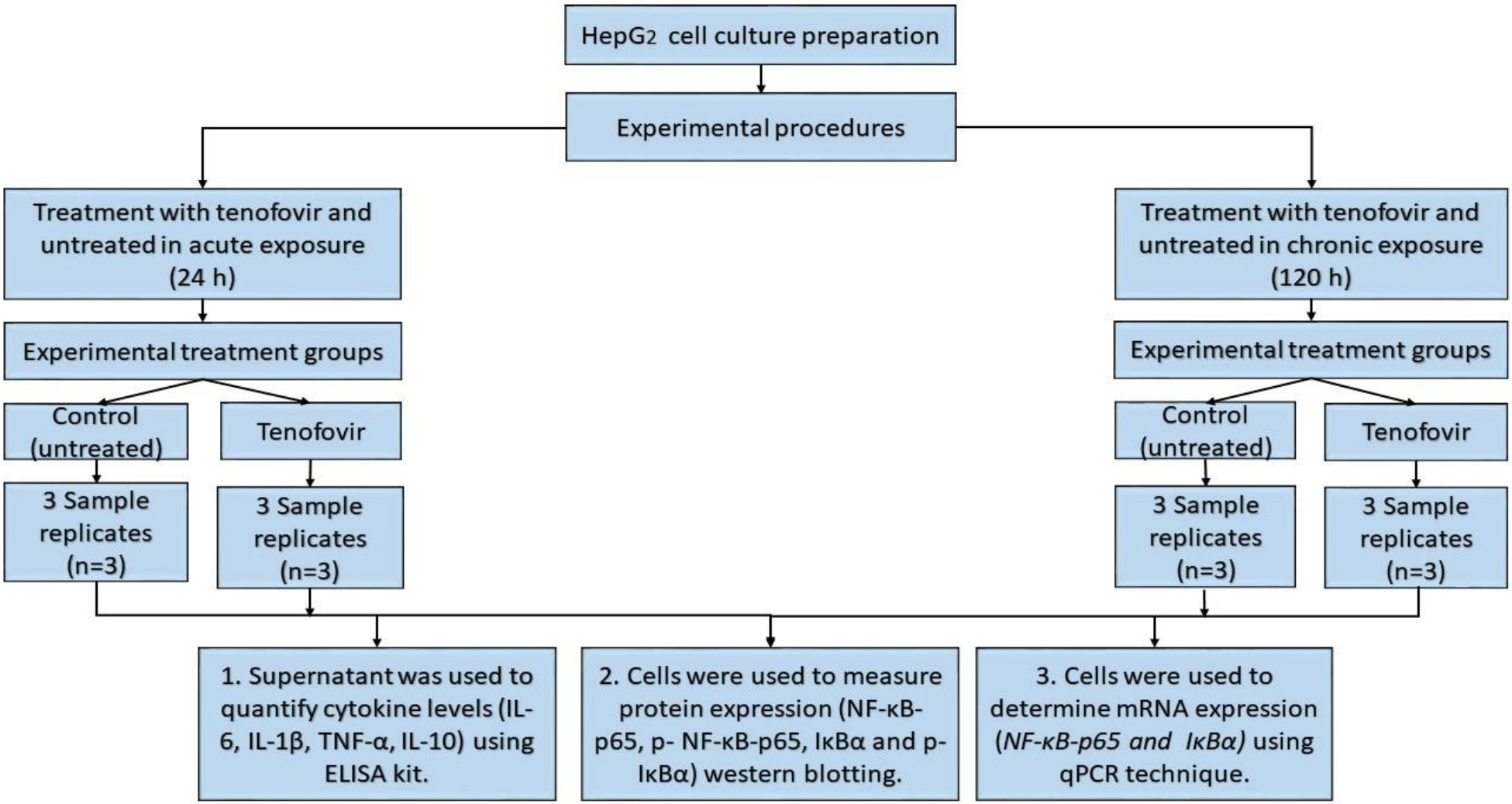

Figure 3.1: Schematic representation of the research design of the study (compiled by the researcher, S Vazi

3.3 MATERIALS

$HepG_2$ cells were obtained from the University of KwaZulu Natal (UKZN) (Durban, SA). Cell culture reagents were purchased from ThermoFisher Scientific (Johannesburg, SA). Tenofovir (SML1795-SMG) was purchased from Sigma–Aldrich (St. Louis, MO). The Enzyme-linked immunosorbent assay (ELISA) kits were purchased from Sigma–Aldrich (Johannesburg, SA). Antibodies used for the Western blot were obtained from Cell Signaling Technology, Inc (Beverly, MA). The Western blot reagents and buffers were purchased from Bio-Rad, SA. The iScript™ cDNA synthesis kit and IQ™ SYBR® green Supermix were purchased from Bio-Rad, SA. All other reagents and consumables were purchased from Merck (Darmstadt, Germany).

3.4 RESEARCH METHODS

3.4.1 CELL CULTURE

3.4.1.1 Introduction

Cell culture is the process of growing cells under a controlled environment (Haycock, 2011). These cells are used in biochemical, cytogenetic and molecular laboratories for diagnostic and research studies (Langdon, 2010). Therefore, cell culture provides a platform to investigate cell biology, biochemistry, physiology and metabolism. Cells cultured in the laboratory can be classified into three categories: Primary, transformed, and self-renewing. Primary cells are isolated directly from living tissue (Gordon and Amini, 2021). Transformed cells are transferred genetic material from one cell to another or genetically altered in order to change a recipient cell's genome (Panganiban et al., 2013). Self-renewing cells are stem cells that divide, maintaining an undifferentiated state. For this study, the $HepG_2$ cell line was used. The $HepG_2$ cell line is derived from the liver tissue of a 15-year-old Caucasian male with differentiated hepatocellular carcinoma (Donato et al., 2015). $HepG_2$ cells are commonly used for drug metabolism and hepatotoxicity studies (Negoro et al., 2021).

3.4.1.2 Protocol

The $HepG_2$ cell line was obtained from UKZN and stored at -80°C. The frozen vial was thawed at 37°C using a bead bath (Dri-block™, DB200/3). The thawed cell line was re-suspended inside a sterile hood (Labtech) into a tissue culture flask 75cm^2 (T75) parent flask, followed by the addition of 10 ml of pre-warmed complete culture media (CCM) to the culture flask. The CCM was prepared by supplementing Minimum Essential Medium (MEM) (gibco, 2534308) with 10% foetal bovine serum (10500-064), 1% L-glutamine (25030-024) and 1% penicillin-streptomycin (15140-122). Thereafter, the cells were placed in an incubator (Heal Force CO_2 incubator, HFZ40) with conditions for optimal cell growth achieved with 5% CO_2 and 95% relative humidity at 37°C. Following 24h of incubation, cells were viewed under the light-inverted microscope (Bio-Smart Scientific, 10109371) for health, attachment and confluency. The CCM was changed as required. Before adding a new CCM, 5 ml of Phosphate buffered saline (PBS) (gibco, 2235064) was used to wash the cells three times. Thereafter, 10 ml of fresh pre-warmed CCM was added, placed in the incubator (Heal Force CO2 incubator, HFZ40), and monitored for growth. Once the $HepG_2$ cells were 80% confluent, the T75 parent flask was trypsinised with 2 ml trypsin (cat no. 25300-054). After that, cells were counted using trypan blue (MKBW2465) in a TC 20™ Automated Cell Counter (Bio-Rad). Following cell count, cells were seeded at the appropriate density into four T25 flasks and subjected to treatment once the cells were 80% confluent.

3.4.2 EXPERIMENTAL TREATMENT

A 1.436 mg of tenofovir powder was dissolved in 5 ml of dimethyl sulfoxide (DMSO) to make a 1 mM stock solution. A volume of 6 µL was required to make 1.2 µM of tenofovir plasma concentration (Nagiah et al., 2015; Venhoff et al., 2007). Acute one-day (24h) and chronic five-day (120h) time duration treatments and untreated controls were conducted. A fresh cell culture medium containing tenofovir was replenished for the chronic five-day (120h) treatment after 48h (Nagiah et al., 2015).

3.5 DATA COLLECTION

3.5.1 ENZYME-LINKED IMMUNOSORBENT ASSAY (ELISA)

3.5.1.1 Introduction

ELISA technique is used to quantify the levels of a target protein in a sample (Ma et al., 2011). The samples used in ELISAs include plasma, serum, cell lysate, saliva, urine and cell culture supernatants (Shah and Maghsoudlou 2016). The ELISA principle is based on an antigen and antibody interaction. The first step involved antibody coating on a polystyrene plate. The second step was adding samples to the wells to be captured by the antibodies. The third step required detecting an antibody-antigen reaction that was visualised using enzymes linked to antibodies such as horseradish peroxidase (HRP) (Sakamoto et al., 2018).

3.5.1.2 Properties of ELISA

This technique utilises an antibody to determine and quantify the presence of the target antigen in biological samples. The target antigen is captured directly (labelled primary antibody) or indirectly (labelled secondary antibody). There are four types of ELISAs: direct, indirect, competitive and sandwich ELISA. For this study, sandwich ELISA was used. This assay measures the antigen using a capture antibody and detects the antibody-antigen complexes with a detection antibody linked to an enzyme. Detection involves assessing conjugated enzyme activity via incubation with the substrate to generate measurable luminescence. The produced colour is measured, and the colour intensity is directly proportional to sample concentration. The data is analysed to determine the concentration of the target molecule in the samples. This study measured levels of released extracellular pro- and anti-inflammatory cytokines at different time exposures.

3.5.1.3 Preparation of reagents

All the reagents were equilibrated to room temperature before use. The following reagents were prepared as needed on the day of the experiment: The 1X Wash buffer PT was prepared by combining 5 ml of Wash Buffer 10X with 45 ml of deionised water; The 10X Capture antibody was prepared by

re-suspending the lyophilised capture antibody with indicated volume of the Sample Diluent NS in the vial; The antibody cocktail was prepared by combining 300 µL of Capture antibody and 300 µL of Detector antibody with 2.4 ml antibody diluent 5BI, followed by gentle mixing

3.5.1.4 Sample preparation

Following the treatment period, the supernatant was collected from the treatment flasks. After that, the supernatant was centrifuged at 2000 x g for 10 minutes using a centrifuge (Hermle, Z 32 HK) and stored at -20℃ until experimentation.

3.5.1.5 Preparation of standards

The standard stock solution was prepared by reconstituting the targeted protein using the volume of sample diluent indicated on the vial. After that, eight eppendorfs were labelled from 1 to 8. Following the manufacturer's guidelines, an appropriate volume was added to each eppendorf. The prepared stock standard was used to complete a serial dilution of 8 concentrations. Eppendorf 8 had no protein and was used as a blank control. Figure 3.2 illustrates the serial dilutions series method.

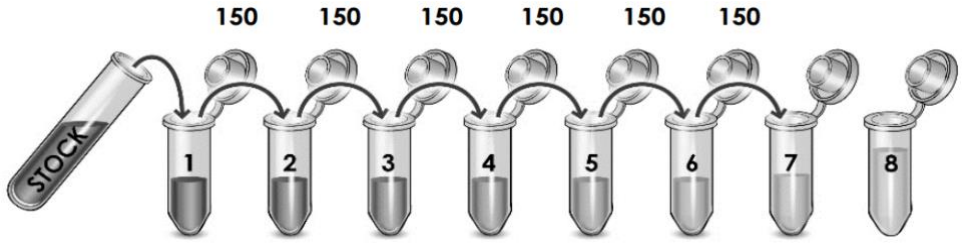

Figure 3.2: Serial dilutions (adapted from the manufacturer's guidelines (ab185986))

3.5.1.6 Protocol

The pro- and anti-inflammatory cytokine levels (IL-6, IL-1β, TNF-α, IL-10) were quantified using SimpleStep human ELISA Kits (ab178013), (ab214025), (ab181421), and (ab185986), respectively.

A volume of 50 µL of sample and standard was added to appropriate wells, followed by 50 µL of antibody cocktail. The plate was sealed and incubated for one hour at room temperature on a plate shaker (Bio–Smart Scientific, DIAB, SK-0110-B) set at 400 rpm. Following incubation, the wells were washed thrice with 350 µL of 1X Wash Buffer PT. The plate was blotted against a paper towel to remove excess liquid during the final wash. Then a volume of 100 µL of Tetramethylbenzidine (TMB) Substrate was added to each well. A plate shaker (Bio–Smart Scientific, DIAB, SK-0110-B) was used to incubate the plate for 10 minutes set at 400 rpm. Following incubation, 100 µL of stop solution was added to each well and mixed on a shaker (Bio–Smart Scientific, DIAB, SK-0110-B) for 1 minute. The absorbance was read within 15 minutes at 450 nm on an ELISA plate reader GloMax^{TM} Discovery (Promega, DTE150-245X-F-W6), and data were expressed as Optical Density (OD). In order to generate a standard curve, the mean absorbance of the standard samples was plotted against the concentration of protein (x-axis) measured in pg/ml. The equation ($y = mx + c$) of the standard curve was used to determine the protein concentration of the sample.

3.5.2 DETERMINATION OF PROTEIN EXPRESSION (WESTERN BLOT)

3.5. 2.1 PROTEIN ISOLATION

3.5.2.1.1 Introduction

Protein isolation from cultured cells is the initial step for many biochemical and analytical techniques, such as Western blotting. The protein was isolated from $HepG_2$ cells using a Cell Lysis solution supplemented with protease inhibitor for Western Blot. The protease inhibitor preserved the protein integrity in the sample (Eslami and Lujan, 2010). The process was carried out on ice to prevent protein degradation.

3.5.2.1.2 Protocol

Following 24h and 120h incubation periods, the protein was extracted according to the manufacturer's guidelines (Sigma, C2978). The cell lysate solution was prepared by diluting cell lytic

(11180733) with protease inhibitor in a 1:100 ratio. Therefore, 50 µL of protease inhibitor was added to 5 ml of cell lytic solution in a 15 ml conical tube and mixed thoroughly. The prepared cell lysate solution was stored at 4℃ until use.

The cells were washed three times with cold PBS following the treatment period. Subsequently, 300 µL of the prepared cell lysate solution was added to cover the cell surface area of the flask. Each treatment flask was incubated for 30 minutes on a shaker (Bio–Smart Scientific, DIAB, SK-0110-B) at 200 rpm. Following incubation, the cells were lysed and removed from the flasks using a cell scraper. The lysed cells were centrifuged for 15 minutes at 12 000 x g, transferred into a 2 ml pre-chilled eppendorf. After that, the protein-containing supernatant was removed, transferred into the pre-chilled eppendorf and stored at -80℃ until use.

3.5.3 QUANTIFICATION AND STANDARDISATION OF PROTEINS

3.5.3.1 Introduction

The bicinchoninic acid (BCA) assay is used to quantify the total concentration of protein in a sample (Shen, 2019). BCA assay employs the principle of Biuret reaction. The cuprous ions (Cu+) bind to the nitrogen atoms present in the protein peptides forming an intense purple colour (Walker, 1996). The BCA-Cu^{2+} complex absorbs light at 562 nm wavelength. The intensity of the purple light is proportional to the protein concentration in the sample (Walker, 1996).

3.5.3.2 Protocol

The isolated protein samples were quantified following the manufacturer's guideline (Pierce™ BCA Protein Assay Kit, cat no. 23225).

The protein samples were allowed to thaw on ice. The working reagent was prepared by mixing 50 parts of reagent A and 1 part of reagent B. The PBS was used as a diluent. Bovine Serum Albumin (BSA) standard ampule was diluted into several labelled eppendorfs.

In a 96-well plate, 25 µL of each standard and protein sample were added in triplicates into an appropriately labelled well. After that, 200 µL of the working reagent was added to each well and mixed thoroughly on a plate shaker (Bio–Smart Scientific, DIAB, SK-0110-B) for 30 seconds at 300 rpm. The 96-well plate was covered with foil and incubated at 37°C for 30 minutes. Following incubation, the 96-well plate was allowed to cool at room temperature for 5 minutes. Using a GloMax plate reader (Promega, DTE150-245X-F-W6), the absorbance was measured at 560 nm. The standard curve was generated (Appendix E) to determine the concentration of sample proteins (pg/ml) present. The proteins were subsequently standardised to 1000 g/ml for the Western blot technique.

3.5.4. WESTERN BLOTTING

3.5.4.1 Introduction

The Western blot technique is employed to identify the target proteins from a sample (Mahmood and Yang, 2012). The technique utilises sodium dodecyl sulphate polyacrylamide gel electrophoresis (SDS-PAGE) to separate proteins. The proteins are separated based on their charge and molecular weights (Mahmood and Yang, 2012). The negative charge of the protein enables migration towards the positive electrode through the polyacrylamide gel. The protein's molecular weight determines the movement through the gel; the large molecular weight proteins migrate slower, while the smaller proteins migrate faster through the matrix (Mahmood and Yang, 2012). Figure 3.3 gives an overview of the standard steps involved in the process of the Western blot technique.

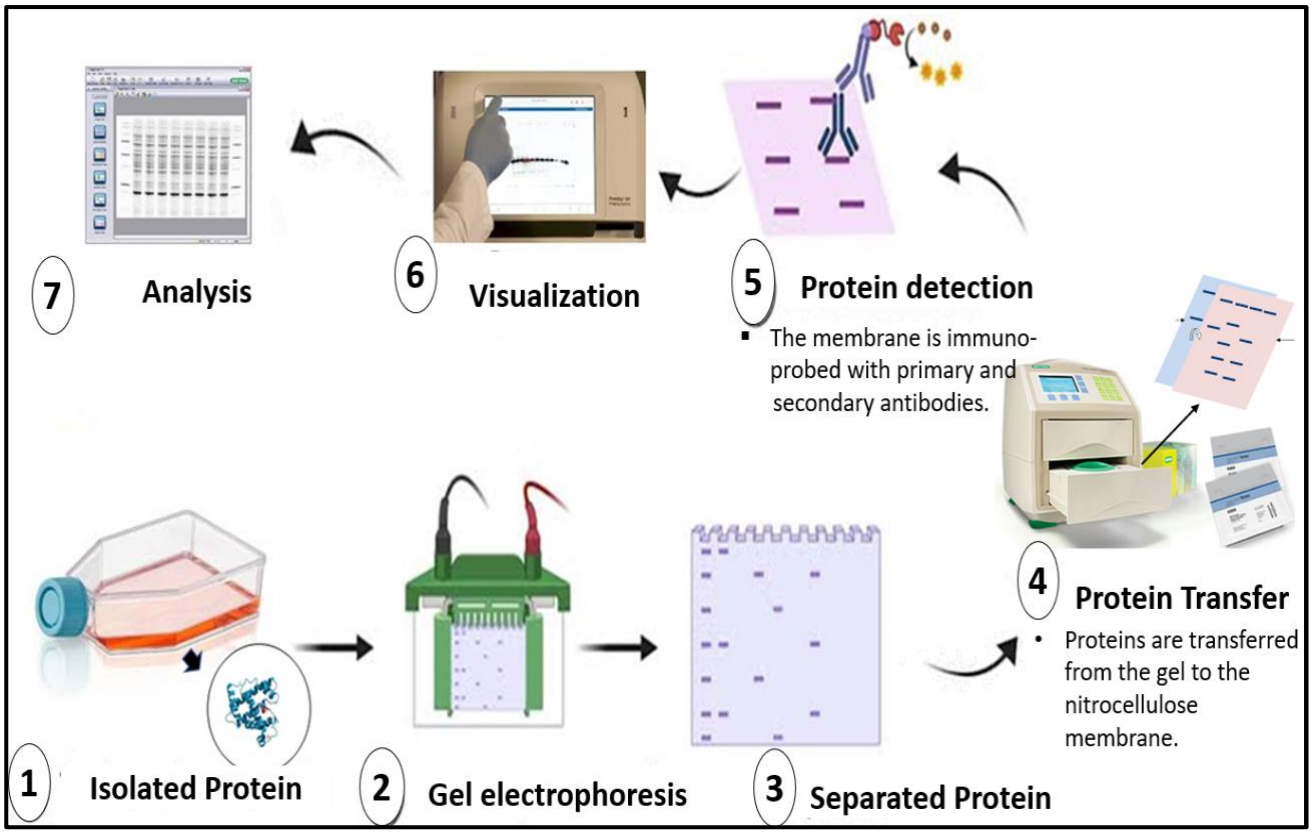

Figure 3.3: Overview of Western blot technique (compiled by the researcher, S Vazi)

3.5.4.2 Preparation of buffers

The Tris-buffered saline with Tween 20 (TTBS, 25 mM Tris pH 7.6, 150 mM NaCl, 0.05% Tween 20) was prepared by mixing 100 ml of 10x Tris-buffered saline (TBS) (1610732) with 900 ml of deionised water and 1ml Tween-20. The Western blot blocking buffer was prepared by dissolving 2.5 g skim milk powder (NCM0249A) in 50 ml of TTBS wash buffer. The 5% BSA was prepared by dissolving 2.5 g BSA (10735078001) in 50 ml of TTBS wash buffer. The 1x Tris-glycine SDS running buffer was prepared by diluting 100 ml of 10X Tris-glycine running buffer (cat. no. 1610734) with 900 ml of deionised water. The prepared buffers were stored at 4°C.

The 2x Laemmli's sample buffer mixture was prepared by mixing 1000 µL of 2x Laemmli buffer (1610737) with 50 µL of 2- mercaptoethanol (1610710).

3.5.4.3 Sample preparation

The standardised protein was allowed to thaw on ice. The prepared Laemmli sample buffer mixture was added to the standardised protein sample in a 1:1 ratio. The prepared samples were heated at 100°C for 5 minutes using the heat block (Benchmark, 034-16031-21020023). The protein samples were immediately loaded into polyacrylamide gels.

3.5.5 SDS-PAGE

3.5.5.1 Introduction

Gel electrophoresis is used to separate mixtures of proteins according to their molecular size (Lee et al., 2012). The protein was separated using the SDS-PAGE. The separation depends on the protein's molecular weight and electric charge (Mahmood and Yang, 2012). Proteins with larger molecular weights migrate slower in the gel, and those with smaller ones migrate faster. The proteins migrate towards the positive charge because they are negatively charged (Mahmood and Yang, 2012).

3.5.5.2 Protocol

The polyacrylamide gels were prepared, and MINI-PROTEAN TGX gels (Bio-Rad, cat. no: 4561033) were set up according to the manufacturer's guidelines. The molecular weight marker (cat no.1610376) (10 µL) was loaded to the first well of the gel. After that, 28 µL of the sample was loaded into the appropriate wells. Once loaded, the SDS-Page tank was filled with running buffer [25 mM Tris, 192 mM glycine, and 0.1% SDS]. SDS-Page gel electrophoresis was run at 150 V for one hour using the Bio-Rad compact power supply. Figure 3.4 illustrates the process of gel electrophoresis.

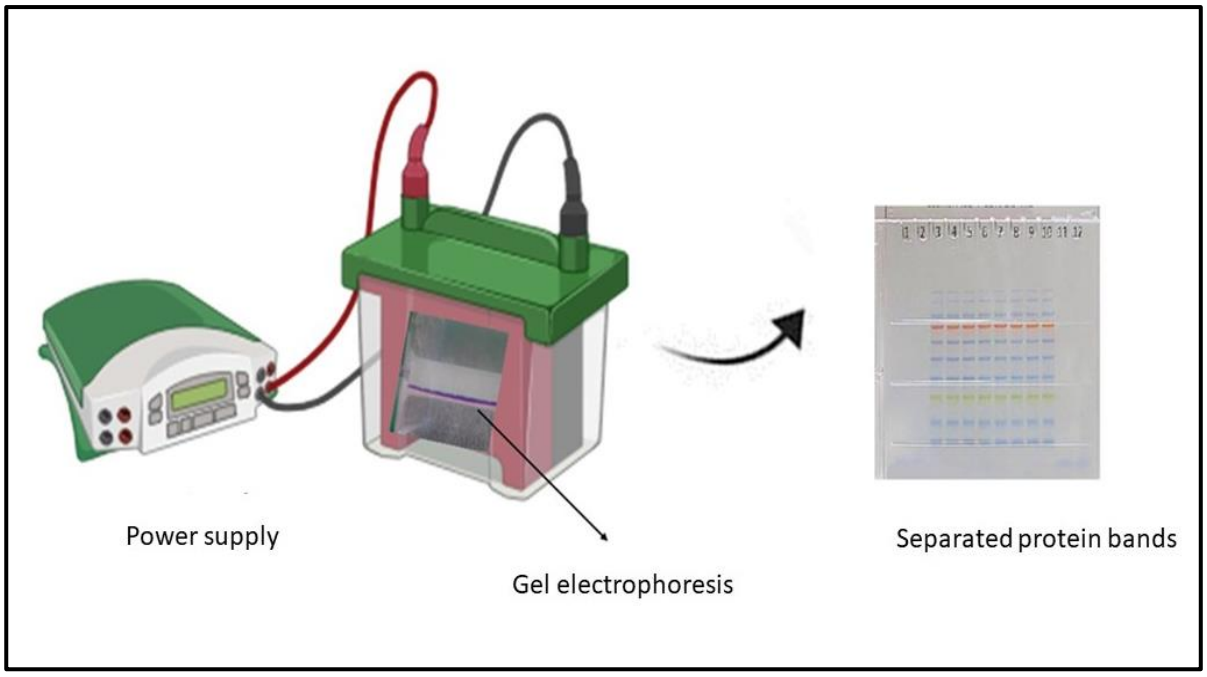

Figure 3.4: Gel electrophoresis (compiled by the researcher, S Vazi)

3.5.6. PROTEIN TRANSFER (ELECTRO-BLOTTING)

3.5.6.1 Introduction

The primary method for transferring the proteins is called electro-blotting. It utilises an electric current to transfer proteins from the gel onto the nitrocellulose membrane (Mahmood and Yang, 2012). In order to maintain their orientation, proteins must be transported from the gel into a membrane.

3.5.6.2 Protocol

The proteins were transferred using the Transblot turbo system (Bio-Rad). After electrophoresis, the cassette was prepared following the manufacturer's guidelines. The gel sandwich was formed with a bottom fibre pad, a nitrocellulose membrane, an electrophoresed gel, and a top fibre pad. The gel sandwich was assembled between two electrodes, and the separated proteins were transferred to the nitrocellulose membrane using a Bio-Rad Trans-Blot Turbo Transfer System (25 V, 3 minutes). The electric current causes the negatively charged proteins to migrate towards the positively charged

electrode resulting in the proteins being embedded into the nitrocellulose membrane. Figure 3.5 illustrates the protein transfer process using the transfer system.

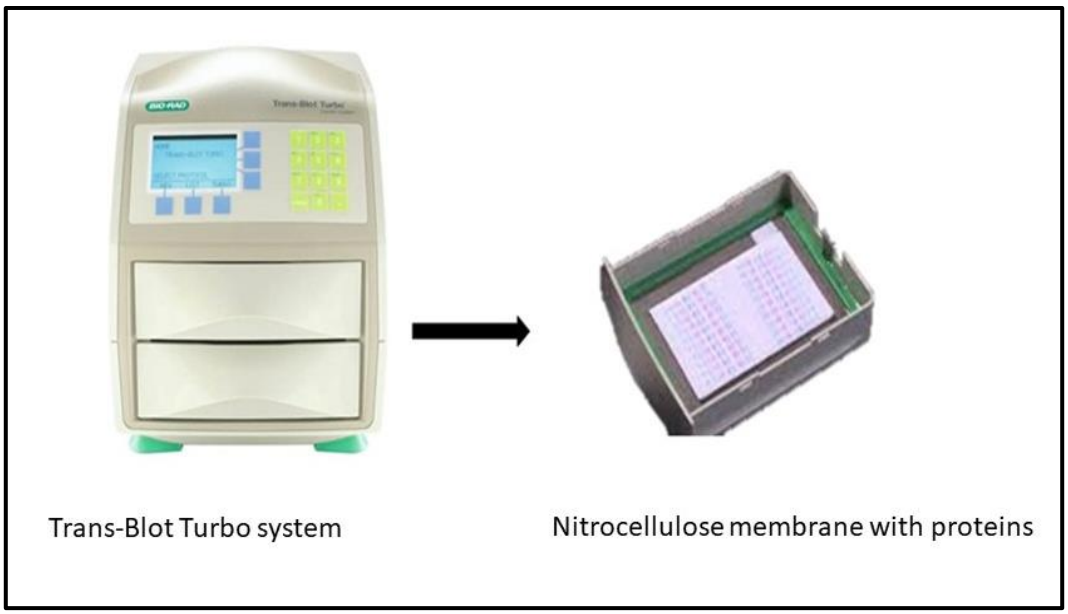

Figure 3.5: Electro-blotting (compiled by the researcher, S Vazi)

3.5.7 BLOCKING

3.5.7.1 Introduction

Non-specific binding is blocked by placing the membrane in a dilute protein solution. In every area where the target proteins are not unbound, the protein is bound to the membrane in the dilute solution. (Mahmood and Yang, 2012). Thus, when the antibody is added, there is no room on the membrane for it to bind other than on the binding sites of the specific target protein. This reduces background noise in the final product of the Western blot.

3.5.7.2 Protocol

Following protein transfer, the nitrocellulose membrane was placed in a clean container using forceps. After that, a volume of 5 ml of 5% non-fat dry milk in TTBS was added to cover the nitrocellulose membrane. In order to block the membrane, the container was placed on a shaker (Bio–Smart Scientific, DIAB, SK-0110-B) for one hour at 300 rpm. Following one hour of incubation, the 5%

non-fat dry milk in TTBS was discarded, and the membrane was washed three times with 15 ml of TTBS for 5 minutes each.

3.5.8. ANTIBODY INCUBATION

3.5.8.1 Introduction

The membrane is incubated with an antibody to detect the target protein. During detection, the membrane is probed for the protein of interest (Mahmood and Yang, 2012). The antibody used for probing the membrane is linked to a reporter enzyme. This enzyme is exposed to an appropriate substrate driving a chemiluminescence reaction and producing bands that can be quantified.

3.5.8.2 Primary antibody incubation

The membrane is incubated with primary antibodies to allow specific detection of the protein of interest (Mahmood and Yang, 2012). During the detection period, the primary antibody binds to the specific amino-acid sequence of the target protein (Mahmood and Yang, 2012). Table 3.1 provides details of the primary antibodies that were used in this study.

Table 3.1: Primary antibody and dilutions used during the Western blot procedure

Primary antibody	**Molecular weight**	**Dilution ratio**
NF-κBp65 Rabbit (Cell Signaling, 8242T)	65	1:1000
IκBα mouse (Cell Signaling, 4814T)	39	1:1000
Phospho-NF-κBp65 Rabbit (Cell Signaling, 3033T)	65	1:1000
Phospho-IκBα Rabbit (Cell Signaling, 2859T)	40	1:1000

In TTBS, the primary antibodies were diluted by 5 ml of 5% BSA. Primary antibodies (Table 3.1) were used to probe the membranes at room temperature for one hour on a shaker. Following one hour

of incubation, the membranes were incubated overnight at 4°C to allow for the binding of primary antibodies to the specific protein. Following overnight incubation, membranes were equilibrated to room temperature for one hour. After that, the primary antibody was removed, and the membrane was washed four times with TTBS wash buffer at 15-minute intervals to remove unbound primary antibodies.

3.5.8.3 Secondary antibodies

Following the removal of the unbound antibodies from the membrane, another antibody is directed at a species-specific portion of the primary antibody. The secondary antibodies are called anti-mouse or anti-goat because of their targeting properties (Mahmood and Yang, 2012). A secondary antibody is usually associated with biotin, or reporter enzymes such as alkaline phosphatase and horseradish peroxidase. This means several secondary antibodies will bind to one primary antibody and enhance the signal. Table 3.2 details the secondary antibodies that were used.

Table 3.2: Secondary antibodies

Secondary antibody	**Source**	**Dilution ratio**
Anti-Rabbit IgG, HRP-linked Antibody (Cell Signaling, 7074S)	Goat	1:5000
Anti-Mouse IgG, HRP-linked Antibody (Cell Signaling, 7076S)	Horse	1:5000

The secondary antibodies (1:5000) were prepared in 5 ml of 5% BSA in TTBS. The secondary antibody depended on the type of primary antibody used. The membranes were then incubated in secondary antibodies conjugated with horseradish peroxidase [goat anti-rabbit (Cell Signaling Technology, 7074S) and Horse anti-mouse (Cell Signaling Technology, 7076S)] with gentle agitation at room temperature for two hours. Following the incubation, the membranes were washed with TTBS four times at 15-minute intervals to remove unbound secondary antibodies. After the TTBS washes, the membrane was rinsed with 5 ml of deionised water at 5-minute intervals.

3.5.9. IMAGING

During imaging, the processed blots are converted into images to visualise the protein bands that can be quantified.

The Bio-Rad Clarity Western ECL Substrate was prepared by mixing reagents in a 1:1 ratio. A volume of 400 µL of ECL substrate was added to cover the membrane. Thereafter, the membrane was placed in ChemiDoc^{TM} MP Imaging System (Bio-Rad, 734BR5336), and the membrane was viewed using the Chemiluminescence protocol. The protein of interest was visible at the expected molecular weight.

3.5.10 RE-PROBING

Re-probing involves re-using the nitrocellulose membrane to probe for a different primary antibody. The stripping buffer removes the bound primary and secondary antibodies during this process.

3.5.10.1 Protocol

The membrane was rinsed once with TTBS wash buffer. After that, a volume of 5 ml stripping buffer (Bio-Rad, 2504) was added to cover the membrane and incubated at 37℃ for 30 minutes. Following incubation, the stripping buffer was discarded, and the membrane was washed with TTBS for 15 minutes. The membrane was blocked in a shaker with every blot-blocking buffer (Bio-Rad, 12010020) for 15 minutes. The membrane was incubated with different primary and secondary antibodies as directed in the previous section and was imaged.

3.5.11 NORMALISATION

3.5.11.1 Introduction

Normalisation is a significant step in obtaining reliable and reproducible results for quantitative Western blot (Faden et al., 2016). The normalisation step allows the researcher to compare changes in protein expression authentically. This occurs through the establishment of the baseline needed to

correct common errors. The normalisation control is a pure protein expected to be expressed constantly across all samples. Such protein is known as a housekeeping protein.

3.5.11.2 Protocol

The nitrocellulose membrane was blocked with 5% BSA and incubated in HRP-conjugated antibody for β-actin (Sigma–Aldrich, ab173838; 1:5000; 30 minutes, RT) as a housekeeping protein and visualised as previously described. Images were analysed using Image Lab Software™ v6.1 (Bio-Rad). The results were expressed as relative band density (RBD) obtained from the proportion of the RBD of the protein of interest and normalised with the RBD of the respective β-actin.

3.5.12 QUANTITATIVE POLYMERASE CHAIN REACTION (qPCR

3.5.12.1 Introduction

The quantitative polymerase chain reaction (qPCR) amplifies fragments of DNA of the target protein. This technique uses isolated RNA to obtain high-quality purified RNA from biological samples. However, RNA is easily degraded by RNases. Therefore, complementary DNA (cDNA) is synthesised from RNA as a convenient way to work with coding sequences. The mRNA carries the protein information from the DNA in a cell nucleus to the cytoplasm. Gene expression refers to the conversion of genetic information into proteins. The qPCR accurately quantifies the number of target genes expressed (Xiao et al., 2018).

The qPCR amplification process involves three steps regulated by temperature in repeated cycles. Step 1 encompasses the denaturation of the double-stranded DNA template at 95°C to yield single-stranded DNA. Step 2 requires annealing the complimentary primers to the target DNA sequence at 50 - 58°C, depending on melting temperature of the primer. In Step 3 extension, Taq polymerase elongates the annealed primer at 72°C by adding nucleotides. These steps are repeated to yield exponential copies of the original DNA. The quantity of the target genes expressed is detected using

SYBR Green dye. The dye is attached to DNA, which generates a fluorescent signal capable of detecting and quantifying (Ponchel et al., 2003).

3.5.12.2 RNA ISOLATION

Following treatment, RNA was isolated using the Tri Reagent™ (T9424). The treatment flasks were washed with PBS. After the wash, 500 µL of Tri Reagent and PBS were added and incubated for 5 minutes at room temperature. Cells were mechanically scraped, transferred into 2 ml eppendorf and stored (-80ºC) until use.

3.5.12.3 RNA PURIFICATION

3.5.12.3.1 Preparation of buffers

A volume of 50 ml RNA pre-wash buffer was prepared by adding 10 ml of ethanol (100%) into 40 ml direct-zol RNA pre-wash concentrate. The 30 ml RNA wash buffer was prepared by diluting 6 ml RNA wash buffer concentrate with 24 ml of 100% ethanol. To reconstitute lyophilized DNase 1, 275 µL RNase-free water (Sabax pour water, cat no: PBS 7624) was added into one vial (A (1500U)) and mixed gently by inversion.

Samples were allowed to thaw at room temperature and centrifuged at 12 000 x g for 30s. The supernatant was transferred into a labelled qPCR tube, and 100% filtered ethanol was added in a 1:1 ratio. The mixture was transferred into a column in a collection tube and centrifuged at 12 000 x g for 30s. The column was transferred into a new collection tube, and the flow-through was discarded. A volume of 400 µL of RNA wash buffer was added into the column and centrifuged at 12 000 x g for 30s. In an RNase-free tube, 5 µL of DNase 1 and 75 µL of digestion buffer was added and mixed gently by inversion. The mixture was added directly to the column and incubated at room temperature for 15 minutes. Following incubation, 400 µL of RNA pre-wash was added into the column and centrifuged at 12 000 x g for 30s. The column was transferred into a new collection tube and repeated the previous step. After that, 700 µL of RNA wash buffer was added into the column and centrifuged

at 12 000 x g for 1 minute. The column was transferred carefully into a new RNase-free tube. To elute RNA, 50 µL of RNase-free water (Sabax pour water, cat no: PBS 7624) was added directly to the column matrix and centrifuged at 12 000 x g for 30s. The eluted RNA was stored at -80˚C until use.

3.5.12.4 RNA QUANTIFICATION

The concentrations of RNA were determined using the Qubit™ RNA HS assay kit (cat no: Q32852). The Qubit™ tubes for samples and standards were prepared and labelled. The Qubit™ working solution was prepared by diluting Qubit™ RNA HS reagent with Qubit™ buffer in a 1:200 ratio. In order to prepare the standard, 10 µL of the standard stock was added to 190 µL of working solution. The samples were prepared by diluting 1 µL of the sample by adding 199 µL of working solution. The standards and samples were vortexed for 2-5s, followed by 2 minutes of incubation at room temperature. The sample and standards were read on the Qubit ™ 4 fluorometer (ThermoFisher Scientific, cat.no: Q10210) and standardised to 1000 ng/µL. The A260/A280 absorbance ratio was used to determine RNA purity.

3.5.12.5 cDNA SYNTHESIS

Complementary DNA (cDNA) was synthesised from RNA for qPCR. The High-Capacity RNA-to-cDNA kit (Cat no: 4387406) was used to convert RNA to cDNA. The reverse transcription mixture was prepared (20 µL per reaction), and the kit components were allowed to thaw on ice.

Table 3.3: Reaction volume and components of the High-Capacity RNA-to- cDNA kit

Component	**Volume per reaction**			
	24h Control	**24h Tenofovir**	**120h Control**	**120h Tenofovir**
2x reverse transcriptase (RT) buffer mix	10 µL	10 µL	10 µL	10 µL
20x RT Enzyme mix	1 µL	1 µL	1 µL	1 µL

RNA sample	8.7 µL	7.06 µL	2.3 µL	2.48 µL
Nuclease-Free water (Sabax pour water, cat # PBS 7624)	0.3 µL	1.94 µL	6.7 µL	6.5 µL
Total per reaction	**20 µL**	**20 µL**	**20 µL**	**20 µL**

The RNase-free tubes were used to prepare the RT reactions and centrifuged at 12 000 x g for 30s. Then 20 µL of RT reaction mix was added into qPCR strips and sealed tightly. The cDNA synthesis thermocycler conditions were 37°C for 60 minutes, 95°C for 5 minutes and a final hold at 4°C (QuantStudio5, Applied Biosystems, ThermoFisher Scientific). The synthesised cDNA was used in qPCR.

3.5.12.6 Quantitative polymerase chain reaction (qPCR)

Quantitative polymerase chain reaction (qPCR) was performed using IQ™ SYBR® Green Supermix Bio-Rad, SA (Cat no. 178880). The gene primer main stocks were prepared according to the manufacturer's guidelines, as shown in Table 3.4.

Table 3. 4: Volumes of TE buffer used to prepare gene primer main stock

Gene primers (100 µM)	**The volume of TE buffer (µL)**
NF-κB p65 sense	247
NF-κB p65 antisense	249
IκBα sense	382
IκBα antisense	228
GAPDH sense	269
GAPDH antisense	279

A working stock was adjusted to a concentration of 25 µM for each gene.

Table 3.5: qPCR reaction mixture

Components	**Optimised reaction volumes (µL)**
SYBR Green Master Mix	5
Sense primer	1
Antisense primer	1
cDNA	1
Nuclease-free water (Sabax pour water, cat no. PBS 7624)	2
Total volume	**10**

In an eppendorf, the qPCR reaction mix components were added. A 9 µL reaction mixture was added to each well in the qPCR plate, followed by the addition of 1 µL of cDNA to appropriate wells. The reaction mix without the cDNA was added as a blank. After that, the plate was covered with a plastic seal. In the presence of air bubbles, the plate was centrifuged at 400 x g for 1 minute. The qPCR run was performed using the QuantStudio™ 5 Real-Time PCR System, Applied Biosystems and analysed using the QuantStudio software. The housekeeping gene, *GAPDH*, was used for normalisation, and the mRNA expression was determined using the ΔCt Livak method (Rao et al., 2013; Livak and Schmittgen, 2001). The primer sequences were as follows:

Table 3.6: Primer sequences used in qPCR assay

Primer sequences		
Genes	**Sense primers:**	**Antisense primers:**
NF-κBp65	5′-ATCCCATCTTTGACAATCGTGC-3′	5′-CTGGTCCCGTGAAATACACCTC-3'
IκBα	5′-TGTCTACACTTAGCCTCTATC-3′	5′-TCTGTGAACTCCGTGAACTC-3′
GAPDH	5′-GCACCGTCAAGGCTGAGAAC-3	5’- TGGTAAGACGCCAGTGGA-3

The qPCR cycle conditions started with 10 minutes of initial denaturation at 95°C, followed by 95°C for 15s, annealing at 58°C for 40s, and an extension at 72°C for 30s for a total of 40 cycles. The melting curve was utilised to validate the specificity of the product amplification. The *NF-κB-p65* and *IκBα* mRNA were expressed as fold-change relative to the control (Yi et al., 2014).

3.6 DATA ANALYSIS

The researcher performed data analysis, verified by the study supervisors and done in consultation with the Department of Biostatistics at the University of the Free State (UFS). Statistical analyses were performed using the GraphPad Prism V9 software package (GraphPad Software Inc., San Diego, California, USA). The analysis involved a comparison of the mean values from results obtained in tenofovir and control exposures. Test samples were measured in triplicate and repeated at least three times to ensure validity and reliability. Two-tailed T-tests were performed when comparing data in acute/chronic exposures with two independent variables. In this study, a p-value <0.05 was used to determine statistical significance.

3.7 VALIDITY AND RELIABILITY

3.7.1 Validity

Scientifically proven techniques for inflammation assessment were employed to measure pro- and anti-inflammatory markers accurately. A live cell count was done before exposure to treatment for all the repeats. The tenofovir concentration used to treat the $HepG_2$ cells was established in previously published studies (Venhoff et al., 2007; Walker et al., 2002). The study techniques were executed under the supervision of the study leader, and a clear and concise protocol (step-by-step) was followed when executing a technique.

3.7.2 Reliability

The test samples were measured in triplicate and repeated at least three times to ensure the consistency of the results. All the successful runs showed consistency in the results obtained. However, a set of results that best represents all the repeats was included in the thesis. Safety and sample handling precautions were followed to avoid contamination and increase the results' accuracy. The protein and RNA samples were stored at -80℃ to avoid degradation; ice was used when handled outside the freezer in a Styrofoam box.

3.8 ETHICAL CONSIDERATIONS

3.8.1 Approval

The research study was approved by the Health Sciences Research Ethics Committee (HSREC) of the University of the Free State (UFS-HSD2021/1624-0002) (Appendix I). The Faculty of Health Sciences (FoHS) management and heads of the departments (Department of Basic Medical Sciences, Department of Human Molecular Biology, Department of Haematology and Cell Biology) also approved the study.

3.9 CONCLUSION

This chapter described and justified the procedures and techniques followed in collecting the data for the study. Furthermore, the overall goal of this chapter was to provide the reader with a step-by-step description of the data collection process.

CHAPTER 4: RESULTS

4.1 INTRODUCTION

This chapter presents the quantitative results of the study derived from the methods. Quantitative data was collected through various experiments, whereby $HepG_2$ cells were exposed to tenofovir for 24h and 120h.

4.1.1 Quantification of IL-6 levels

The results show a significant increase in IL - 6 levels when cells were treated with tenofovir for 24 h [tenofovir (36.321 ± 7.926) vs control (28.991 ± 4.881), p = 0.040]. However, at 120 h, IL - 6 levels were significantly decreased compared to the control [tenofovir (39.252 ± 8.502) vs control (77.885 ± 5.413), $^{**}p = 0.003$]. Quantitative data are presented as mean ± SD. Statistical analysis was performed using two-tailed T-tests where $p < 0.05$ was considered significant. Figure 4.5 illustrates the levels of IL-6 at different time exposures in $HepG_2$ cells.

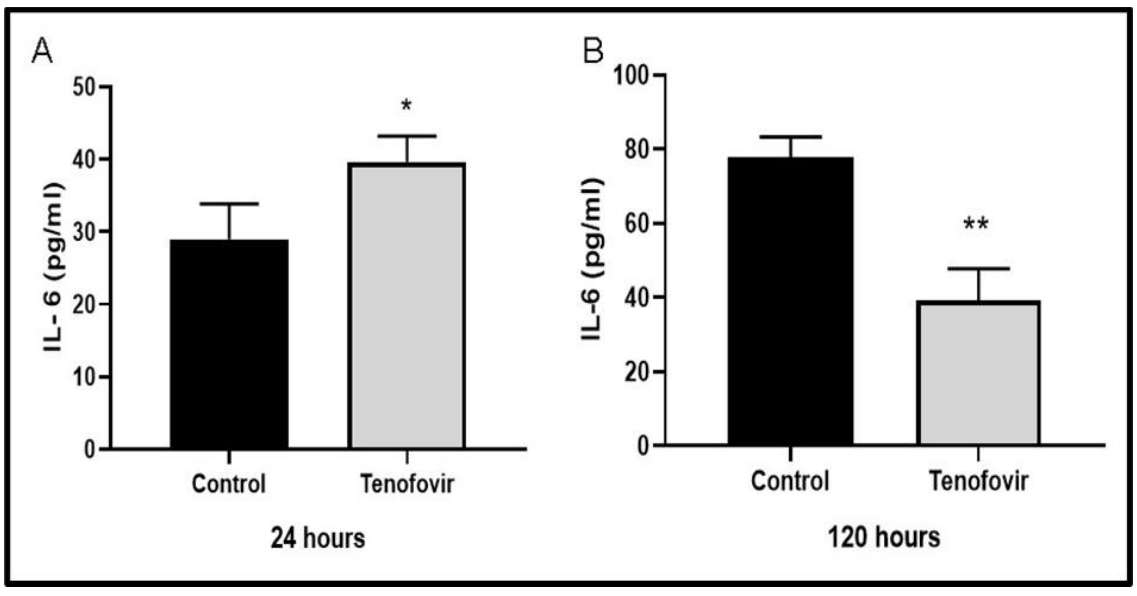

Figure 4.2: Quantitative ELISA analysis of IL-6 levels in $HepG_2$ cells following exposure to tenofovir at 24h (A) and 120h (B).

4.1.2 Quantification of IL-1β levels

The results show a significant decrease in IL - 1β levels when cells were treated with tenofovir for 24 h [tenofovir (63.32 ± 10.680) vs control (167.55 ± 94.220), $p = 0.003$]. However, at 120 h there was a non-significant increase in IL - 1β levels when compared to the control [tenofovir (62.140 ± 9.630) vs control (59.170 ± 3.450), $p = 0.642$]. Quantitative data are presented as mean ± SD. Statistical analysis was performed using two-tailed T-tests where $p < 0.05$ was considered significant. Figure 4.5 illustrates the levels of IL- 1β at different time exposures in $HepG_2$ cells.

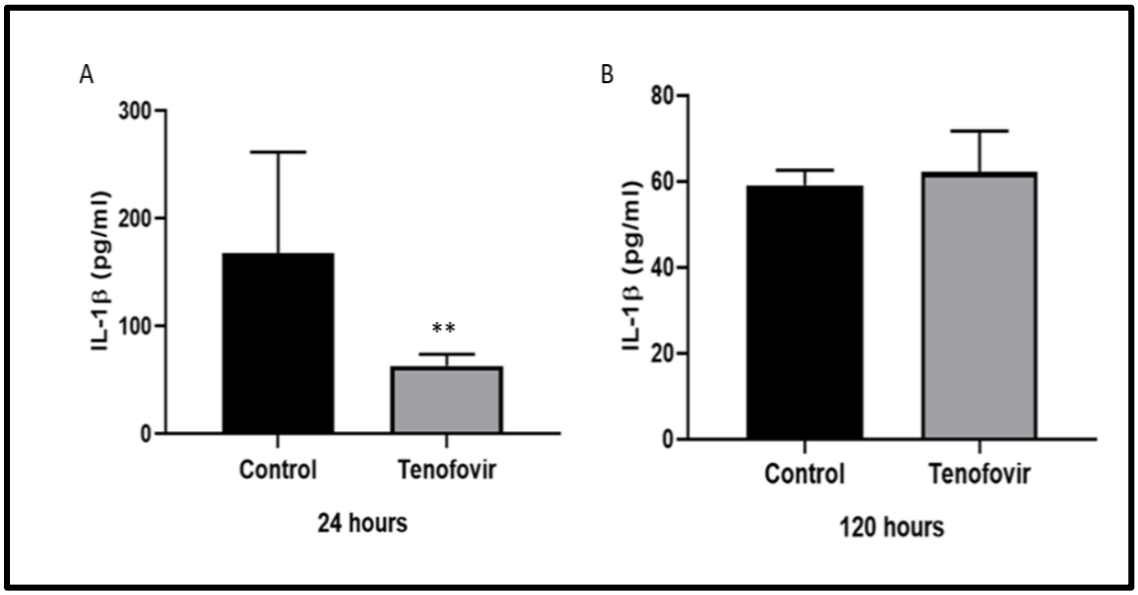

Figure 4.3: Quantitative ELISA analysis of IL- 1β levels in $HepG_2$ cells following exposure to tenofovir at 24h (A) and 120h (B).

4.1.3 Quantification of TNF-α levels

The observations demonstrate a non-significant decrease in TNF-α levels at 24 h relative to the control [tenofovir (112.600 ± 27.116) vs control (140.208 ± 89.738), $p = 0.637$]. However, at 120 h, there was a non-significant increase in TNF-α levels relative to the control [tenofovir (119.315 ± 44.316) vs control (76.140 ± 31.708), $p = 0.242$]. Quantitative data are presented as mean ± SD. Statistical analysis was performed using two-tailed T-tests where $p < 0.05$ was considered significant. Figure 4.5 illustrates the levels of TNF-α at different time exposures in $HepG_2$ cells.

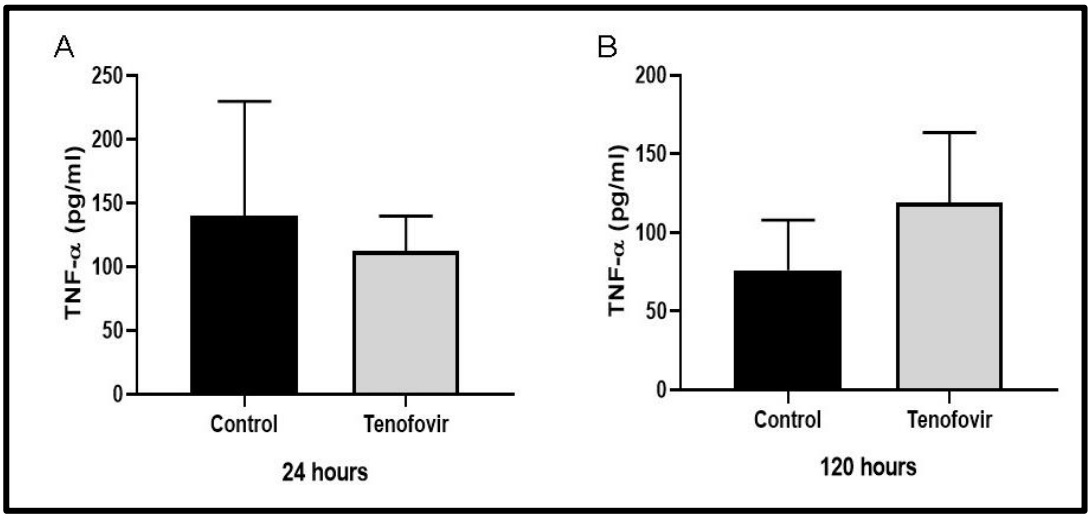

Figure 4.4: Quantitative ELISA analysis of TNF-α levels in $HepG_2$ cells following exposure to tenofovir at 24h (A) and 120h (B).

4.1.4 Quantification of IL-10 levels

The findings demonstrate a significant increase in IL - 10 levels when cells were treated with tenofovir for 24 h [tenofovir (43.671 ± 2.644) vs control (34.797 ± 0.591), $p = 0.005$]. In contrast, a significant decrease in IL -10 levels at 120h when compared to the control [tenofovir (43.671 ± 2.644) vs control (34.797 ± 0.591), $p = 0.014$] was observed. Quantitative data are presented as mean ± SD. Statistical analysis was performed using two-tailed T-tests where $p < 0.05$ was considered significant. Figure 4.5 illustrates the levels of IL - 10 at different time exposures in $HepG_2$ cells.

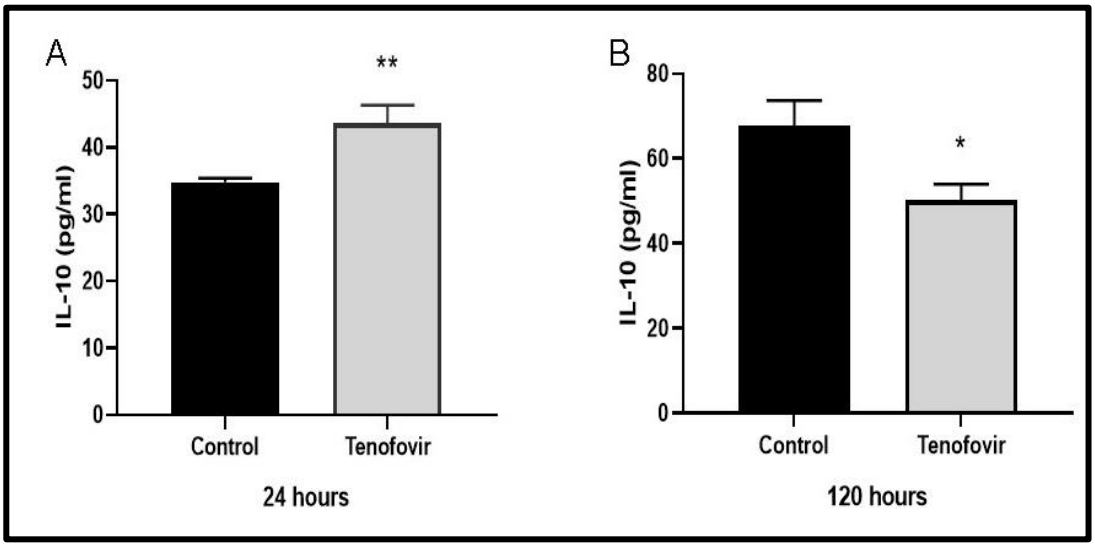

Figure 4.5: Quantitative ELISA analysis of IL-10 levels in $HepG_2$ cells following exposure to tenofovir at 24h (A) and 120h (B).

4.4 QUANTITATIVE POLYMERASE CHAIN (qPCR)

4.4.2.1 Determination of *NF-κBp65* expression at different time intervals

Graph A shows a significant 1.704 ± 0.329 (*$p < 0.0207$) increase in NF-κBp65 mRNA expression in the tenofovir-treated $HepG_2$ cells at 24h (Figure 4.6A), and Graph B decreased by 0.298 ± 0.083 (***$p < 0.0001$) at 120h of exposure (Figure 4.6B). Quantitative data are presented as relative fold change ± SD. Statistical analysis was performed using two-tailed T-tests where $p < 0.05$ was considered significant.

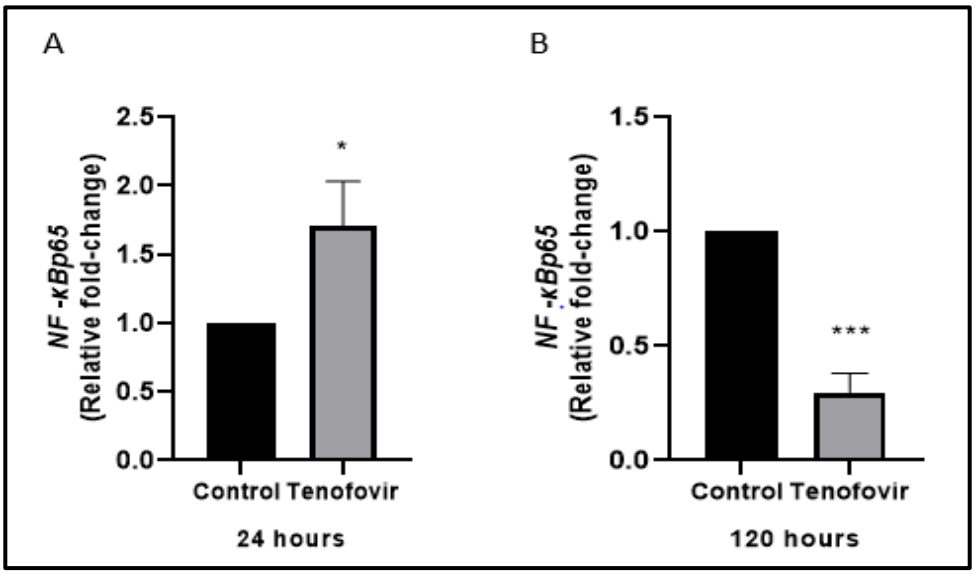

Figure 4.6: ***NF-κBp65*** **expression in $HepG_2$ cells after exposure to tenofovir at 24h (A) and 120h (B)**.

4.4.2.2 Determination of *IκBα* expression

Graph A shows a significant 0.204 ± 0.123 (***$p < 0.0004$) decrease in IκBα mRNA expression in the tenofovir-treated $HepG_2$ cells at 24h (Figure 4.7A), and Graph B decreased by 0.521 ± 0.135 (**$p < 0.0033$) at 120h of exposure (Figure 4.7B). Quantitative data are presented as relative fold change ± SD. Statistical analysis was performed using two-tailed T-tests where $p < 0.05$ was considered significant.

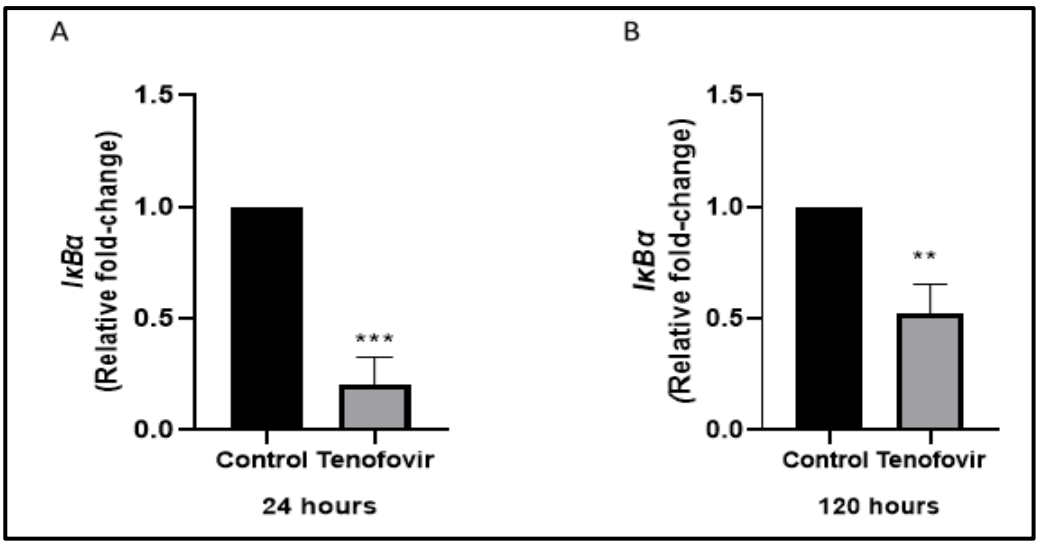

Figure 4.7: *IκBα* expression in $HepG_2$ cells after exposure to tenofovir at 24h (A) and 120h (B).

4.5 WESTERN BLOT

4.5.2.1 Determination of NF-κBp65 protein at different time intervals

NF-κBp65 is the NF-κB subunit most studied amongst NF-κB proteins. The levels of NF-κBp65 correlate with the activation of the NF-κB pathway. Therefore, to understand the effect of tenofovir on the NF-κB pathway, NF-κBp65 protein expression was determined. The NF-κBp65 protein expression was increased in the $HepG_2$-treated cells at 24h (2.464-fold). At 120h, tenofovir caused a decrease in the NF-κBp65 protein expression (0.843-fold).

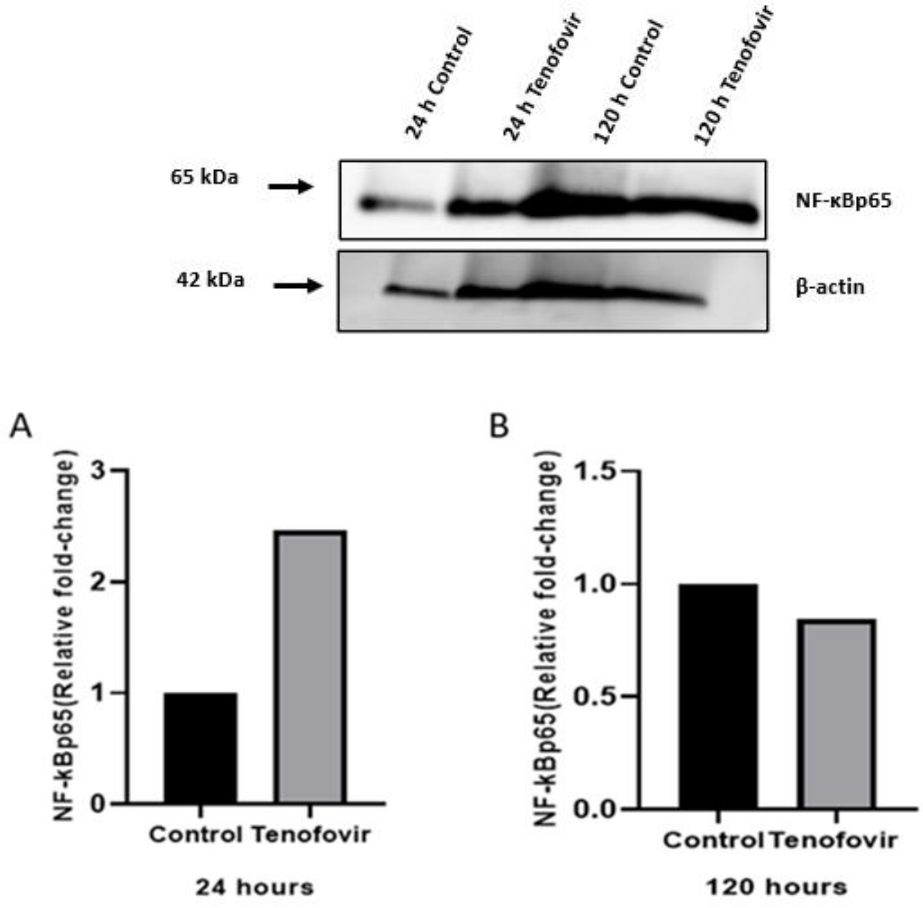

Figure 4.8: NF-κBp65 protein expression in $HepG_2$ cells after exposure to tenofovir at 24h (A) and 120h (B). The data is expressed as a relative fold-change (n=1).

4.5.2.2 Determination of p-NF-κBp65 protein at different time intervals

Phosphorylated NF-κBp65 (p-NF-κBp65) was assessed as a response to tenofovir exposure. p-NF-κBp65 protein is expressed in the NF-κB pathway activation. Tenofovir upregulated the p-NF-κBp65 expression at 24h (2.620-fold) and 120h (6.231-fold).

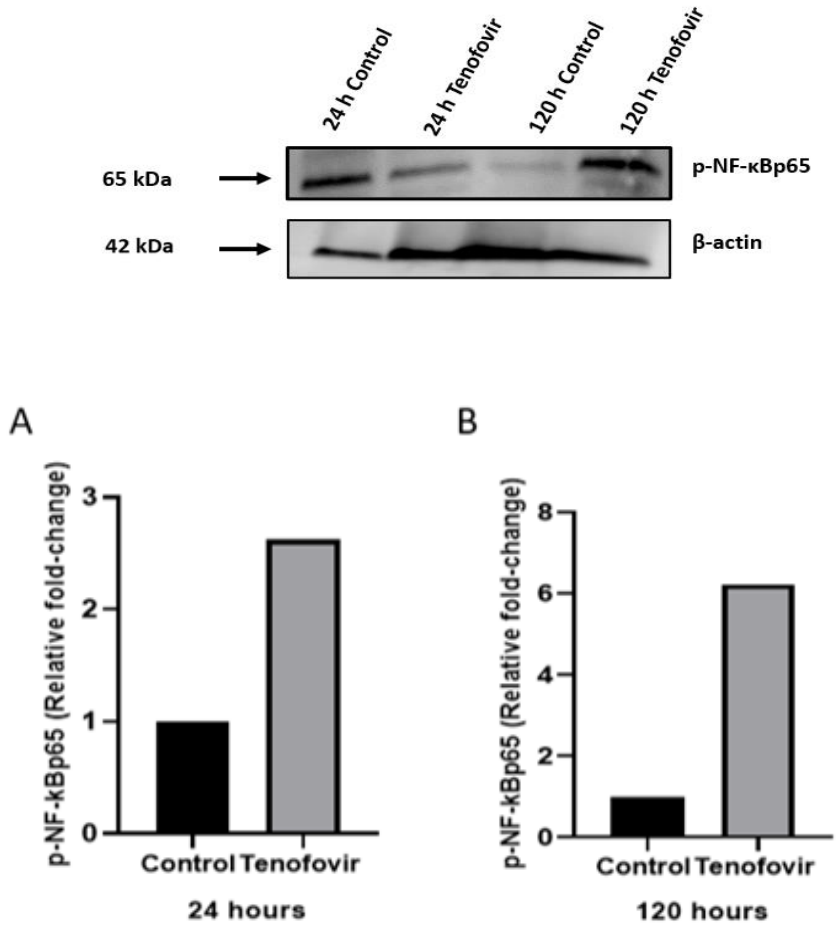

Figure 4.9: p-NF-κBp65 protein expression in HepG$_2$ cells after exposure to tenofovir at 24h (A) and 120h (B). The data is expressed as a relative fold-change (n=1).

4.5.2.3 Determination of IκBα protein at different time intervals

The IκBα protein limits NF-κB activity through a negative feedback loop. Tenofovir downregulated the IκBα protein expression at 24h (0.292-fold). After 120h, the IκBα protein expression was upregulated in the tenofovir-treated $HepG_2$ cells compared to the control (4.417-fold).

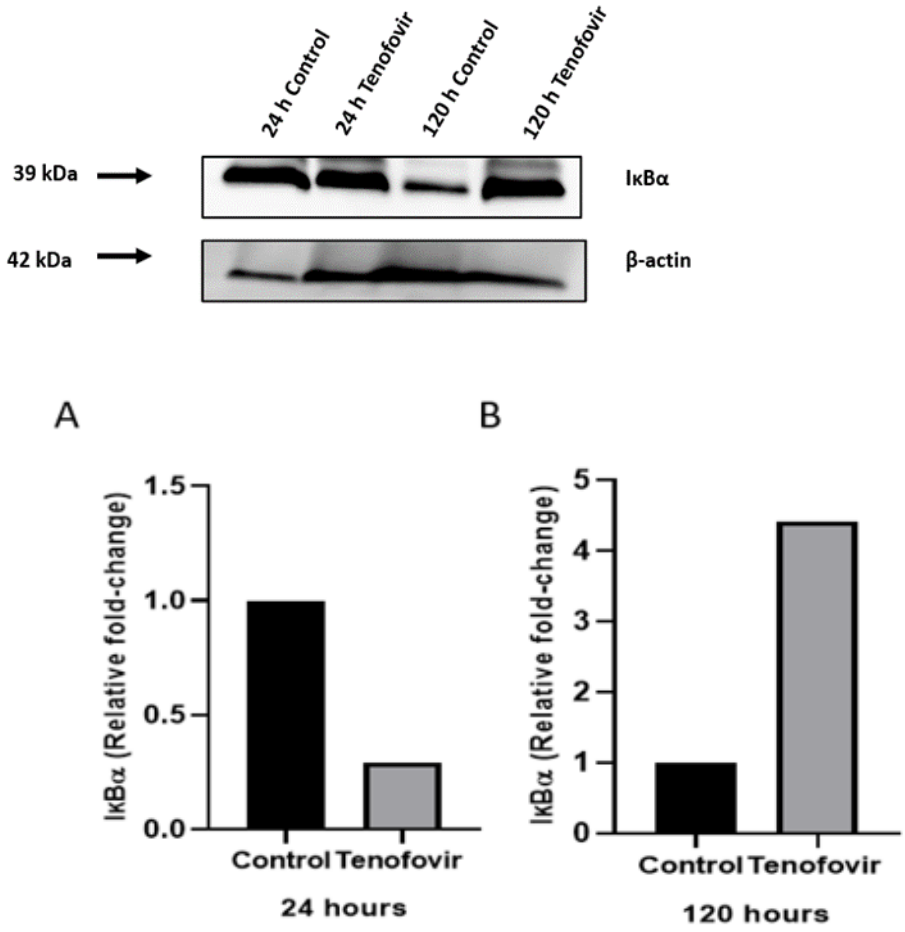

Figure 4.10: IκBα protein expression in $HepG_2$ cells after exposure to tenofovir for 24h (A) and 120h (B). The data is expressed as a relative fold-change (n=1).

4.5.2.4 Determination of p-IκBα protein at different time intervals

The p-IκBα is essential for the activation of the NF-κB signalling pathway. After 24h, p-IκBα protein was higher in the tenofovir-treated group compared to the control (1.290-fold). At 120h, tenofovir decreased the expression of p-IκBα (0.573-fold).

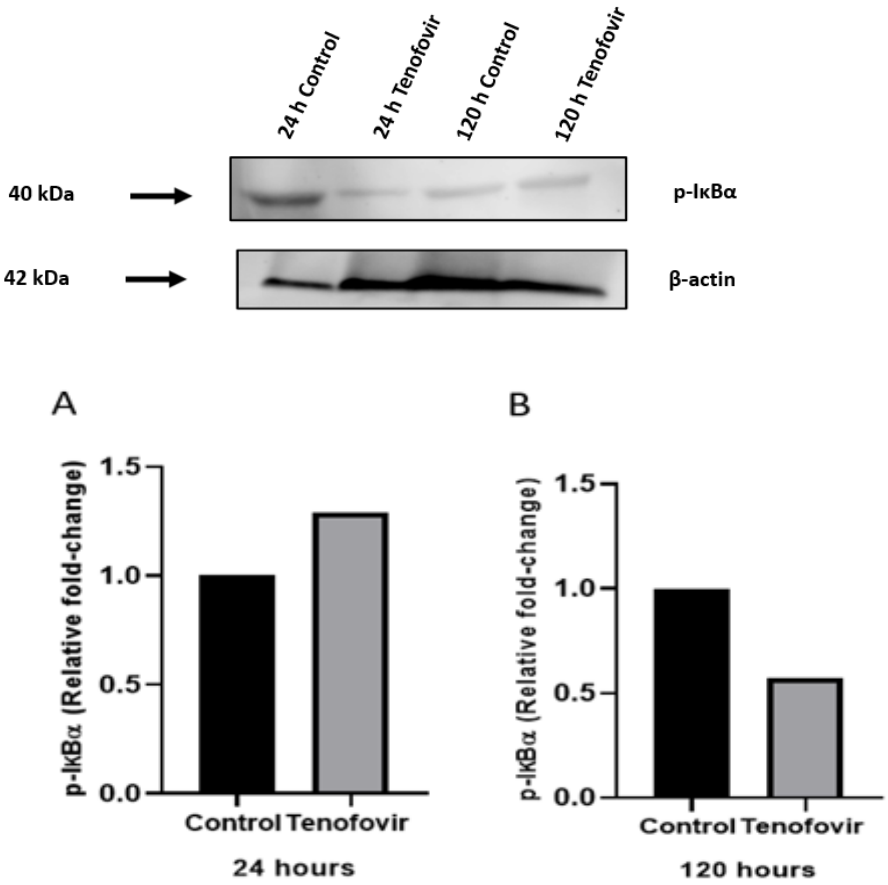

Figure 4.11: p-IκBα protein expression in HepG$_2$ cells after exposure to tenofovir for 24h (A) and 120h (B). The data is expressed as a relative fold-change (n=1).

4.6 SUMMARY OF THE RESULTS

The overall quantitative evaluation of cytokines i shows that at 24h, significantly lower levels of IL-1β and higher levels of IL-6 and IL-10 in the tenofovir-treated group were observed. However, at 120h, significantly lower levels of IL-6 and IL-10 were observed in the tenofovir-treated group compared to the control group.

Quantitative PCR demonstrated a significant increase of *NF-κBp65* mRNA expression in the tenofovir-treated $HepG_2$ cells at 24h. However, at 120h, tenofovir-treated showed a significant decrease in *NF-κBp65* mRNA expression in $HepG_2$ cells. The *IκBα* mRNA expression demonstrated a significant decrease at both time frames.

Furthermore, at 24h, the western blot results demonstrated a decrease in IκBα and an increase in NF-κBp65, p-NF-κBp65 and p-IκBα protein expression. After 120h, tenofovir upregulated p-NF-κBp65 and IκBα protein expression. However, NF-κBp65 and p-IκBα were down-regulated at 120h.

4.7 CONCLUSION

Chapter 4 presented the quantitative results of the inflammatory cytokines (IL-6, IL-1β, TNF-α, and IL-10), mRNA expression (*NF-κBp65* and *IκBα*) and protein expression (p-NF-κBp65, p-IκBα, NF-κBp65 and IκBα). In order to answer the research questions, inflammatory cytokines were quantified using a sandwich ELISA assay, and mRNA expression was determined using qPCR and protein expression with the Western blot technique. The findings are presented in the form of figures and tables. A detailed discussion of the inflammatory properties of tenofovir will follow in Chapter 5.

CHAPTER 5: DISCUSSION OF THE FINDINGS

5.1 INTRODUCTION

This chapter presents the contribution of the study by addressing the research questions (cf 1.5) and the objectives (cf 1.6). The study's quantitative findings (Chapter 4) demonstrated that tenofovir has pro- and anti-inflammatory properties in $HepG_2$ human liver cells. A discussion of the findings of the quantitative data is presented here.

The following diagram summarises tenofovir's pro- and anti-inflammatory properties in $HepG_2$ human liver cells at different time exposures and the proposed mechanisms of action

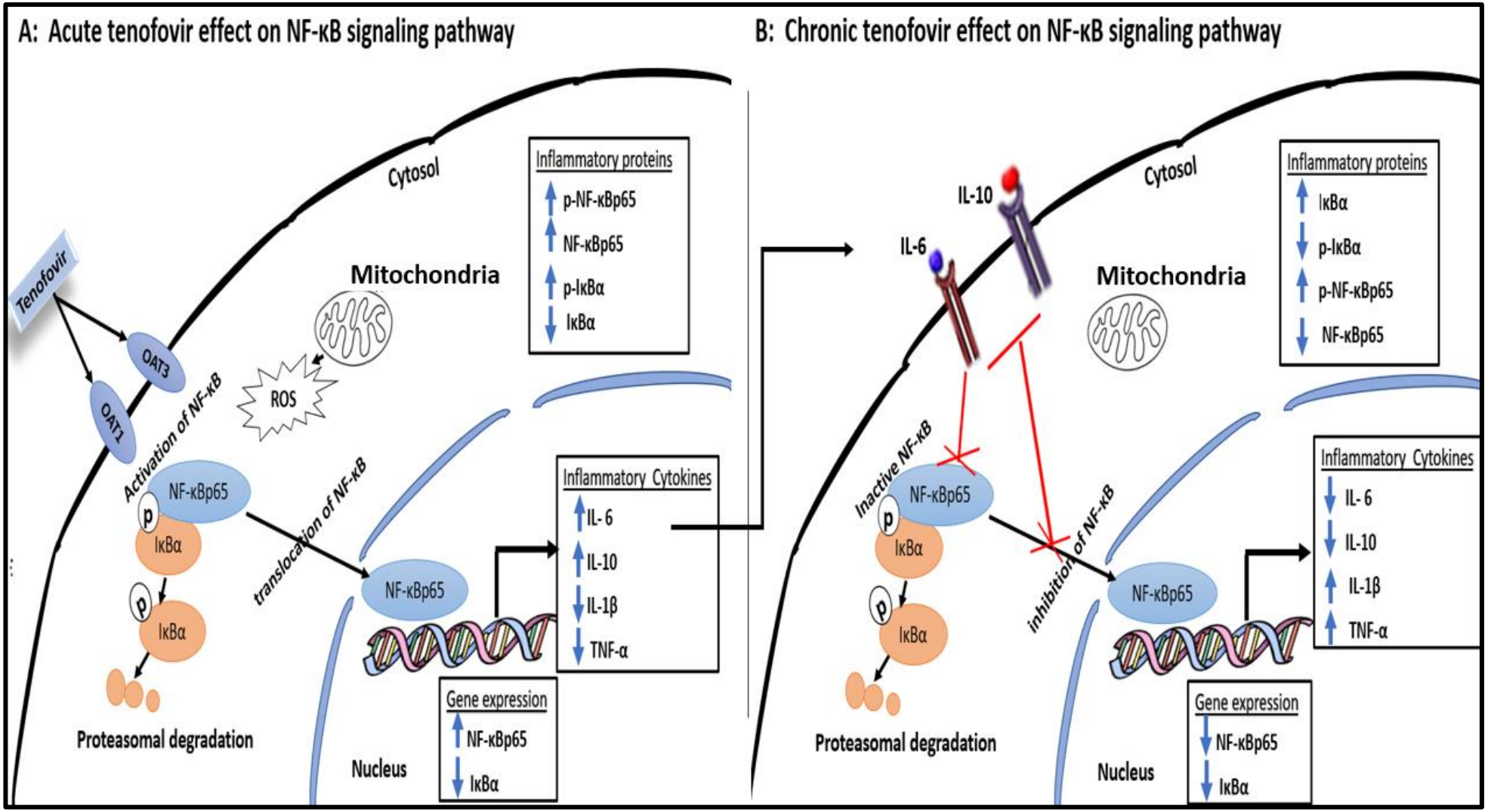

Figure 5.1: Tenofovir's pro- and anti-inflammatory properties in HepG$_2$ human liver cells at different time exposures (compiled by the researcher, S Vazi).

5.2 DISCUSSION

Tenofovir, a reverse transcriptase inhibitor, is an effective HIV therapeutic drug (Hall et al., 2011; Post and Sinxadi, 2022; Milián et al., 2017). However, immune activation and mitochondrial toxicity often persist despite successful viral suppression, especially with long-term use. It is widely used in combination with other ARV drugs to treat HIV infection. However, tenofovir has several side effects, especially with long-term use. Numerous case reports have described severe cases of mitochondrial toxicity associated with tenofovir exposure (Tourret et al., 2013; Nagiah et al., 2015; Zhao et al., 2017; Milian et al., 2017). Disruptions to mitochondrial function increase the production of ROS via defective oxidative phosphorylation (Nagiah et al., 2015). Increased free radical production depletes the antioxidant defence response over time, eventually resulting in oxidative damage (Zhao et al., 2017). Reactive oxygen species are signalling molecules that initiate and perpetuate the inflammatory process during oxidative stress (Zhang et al., 2019). This has an impact on the genes being expressed. Reactive oxygen species directly influence NF-κB transcription factors (Liu et al., 2017). The NF-κB pathway is central in regulating the gene transcription and encoding of inflammatory cytokines (Zhang et at., 2021).

5.3 TENOFOVIR'S EFFECT ON NF-KB SIGNALING PATHWAY AT ACUTE EXPOSURE

The present study investigated NF-κB signalling pathway activation in $HepG_2$ human liver cells following exposure to tenofovir for 24h. For this, gene expression, protein expression and inflammatory cytokine levels were determined by qPCR, western blot, and ELISAs, respectively. The NF-κB gene expression analysis revealed increased mRNA and protein expression in the NF-κB signalling pathway at acute exposure when compared to the control (Figure 5.1A). This suggests that tenofovir affects the NF-κB signaling pathway via regulating gene expression. This is supported by Ramamoorthy et al. (2017), who found that tenofovir affects the NF-κB signalling pathway by increasing mRNA and protein expressions in kidney cells.

NF-κB pathway is responsive to oxidative stress (Van den Berg et al., 2001). In response to oxidative stress, the NF-κB subunit translocates into the nucleus (Bonnard et al., 2000). Increased ROS levels reduce the mitochondrial intracellular thiol group, modulating redox potential (Ramamoorthy et al., 2017). The redox imbalance initiated by oxidative stress can negatively affect redox-sensitive gene regulation (Hansen and Harris, 2004), including upregulation of the inflammatory genes (Ramamoorthy et al., 2017). A study in human microvascular endothelial cells has shown that mitochondrial ROS causes changes in the cytoplasmic redox state, activating the NF-κB pathway (Kim et al., 2008). In the current study, the results demonstrated that acute tenofovir exposure initiates and activates the NF-κB pathway. This NF-κB pathway activation is evident through the increase of the *NF-κBp65* gene (*$p < 0.0207$; figure 4.6A) and NF-κBp65 and phosphorylated NF-κBp65 protein (Figure 4.8A and 9A, respectively) following 24h of tenofovir exposure.

The *IκBα* subunit inhibits NF-κB in the cytoplasm (Mercurio et al., 1997). *IκBα* binds to the *NF-κBp65* subunit and limits its translocation into the nucleus (Arenzana-Seisdedos et al., 1997). The present study found that *IκBα* gene expression was significantly decreased at acute exposure (***$p <$ 0.0004; figure 4.7A) when compared to the control. This indicates that the freely available *NF-κBp65* could translocate into the nucleus to increase/decrease the transcription of genes.

The activated NF-κB pathway controls the transcription of genes that regulate inflammation (Melchjorsen et al., 2011). Therefore, to further corroborate these findings, the researcher assessed pro- and anti-inflammatory cytokine levels at acute exposure in tenofovir-treated $HepG_2$ cells.

Interestingly, IL-1β levels (**$p <$ 0,003; Figure 4.3A) were significantly decreased, while no change in TNF-α levels was observed at acute exposure. The ability of tenofovir to reduce the levels of pro-inflammatory cytokines, such as IL-1β, may therefore be generally beneficial during very early HIV infection.

In addition, tenofovir elevated IL-10 (**$p < 0.005$; Figure 4.5A) and IL-6 (*$p < 0.040$; Figure 4.2A) levels at acute exposure. The elevation of these cytokines represents a compensatory mechanism to the active NF-κB pathway. Melchjorsen et al. (2011) found that tenofovir selectively regulates the production of IL-10 in monocytes and PBMCs. These findings suggest that nuclear NF-κB binds to the anti-inflammatory gene promoter and initiates IL-10 and IL-6 mRNA transcription. These genes are subsequently translated into proteins, and cytokines are then released. The anti-inflammatory cytokines inhibit the translocation of the *NF-κBp65* subunit (Driessler et al., 2004). The current results show that tenofovir is responsible for the negative feedback effect on the activated NF-κB pathway by increasing anti-inflammatory markers at acute exposure.

5.4 TENOFOVIR'S EFFECT ON NF-KB SIGNALLING PATHWAY AT CHRONIC EXPOSURE

The long-term use of tenofovir in antiretroviral therapy is linked with liver and renal damage and the activation of the NF-κB pathway at a molecular level (Ramamoorthy et al., 2017). This study demonstrated increased NF-κB inhibitory protein (IκBα) expression at chronic exposure (Figure 4.10B). The acute elevation of IL-10 (**$p < 0.005$; Figure 4.5A) and IL-6 (*$p < 0.040$; Figure 4.2A) inhibits the NF-κB pathway at chronic exposure. Maiti et al. (2014) reported that secreted anti-inflammatory cytokines bind to cell surface receptors forming a ligand-receptor complex. This complex inhibits the NF-κB pathway activation and translocation into the nucleus.

This study further investigated the NF-κB pathway activity at chronic exposure. The results demonstrated the decrease of *NF-κBp65* gene expression (***$p < 0.0001$; Figure 4.6). Interestingly, the phosphorylated NF-κBp65 protein expression was increased compared to the control group (Figure 4.9B). The cause of higher p-NF-κBp65 protein levels may be due to its sequential post-translational modifications. This is based on post-translational modifications modulating the expression, strength, and duration of the NF-κBp65 activity (Lu, 2015; Oeckinghaus and Ghosh, 2009).

Furthermore, tenofovir increased IκBα protein expression (Figure 4.10B) in $HepG_2$ cells leading to inhibition of the NF-κB pathway. Maiti et al. (2014) noted that the consequence of higher levels of IκBα is an increased association between IκBα and NF-κBp65 in the cytosol (Maiti et al., 2014). The IκBα:NF-κBp65 association decreases the availability of free (active) NF-κBp65 to translocate into the nucleus and activate pro-inflammatory genes. The presence of an NF-κB inhibitor (IκBα), a normal regulatory activity of the NF-κB pathway, restores homeostasis (Hoffmann et al., 2002).

Phosphorylation of IκBα proteins regulates NF-κB complexes in the cytosol (Ramamoorthy et al., 2017). The phosphorylated IκBα proteins are subsequently ubiquitinated and degraded via the proteasomal pathway. Degradation of IκBα proteins frees the NF-κB proteins, which translocate into the nucleus to activate gene expression (Maiti et al., 2014). The present study demonstrated decreased p-IκBα protein expression at chronic exposure (Figure 4.11B). This finding supports the previous statement that the NF-κB pathway was inhibited at chronic exposure to tenofovir.

NF-κB is a critical mediator of pro-inflammatory cytokine production. Therefore, the therapeutic potential of inhibiting the NF-κB pathway is an important target for drug development and discovery (Roberti et al., 2022; Liu et al., 2017). The effect of tenofovir on inflammatory cytokine production has been extensively documented (Parienti et al., 2021; Biswas et al., 2014; Melchjorsen et al., 2011). The current study demonstrated a non-significant increase in pro-inflammatory cytokine (IL-1β and TNF-α) production at chronic exposure.

Zulu et al. (2017) documented the upregulation of IL-1β and TNF-α levels in hippocampal tissue after eight weeks of tenofovir exposure. Similarly, elevated levels of TNF-α and IL-1β in murine peritoneal macrophage cultures were seen (Zídek et al., 2001). Furthermore, Ramamoorthy et al. (2017) showed that increased TNF-α levels influence the pathophysiology of tenofovir-induced renal damage in rat kidney cells.

The researcher also investigated the anti-inflammatory activity of tenofovir in $HepG_2$ human liver cells at chronic exposure. Interestingly, IL-10 (*$p < 0.014$; Figure 4.5B) and IL-6 (****$p < 0.0001$;

Figure 4.2B) levels were significantly downregulated. The anti-inflammatory cytokines decline post NF-κB pathway inhibition suggests an establishment of cellular homeostasis. Melchjorsen et al. (2011) also reported decreased production of IL-10 following chronic exposure to tenofovir in monocytes. In other studies, tenofovir was reported to increase IL-6 levels at chronic exposure (Dumond et al., 2020; Biswas et al., 2013; McDonald et al., 2013).

Elucidation of tenofovir's inflammatory properties at chronic exposure is essential. Tenofovir's long-term use is linked to mitochondrial toxicity and the generation of ROS. However, the current study demonstrated a non-significant increase in pro-inflammatory cytokines and significantly decreased anti-inflammatory cytokines, IL-10 and IL-6, at prolonged exposure. The results suggest that tenofovir potentially has pro-inflammatory activity in $HepG_2$ cells at chronic exposure.

In summary, the ability of tenofovir to inactivate the NF-κB signalling pathway may play a critical role in the therapeutics of tenofovir. Acute tenofovir exposure in $HepG_2$ cells resulted in anti-inflammatory activity by increasing anti-inflammatory cytokines (IL-10 and IL-6). This suggests that the increased of anti-inflammatory markers contributes to the feedback control of the inflammatory response. While prolonged tenofovir exposure in $HepG_2$ cells resulted in increased pro-inflammatory activity with decreased anti-inflammatory cytokines (IL-10 and IL-6). Eric et al. (2016) indicated that antiretroviral drugs with anti-inflammatory activity could improve the functioning of blood vessels in HIV-positive individuals as they are at high risk of cardiovascular diseases.

CHAPTER 6: CONCLUSION, RECOMMENDATIONS AND LIMITATIONS OF THE STUDY.

6.1 INTRODUCTION

Antiretroviral drugs are responsible for several side effects and life-threatening diseases, such as lactic acidosis and hepatotoxicity in HIV-positive individuals (Ezhilarasan et al., 2017; Kalyesubula et al., 2011). These diseases arise from toxicity associated with the long-term use of ARVs. Tenofovir is among the ARV drugs found to damage liver cells through the generation of ROS. Existing literature states that ROS is responsible for the NF-κB pathway activation. The NF-κB pathway is the primary regulator of inflammation. Given this, the study aimed to determine tenofovir's potential pro- and anti-inflammatory properties in $HepG_2$ human liver cells. The rationale for investigating the inflammatory properties of tenofovir was to improve understanding of its mechanism of action and its associated side effects in liver cells.

6.2 CONCLUSION

This study found that tenofovir has anti-inflammatory activity in $HepG_2$ human liver cells at acute exposure. Tenofovir reduced the expression of pro-inflammatory cytokines and enhanced the expression of anti-inflammatory cytokines. In addition, the results of this study indicated that tenofovir increased pro-inflammatory cytokines and downregulated anti-inflammatory cytokines at chronic exposure. The increased pro-inflammatory activity with an inadequate anti-inflammatory response as compensation might result in severe clinical outcomes. Therefore, these results imply that tenofovir's long-term exposure might promote a chronic inflammatory response in liver cells. However, more studies confirming and validating these findings are needed.

6.3 RECOMMENDATIONS

In light of the study's findings, the following recommendations are made: Firstly, to have a more comprehensive understanding of tenofovir's inflammatory properties, a study assessing oxidative

stress leading to NF-κB pathway activation would provide insight into how the NF-κB pathway responds to several stimuli, including cytokines and stress. Secondly, besides the liver, the kidneys are major excretory organs prone to ARV toxicity. Therefore, future studies investigating tenofovir's inflammatory properties in kidney cells are also warranted. Thirdly, the $HepG_2$ cells were only treated for 24h and 120h periods. Results could differ if shorter or longer periods were investigated. Lastly, this study was carried out on an immortalised cell line *in vitro*; therefore, future studies need to be conducted in an *in vivo* model to validate the *in vitro* study results.

6.4 LIMITATIONS OF THE STUDY

The researcher recognises the following limitations of the study: Firstly, the results of this study were obtained in a unicellular culture model and may differ in a multicellular model such as primary liver cells. Secondly, although the first result of the Western blot was completed, and data showed differential protein expression between the treatment groups, the second and third repeats could not be completed due to limited resources and funding.

REFERENCES

1. Abdulrasool, H. and Briggs, C., 2018. Anatomical variation of arterial blood supply of liver segment IV. Europe Journal of anatomy, pp.375-377.
2. Abraham, P., Ramamoorthy, H. and Isaac, B., 2013. Depletion of the cellular antioxidant system contributes to tenofovir disoproxil fumarate-induced mitochondrial damage and increased oxido-nitrosative stress in the kidney. Journal of biomedical science, 20(1), pp.1-15.
3. Adebayo, O.A., Akinloye, O. and Adaramoye, O.A., 2020. Cerium oxide nanoparticles attenuate oxidative stress and inflammation in the liver of diethylnitrosamine-treated mice. Biological trace element research, 193(1), pp.214-225.
4. Ahmed, D., Roy, D. and Cassol, E., 2018. Examining relationships between metabolism and persistent inflammation in HIV patients on antiretroviral therapy. Mediators of inflammation, 2018.
5. Alía, M., Ramos, S., Mateos, R., Bravo, L. and Goya, L., 2005. Response of the antioxidant defence system to tert-butyl hydroperoxide and hydrogen peroxide in a human hepatoma cell line ($HepG_2$). Journal of biochemical and molecular toxicology, 19(2), pp.119-128.
6. Almazroo, O.A., Miah, M.K. and Venkataramanan, R., 2017. Drug metabolism in the liver. Clinics in liver disease, 21(1), pp.1-20.
7. Alonzo, A.A. and Reynolds, N.R., 1995. Stigma, HIV and AIDS: An exploration and elaboration of a stigma trajectory. Social science & medicine, 41(3), pp.303-315.
8. Anderson, E.M. and Maldarelli, F., 2018. The role of integration and clonal expansion in HIV infection: live long and prosper. Retrovirology, 15(1), pp.1-22.
9. Spearman, C.W., 2023. The burden of chronic liver disease in west Africa: a time for action. The Lancet Global Health, 11(9), pp. e1319-e1320.

10. Arenzana-Seisdedos, F., Turpin, P., Rodriguez, M., Thomas, D., Hay, R.T., Virelizier, J.L. and Dargemont, C., 1997. Nuclear localization of I kappa B alpha promotes active transport of NF-kappa B from the nucleus to the cytoplasm. Journal of cell science, 110(3), pp.369-378.

11. Bakasis, A.D. and Androutsakos, T., 2021. Liver Fibrosis during Antiretroviral Treatment in HIV-Infected Individuals. Truth or Tale. Cells, 10(5), p.1212.

12. Baynes, H.W., Tegene, B., Gebremichael, M., Birhane, G., Kedir, W. and Biadgo, B., 2017. Assessment of the effect of Antiretroviral therapy on renal and liver functions among HIV-infected patients: a retrospective study. HIV/AIDS (Auckland, NZ), 9, pp.1-7.

13. Biswas, N., Rodriguez-Garcia, M., Crist, S.G., Shen, Z., Bodwell, J.E., Fahey, J.V. and Wira, C.R., 2013. Effect of tenofovir on nucleotidases and cytokines in HIV-1 target cells. PloS one, 8(10), p.e78814.

14. Biswas, N., Rodriguez-Garcia, M., Shen, Z., Crist, S.G., Bodwell, J.E., Fahey, J.V. and Wira, C.R., 2014. Effects of tenofovir on cytokines and nucleotidases in HIV-1 target cells and the mucosal tissue environment in the female reproductive tract. Antimicrobial agents and chemotherapy, 58(11), pp.6444-6453.

15. Blas-García, A., Apostolova, N., Ballesteros, D., Monleon, D., Morales, J.M., Rocha, M., Victor, V.M. and Esplugues, J.V., 2010. Inhibition of mitochondrial function by efavirenz increases lipid content in hepatic cells. Hepatology, 52(1), pp.115-125.

16. Blattner, W.A., 1989. Retroviruses. In Viral infections of humans (pp. 545-592). Springer, Boston, MA.

17. Bonnard, M., Mirtsos, C., Suzuki, S., Graham, K., Huang, J., Ng, M., Itié, A., Wakeham, A., Shahinian, A., Henzel, W.J. and Elia, A.J., 2000. Deficiency of T2K leads to apoptotic liver degeneration and impaired NF-κB-dependent gene transcription. The EMBO journal, 19(18), pp.4976-4985.

18. Bordes, C., Leguelinel-Blache, G., Lavigne, J.P., Mauboussin, J.M., Laureillard, D., Faure, H., Rouanet, I., Sotto, A. and Loubet, P., 2020. Interactions between antiretroviral therapy

and complementary and alternative medicine: a narrative review. Clinical Microbiology and Infection, 26(9), pp.1161-1170.

19. Bosh, K.A., Hall, H.I., Eastham, L., Daskalakis, D.C. and Mermin, J.H., 2021. Estimated Annual Number of HIV Infections─ the United States, 1981–2019. Morbidity and Mortality Weekly Report, 70(22), p.801.

20. Calza, L., Colangeli, V., Magistrelli, E., Rossi, N., Rosselli Del Turco, E., Bussini, L., 2017. Prevalence of metabolic syndrome in HIV-infected patients naive to antiretroviral therapy or receiving the first-line treatment. HIV clinical trials, 18(3), pp.110-117.

21. Cames, C., Pascal, L., Ba, A., Mbodj, H., Ouattara, B., Diallo, N.F., et al., 2018. Low prevalence of lipodystrophy in HIV-infected Senegalese children on long-term Antiretroviral treatment: the ANRS 12279 MAGGSEN Pediatric Cohort Study. BMC infectious diseases, 18(1), pp.1-9.

22. Castillo-Mancilla, J.R., Meditz, A., Wilson, C., Zheng, J.H., Palmer, B.E., Lee, E.J., Gardner, E.M., Seifert, S., Kerr, B., Bushman, L.R. and MaWhinney, S., 2015. Reduced immune activation during tenofovir-emtricitabine therapy in HIV-negative individuals. Journal of acquired immune deficiency syndromes, 68(5), p.495.

23. Castro-Nallar, E., Pérez-Losada, M., Burton, G.F. and Crandall, K.A., 2012. The evolution of HIV: inferences using phylogenetics. Molecular phylogenetics and evolution, 62(2), pp.777-792.

24. Centers for Disease Control (CDC), 1982. A cluster of Kaposi's sarcoma and Pneumocystis carinii pneumonia among homosexual male residents of Los Angeles and Orange Counties, California. MMWR. Morbidity and mortality weekly report, 31(23), pp.305-307.

25. Chen, L., Deng, H., Cui, H., Fang, J., Zuo, Z., Deng, J., Li, Y., et al., 2018. Inflammatory responses and inflammation-associated diseases in organs. Oncotarget, 9(6), pp.7204.

26. Chibawara, T., Mbuagbaw, L., Kitenge, M. and Nyasulu, P., 2019. Effects of antiretroviral therapy in HIV-positive adults on new HIV infections among young women: a systematic review protocol. Systematic reviews, 8, pp.1-6.

27. Chittick, G.E., Zong, J., Blum, M.R., Sorbel, J.J., Begley, J.A., Adda, N. and Kearney, B.P., 2006. Pharmacokinetics of tenofovir disoproxil fumarate and ritonavir-boosted saquinavir mesylate administered alone or in combination at a steady state. Antimicrobial agents and chemotherapy, 50(4), pp.1304-1310.

28. Cressey, T.R., Siriprakaisil, O., Kubiak, R.W., Klinbuayaem, V., Sukrakanchana, P.O., Quame-Amaglo, J., Okochi, H., Tawon, Y., Cressey, R., Baeten, J.M. and Gandhi, M., 2020. Plasma pharmacokinetics and urinary excretion of tenofovir following cessation in adults with controlled levels of adherence to tenofovir disoproxil fumarate. International Journal of Infectious Diseases, 97, pp.365-370.

29. Costanzo, L. S., 2018. Physiology (Sixth edition.). Philadelphia, PA: Elsevier. (Accessed: 22/10/2021). http://pi.lib.uchicago.edu/1001/cat/bib/11052611

30. Dawany, N., 2010. Large-Scale Integration of Microarray Data: Investigating the Pathologies of Cancer and Infectious Diseases (Vol. 71, No. 08).

31. Dayakar, A., Chandrasekaran, S., Kuchipudi, S.V. and Kalangi, S.K., 2019. Cytokines: key determinants of resistance or disease progression in visceral leishmaniasis: opportunities for novel diagnostics and immunotherapy. Frontiers in immunology, 10(1), pp.670.

32. De Clercq, E., 1995. Toward improved anti-HIV chemotherapy: therapeutic strategies for intervention with HIV infections. Journal of medicinal chemistry, 38(14), pp.2491-2517.

33. Deng, L., Zeng, Q., Wang, M., Cheng, A., Jia, R., Chen, S., Zhu, D., et al., 2018. Suppression of NF-κB activity: a viral immune evasion mechanism. Viruses, 10(8), pp.409.

34. Donato, M.T., Tolosa, L. and Gómez-Lechón, M.J., 2015. Culture and functional characterization of human hepatoma HepG2 cells. Protocols in in vitro hepatocyte research, pp.77-93.

35. Dorrington, M.G. and Fraser, I.D., 2019. NF-κB signalling in macrophages: dynamics, crosstalk, and signal integration. Frontiers in immunology, 10, pp.705.

36. Driessler, F., Venstrom, K., Sabat, R., Asadullah, K. and Schottelius, A.J., 2004. Molecular mechanisms of interleukin-10-mediated inhibition of NF-κ B activity: a role for p50. Clinical & Experimental Immunology, 135(1), pp.64-73.

37. Dumitrescu, T.P., Peddiraju, K., Fu, C., Bakshi, K., Yu, S., Zhang, Z., Tenorio, A.R., Spancake, C., Joshi, S., Wolstenholme, A. and Adkison, K., 2020. Bioequivalence and Food Effect Assessment of 2 Fixed-Dose Combination Formulations of Dolutegravir and Lamivudine. Clinical Pharmacology in Drug Development, 9(2), pp.189-202.

38. Dumond, J.B., Bay, C.P., Nelson, J.A., Davalos, A., Edmonds, A., De Paris, K., Sykes, C., Anastos, K., Sharma, R., Kassaye, S. and Tamraz, B., 2020. Intracellular tenofovir and emtricitabine concentrations in younger and older women with HIV receiving tenofovir disoproxil fumarate/emtricitabine. Antimicrobial agents and chemotherapy, 64(9), pp.10-1128.

39. Edagwa, B., McMillan, J., Sillman, B. and Gendelman, H.E., 2017. Long-acting slow effective release Antiretroviral therapy. Expert opinion on drug delivery, 14(11), pp.1281-1291.

40. Edwards, C.T., Holmes, E.C., Wilson, D.J., Viscidi, R.P., Abrams, E.J., Phillips, R.E. and Drummond, A.J., 2006. Population genetic estimation of the loss of genetic diversity during horizontal transmission of HIV-1. BMC evolutionary biology, 6(1), pp.1-10.

41. Eggleton, J.S. and Nagalli, S., 2020. Highly Active Antiretroviral Therapy (HAART). Statistics Pearls: Treasure Island (FL), Accessed: 25 Mar 2021. https://europepmc.org/article/nbk/nbk554533#free-full-text

42. Elias, A., Ijeoma, O., Edikpo, N.J., Oputiri, D. and Geoffrey, O.B.P., 2013. Tenofovir Renal Toxicity: Evaluation of Cohorts and Clinical Studies—Part One. Pharmacology & Pharmacy, 4(09), pp.651-662.

43. Eric, N., Janet, L. and Grinspoon, S.K., 2016. Inflammation, immune activation, and cardiovascular disease in HIV. AIDS (London, England), 30(10), p.1495.

44. Ezhilarasan, D., Srilekha, M. and Raghu, R., 2017. HAART and hepatotoxicity. Journal of Applied Pharmaceutical Science, 7, pp.220-226.

45. Faden, F., Eschen-Lippold, L. and Dissmeyer, N., 2016. Normalized quantitative Western blotting based on standardized fluorescent labeling. Plant Proteostasis: Methods and Protocols, pp.247-258.

46. Fantauzzi, A. and Mezzaroma, I., 2014. Dolutegravir: clinical efficacy and role in HIV therapy. Therapeutic advances in chronic disease, 5(4), pp.164-177.

47. Feeney, E.R., van Vonderen, M.G., Wit, F., Danner, S.A., van Agtmael, M.A., Villarroya, F., Domingo, P., Capeau, J., Reiss, P., and Mallon, P.W., 2012. Zidovudine/lamivudine but not nevirapine in combination with lopinavir/ritonavir decreases subcutaneous adipose tissue mitochondrial DNA. Aids, 26(17), pp.2165-2174.

48. Fernandez-Fernandez, B., Montoya-Ferrer, A., Sanz, A.B., Sanchez-Nino, M.D., Izquierdo, M.C., Poveda, J., Sainz-Prestel, V., Ortiz-Martin, N., Parra-Rodriguez, A., Selgas, R. and Ruiz-Ortega, M., 2011. Tenofovir nephrotoxicity: 2011 update. AIDS research and treatment, 2011.

49. Fields, J.A., Swinton, M.K., Carson, A., Soontornniyomkij, B., Lindsay, C., Han, M.M., Frizzi, K., Sambhwani, S., Murphy, A., Achim, C.L. and Ellis, R.J., 2019. Tenofovir disoproxil fumarate induces peripheral neuropathy and alters inflammation and mitochondrial biogenesis in the brains of mice. Scientific reports, 9(1), pp.1-16.

50. Finzi, A., Xiang, S.H., Pacheco, B., Wang, L., Haight, J., Kassa, A., Danek, B., Pancera, M., Kwong, P.D. and Sodroski, J., 2010. Topological layers in the HIV-1 gp120 inner domain regulate gp41 interaction and CD4+ -triggered conformational transitions. Molecular cell, 37(5), pp.656-667.

51. Fletcher, C.V., Podany, A.T., Thorkelson, A., Winchester, L.C., Mykris, T., et al., 2020. The Lymphoid Tissue Pharmacokinetics of Tenofovir Disoproxil Fumarate and Tenofovir Alafenamide in HIV-Infected Persons. Clinical Pharmacology & Therapeutics, 108(5), pp.971-975.

52. Gallo, R.C. and Montagnier, L., 2003. The discovery of HIV as the cause of AIDS. New England Journal of Medicine, 349(24), pp.2283-2285.

53. Ganesan, M., Poluektova, L.Y., Kharbanda, K.K. and Osna, N.A., 2018. Liver as a target of human immunodeficiency virus infection. World journal of gastroenterology, 24(42), p.4728.

54. Ganta, K.K. and Chaubey, B., 2019. Mitochondrial dysfunctions in HIV infection and antiviral drug treatment. Expert opinion on drug metabolism & toxicology, 15(12), pp.1043-1052.

55. Gao, F., Yue, L., Robertson, D.L., Hill, S.C., Hui, H., Biggar, R.J., Neequaye, A.E., Whelan, T.M., Ho, D.D. and Shaw, G.M., 1994. Genetic diversity of human immunodeficiency virus type 2: evidence for distinct sequence subtypes with differences in virus biology. Journal of virology, 68(11), pp.7433-7447.

56. Ghosh, S. and Hayden, M., 2012. Celebrating 25 years of NF-κB research. Immunological Reviews, 246(1), p.5.

57. Giuliani, C., Bucci, I. and Napolitano, G., 2018. The role of the transcription factor Nuclear Factor-kappa B in thyroid autoimmunity and cancer. Frontiers in endocrinology, 9, pp.471.

58. Gordon, J. and Amini, S., 2021. General overview of neuronal cell culture. Neuronal Cell Culture: Methods and Protocols, pp.1-8.

59. Greene, W.C., 2007. A history of AIDS: looking back to see ahead. European journal of immunology, 37(S1), pp. S94-S102.

60. Grigsby, I.F., Pham, L., Mansky, L.M., Gopalakrishnan, R. and Mansky, K.C., 2010. Tenofovir-associated bone density loss. Therapeutics and clinical risk management, 6, p.41.

61. Gulati, K., Guhathakurta, S., Joshi, J., Rai, N., and Ray, A.J.M.I., 2016. Cytokines and their role in health and disease: a brief overview. MedCrave Online Journal of Immunology, 4(2), pp.1-9.

62. Gulick, R.M., 2003. New antiretroviral drugs. Clinical microbiology and infection, 9(3), pp.186-193.

63. Hall, A.M., Hendry, B.M., Nitsch, D. and Connolly, J.O., 2011. Tenofovir-associated kidney toxicity in HIV-infected patients: a review of the evidence. American Journal of kidney diseases, 57(5), pp.773-780.

64. Hall, J.E., 2015. Pocket Companion to Guyton & Hall Textbook of Medical Physiology E-Book. Elsevier Health Sciences.

65. Hamlin, A.N., Tillotson, J. and Bumpus, N.N., 2019. Genetic variation of kinases and activation of nucleotide analogue reverse transcriptase inhibitor Tenofovir. Pharmacogenomics, 20(02), pp.105-111.

66. Han, J., Remete, A.M., Dobson, L.S., Kiss, L., Izawa, K., Moriwaki, H., et al., 2020. Next generation organofluorine containing blockbuster drugs. Journal of Fluorine Chemistry, p.109639.

67. Hansen, J.M. and Harris, C., 2004. A novel hypothesis for thalidomide-induced limb teratogenesis: redox misregulation of the NF-κB pathway. Antioxidants and Redox Signaling, 6(1), pp.1-14.

68. Hashemi, S.P., 2019. Small molecules are effective for disruption of HIV-1 latency (Doctoral dissertation, University of British Columbia), http://hdl.handle.net/2429/71810. Accessed: 5 April 2022.

69. Haycock, J.W., 2011. 3D cell culture: a review of current approaches and techniques (pp. 1-15). Humana Press.

70. Hernaez, R., Solà, E., Moreau, R. and Ginès, P., 2017. Acute-on-chronic liver failure: an update. Gut, 66(3), pp.541-553.

71. Hoffmann, A., Levchenko, A., Scott, M.L. and Baltimore, D., 2002. The IκB-NF-κB signaling module: temporal control and selective gene activation. science, 298(5596), pp.1241-1245.

72. Holec, A.D., Mandal, S., Prathipati, P.K. and Destache, C.J., 2017. Nucleotide reverse transcriptase inhibitors: a thorough review, present status, and future perspective as HIV therapeutics. Current HIV research, 15(6), pp.411-421.

73. Hoofnagle, J.H., 2013. LiverTox: a website on drug-induced liver injury. In Drug-induced liver disease (pp. 725-732). Academic Press.

74. James, A.M., Ofotokun, I., Sheth, A., Acosta, E.P. and King, J.R., 2012. Tenofovir: once-daily dosage in the management of HIV infection. Clinical Medicine Insights: Therapeutics, 4, pp.CMT-S8316.

75. Kalyesubula, R., Kagimu, M., Opio, K.C., Kiguba, R., Semitala, C.F., Schlech, W.F. and Katabira, E.T., 2011. Hepatotoxicity from first line antiretroviral therapy: an experience from a resource limited setting. African health sciences, 11(1).

76. Kandel, C. E., and Walmsley, S. L. 2015. Dolutegravir – A review of the pharmacology, efficacy, and safety in the treatment of HIV. Drug Design, Development and Therapy, 9, 3547–3555. https://doi.org/10.2147/DDDT.S84850. Accessed: 15 February 2021.

77. Kany, S., Vollrath, J.T. and Relja, B., 2019. Cytokines in inflammatory disease. International journal of molecular sciences, 20(23), pp.6008.

78. Kaspar, M.B. and Sterling, R.K., 2017. Mechanisms of liver disease in patients infected with HIV. BMJ open gastroenterology, 4(1), pp. e000166.

79. Kim, S.R., Bae, Y.H., Bae, S.K., Choi, K.S., Yoon, K.H., Koo, T.H., Jang, H.O., Yun, I., Kim, K.W., Kwon, Y.G. and Yoo, M.A., 2008. Visfatin enhances ICAM-1 and VCAM-1 expression through ROS-dependent NF-κB activation in endothelial cells. Biochimica et Biophysica Acta (BBA)-Molecular Cell Research, 1783(5), pp.886-895.

80. Kouanfack, C., Mpoudi-Etame, M., Eymard-Duvernay, S., Leroy, S., Boyer, S., 2019. Dolutegravir-Based or Low-Dose Efavirenz-Based Regimen for the Treatment of HIV-1. The New England Journal of Medicine, 381(9), pp.816-826.

81. Kuntz, E., and Kuntz, H.D., 2006. Hepatology, Principles, and practice: history, morphology, biochemistry, diagnostics, clinic, therapy. Springer Science & Business Media.

82. Langdon, S.P., 2010. Cancer cell culture (Vol. 5, No. 9). Humana. pp.1940-6037. https://doi.org/10.1385/1592594069

83. Lataillade, M. and Kozal, M.J., 2006. The hunt for HIV-1 integrase inhibitors. AIDS Patient Care & STDs, 20(7), pp.489-501.

84. Lee, A.R., Cho, J.Y., Kim, J.C., Dezhbord, M., Choo, S.Y., Ahn, C.H., et al., 2021. Distinctive HBV Replication Capacity and Susceptibility to Tenofovir Induced by a Polymerase Point Mutation in Hepatoma Cell Lines and Primary Human Hepatocytes. International Journal of Molecular Sciences, 22(4), pp.1606.

85. Lingappan, K., 2018. NF-κB in oxidative stress. Current opinion in toxicology, 7, pp.81-86.

86. Liu, T., Zhang, L., Joo, D. and Sun, S.C., 2017. NF-κB signaling in inflammation. Signal transduction and targeted therapy, 2(1), pp.1-9.

87. Lonardo, A., Arab, J.P. and Arrese, M., 2021. Perspectives on precision medicine approach to NAFLD diagnosis and management. Advances in Therapy, 38(5), pp.2130-2158.

88. Lu, D.Y., Wu, H.Y., Yarla, N.S., Xu, B., Ding, J., and Lu, T.R., 2018. HAART in HIV/AIDS treatments: future trends. Infectious Disorders-Drug Targets, 18(1), pp.15-22.

89. Ma, L.N., Zhang, J., Chen, H.T., Zhou, J.H., Ding, Y.Z. and Liu, Y.S., 2011. An overview on ELISA techniques for FMD. Virology journal, 8(1), pp.1-9.

90. Macías, J., Mancebo, M., Merino, D., Téllez, F., Montes-Ramírez, M.L. et al., 2017. Changes in Liver Steatosis After Switching from Efavirenz to Raltegravir Among Human Immunodeficiency Virus-Infected Patients with Nonalcoholic Fatty Liver Disease. Clinical Infectious Diseases, 65(6), pp.1012-1019.

91. Mahadevan, V., 2020. Anatomy of the liver. Surgery (Oxford), 38(8), pp.427-431.

92. Mahmood, T. and Yang, P.C., 2012. Western blot: technique, theory, and trouble shooting. North American journal of medical sciences, 4(9), p.429.

93. Maiti, S., Dai, W., Alaniz, R.C., Hahn, J. and Jayaraman, A., 2014. Mathematical modeling of pro-and anti-inflammatory signaling in macrophages. Processes, 3(1), pp.1-18.

94. Marcus, L. and MacDonell, S., 2020. Human immunodeficiency virus in South Africa. (Accessed, 23 March 2022). https://www.spotlightnsp.co.za/2019/07/18/hiv-in-sa-seven-graphs-that-tell-the-story/. Accessed: 15 April 2021.

95. Margolis, A.M., Heverling, H., Pham, P.A. and Stolbach, A., 2014. A review of the toxicity of HIV medications. Journal of Medical Toxicology, 10(1), pp.26-39.

96. Marinda, E., Simbayi, L., Zuma, K., Zungu, N., Moyo, S., Kondlo, L., Jooste, S., Nadol, P., Igumbor, E., Dietrich, C. and Briggs-Hagen, M., 2020. Towards achieving the 90–90–90 HIV targets: results from the South African 2017 national HIV survey. BMC Public Health, 20(1), pp.1-12.

97. Matta, M.K., Pilli, N.R., Inamadugu, J.K., Burugula, L. and JVLN, S.R., 2012. Simultaneous quantitation of lamivudine, zidovudine and nevirapine in human plasma by liquid chromatography-tandem mass spectrometry and application to a pharmacokinetic study. Acta Pharmaceutica Sinica B, 2(5), pp.472-480.

98. McDonald, B., Moyo, S., Gabaitiri, L., Gaseitsiwe, S., Bussmann, H., Koethe, J.R., Musonda, R., Makhema, J., Novitsky, V., Marlink, R.G. and Wester, C.W., 2013. Persistently elevated serum interleukin-6 predicts mortality among adults receiving combination antiretroviral therapy in Botswana: results from a clinical trial. AIDS research and human retroviruses, 29(7), pp.993-999.

99. McMillan, J.M., Cobb, D.A., Lin, Z., Banoub, M.G., Dagur, R.S., Woods, A.A.B., et al., 2018. Antiretroviral drug metabolism in humanized PXR-CAR-CYP3A-NOG mice. Journal of Pharmacology and Experimental Therapeutics, 365(2), pp.272-280.

100. Melchjorsen, J., Risør, M.W., Søgaard, O.S., O'Loughlin, K.L., Chow, S., Paludan, S.R., et al., 2011. Tenofovir selectively regulates the production of inflammatory cytokines and shifts the IL-12/IL-10 balance in human primary cells. JAIDS Journal of Acquired Immune Deficiency Syndromes, 57(4), pp.265-275.

101. Mendelsohn, A. S., and Ritchwood, T., 2020. COVID-19 and Antiretroviral Therapies: South Africa's Charge Towards 90–90–90 amid a Second Pandemic. AIDS and Behavior, 24(10), 2754–2756. https://doi.org/10.1007/s10461-020-02898-y. Accessed: 05 April 2021.

102. Mercurio, F., Zhu, H., Murray, B.W., Shevchenko, A., Bennett, B.L., Li, J.W., Young, D.B., Barbosa, M., Mann, M., Manning, A. and Rao, A., 1997. IKK-1 and IKK-2: cytokine-activated IκB kinases essential for NF-κB activation. Science, 278(5339), pp.860-866.

103. Milián, L., Peris, J.E., Gandía, P., Andújar, I., Pallardó, L., Górriz, J.L. and Blas-García, A., 2017. Tenofovir-induced toxicity in renal proximal tubular epithelial cells: involvement of mitochondria. Aids, 31(12), pp.1679-1684.

104. Mohan, H., Lenis, M.G., Laurette, E.Y., Tejada, O., Sanghvi, T., Leung, K.Y., Cahill, L.S., Sled, J.G., Delgado-Olguín, P., Greene, N.D. and Copp, A.J., 2021. Dolutegravir in pregnant mice is associated with increased rates of fetal defects at therapeutic but not at supratherapeutic levels. EBioMedicine, 63.

105. Tseng, A., Seet, J. and Phillips, E.J., 2015. The evolution of three decades of antiretroviral therapy: challenges, triumphs and the promise of the future. British journal of clinical pharmacology, 79(2), pp.182-194.

106. Morgan, M.J. and Liu, Z.G., 2011. Crosstalk of reactive oxygen species and NF-κB signaling. Cell research, 21(1), pp.103-115.

107. Morrison, M., Hughes, H.Y., Naggie, S. and Syn, W.K., 2019. Nonalcoholic fatty liver disease among individuals with HIV mono-infection: a growing concern. Digestive diseases and sciences, 64(12), pp.3394-3401.

108. Moure, R., Domingo, P., Villarroya, J., Gasa, L., Gallego-Escuredo, J.M., Quesada-López, T., et al., 2018. Reciprocal effects of Antiretroviral drugs used to treat HIV infection on the fibroblast growth factor 21/β-Klotho system. Antimicrobial agents and chemotherapy, 62(6), pp. e00029-18.

109. National Institute of Allergy and Infectious Diseases (NIAID). 2020. Antiretroviral Drug Discovery and Development. https://www.niaid.nih.gov/diseases-conditions/antiretroviral-drug-development. Accessed: 26 April 2022.

110. Mustafa, M.F., Fakurazi, S., Abdullah, M.A. and Maniam, S., 2020. Pathogenic mitochondria DNA mutations: current detection tools and interventions. Genes, 11(2), p.192.

111. Mzoughi, O., Teixido, M., Planès, R., Serrero, M., Hamimed, I., et al., 2019. Trimeric heptad repeats synthetic peptides HR1 and HR2 efficiently inhibit HIV-1 entry. Bioscience reports, 39(9), pp. BSR20192196.

112. Nagel, D., Vincendeau, M., Eitelhuber, A.C. and Krappmann, D., 2014. Mechanisms and consequences of constitutive NF-κB activation in B-cell lymphoid malignancies. Oncogene, 33(50), pp.5655-5665.

113. Nagiah, S., Phulukdaree, A. and Chuturgoon, A., 2015. Mitochondrial and oxidative stress response in HepG2 cells following acute and prolonged exposure to antiretroviral drugs. Journal of cellular biochemistry, 116(9), pp.1939-1946.

114. Nassir, F., Rector, R.S., Hammoud, G.M. and Ibdah, J.A., 2015. Pathogenesis and prevention of hepatic steatosis. Gastroenterology & hepatology, 11(3), pp.167.

115. National Institute of Allergy and Infectious Diseases (NIAID), 2018. Human immunodeficiency virus cycle. (Accessed; 20 January 2022). (https://www.niaid.nih.gov/diseases-conditions/hiv-replication-cycle).

116. Negoro, R., Tasaka, M., Deguchi, S., Takayama, K. and Fujita, T., 2022. Generation of HepG2 Cells with High Expression of Multiple Drug-Metabolizing Enzymes for Drug Discovery Research Using a PITCh System. Cells, 11(10), p.1677.

117. Oeckinghaus, A. and Ghosh, S., 2009. The NF-κB family of transcription factors and its regulation. Cold Spring Harbor perspectives in biology, 1(4), p.a000034.

118. Olojede, S.O., Lawal, S.K., Faborode, O.S., Dare, A., Aladeyelu, O.S., Moodley, R., Rennie, C.O., Naidu, E.C. and Azu, O.O., 2022. Testicular ultrastructure and hormonal changes following administration of tenofovir disoproxil fumarate-loaded silver nanoparticle in type-2 diabetic rats. Scientific Reports, 12(1), p.9633.

119. Paemanee, A., Sornjai, W., Kittisenachai, S., Sirinonthanawech, N., Roytrakul, S., Wongtrakul, J. and Smith, D.R., 2017. Nevirapine induced mitochondrial dysfunction in HepG2 cells. Scientific reports, 7(1), pp.1-11.

120. Paniagua, A. and Amariles, P., 2017. Hepatotoxicity by drugs, pharmacokinetics and adverse effects of drugs-mechanism and risk factors. Malangu N, IntechOpen, UK. DOI: 10.5772/intechopen.72005.

121. Panganiban, R.A.M., Snow, A.L. and Day, R.M., 2013. Mechanisms of radiation toxicity in transformed and non-transformed cells. International journal of molecular sciences, 14(8), pp.15931-15958.

122. Pant, K. and Singh, A., 2018. Overview of Chemokine Co-Receptor-5 (CCR-5) HIV-1 Entry Inhibitors. Journal of Drug Delivery and Therapeutics, 8(4), pp.73-79.

123. Paoletti, A., Allouch, A., Caillet, M., Saïdi, H., Subra, F., Nardacci, R., Wu, Q., Muradova, Z., Voisin, L., Raza, S.Q. and Law, F., 2019. HIV-1 envelope overcomes NLRP3-mediated inhibition of F-actin polymerization for viral entry. Cell reports, 28(13), pp.3381-3394

124. Pau, A.K. and George, J.M., 2014. Antiretroviral therapy: current drugs. Infectious Disease Clinics, 28(3), pp.371-402.

125. Pitman, M.C., Lau, J.S., McMahon, J.H. and Lewin, S.R., 2018. Barriers and strategies to achieve a cure for HIV. The Lancet HIV, 5(6), pp. e317-e328.

126. Ponchel, F., Toomes, C., Bransfield, K., Leong, F.T., Douglas, S.H., Field, S.L., Bell, S.M., Combaret, V., Puisieux, A., Mighell, A.J. and Robinson, P.A., 2003. Real-time PCR based on

SYBR-Green I fluorescence: an alternative to the TaqMan assay for a relative quantification of gene rearrangements, gene amplifications and micro gene deletions. BMC biotechnology, 3, pp.1-13.

127. Post, F.A. and Sinxadi, P., 2022. Tenofovir disoproxil and renal mitochondrial toxicity: more studies in Africans are needed. AIDS, 36(7), pp.1047-1048.

128. Raffi, F., Pozniak, A. L., and Wainberg, M. A. 2014. Has the time come to abandon efavirenz for first-line antiretroviral therapy? Journal of Antimicrobial Chemotherapy, 69(7), 1742–1747. https://doi.org/10.1093/jac/dku058. Accessed: 25 Mar 2021.

129. Ramamoorthy, H., Abraham, P., Isaac, B., and Selvakumar, D., 2017. The role of the NF-κB inflammatory signalling pathway in Tenofovir disoproxil fumarate (TDF) induced renal damage in rats. Food and Chemical Toxicology, 99, pp.103-118.

130. Rao, X., Huang, X., Zhou, Z. and Lin, X., 2013. An improvement of the 2ˆ (–delta CT) method for quantitative real-time polymerase chain reaction data analysis. Biostatistics, bioinformatics, and biomathematics, 3(3), pp.71.

131. Reis, W., Gaio, J., Chau, T., Ramos, F. and Reis, C., 2020. Antivirals. In Pharmacology in Clinical Neurosciences (pp. 499-678). Springer, Singapore

132. Roberti, A., Chaffey, L.E. and Greaves, D.R., 2022. NF-κB Signaling and Inflammation—Drug Repurposing to Treat Inflammatory Disorders. Biology 2022, 11, 372.

133. Sadiq, U., Shrestha, U. and Guzman, N., 2018. Prevention Of Opportunistic Infections In HIV/AIDS. StatPearls Publishing, Treasure Island (FL), PMID: 30020717 https://europepmc.org/article/nbk/nbk513345#impact.

134. Sahin, K., 2020. Investigation of novel indole-based HIV-1 protease inhibitors using virtual screening and text mining. Journal of Biomolecular Structure and Dynamics, pp.1-11.

135. Schneider, W.H. ed., 2021. The Histories of HIVs: The Emergence of the Multiple Viruses that Caused the AIDS Epidemics. Ohio University Press.

136. Schwetz, T.A. and Fauci, A.S., 2019. The extended impact of human immunodeficiency virus/AIDS research. The Journal of infectious diseases, 219(1), pp.6-9.

137. Sakamoto, S., Putalun, W., Vimolmangkang, S., Phoolcharoen, W., Shoyama, Y., Tanaka, H. and Morimoto, S., 2018. Enzyme-linked immunosorbent assay for the quantitative/qualitative analysis of plant secondary metabolites. Journal of natural medicines, 72, pp.32-42.

138. Serra, P.A., Taveira, N. and Guedes, R.C., 2021. Computational Modulation of the V3 Region of Glycoprotein gp125 of HIV-2. International journal of molecular sciences, 22(4), p.1948.

139. Shah, K. and Maghsoudlou, P., 2016. Enzyme-linked immunosorbent assay (ELISA): the basics. British journal of hospital medicine, 77(7), pp.C98-C101.

140. Shamsabadi, A.A., 2014. Investigation into the hepatotoxic effects of Highly Active Antiretroviral Therapy (HAART) medications, Available from: https://cris.brighton.ac.uk/ws/portalfiles/portal/4753485/Anahid+Amiri+Shamsabadi+MPhil+2014.pdf. Accessed: 11 March 2021].

141. Shamsi, T.S., 2019. Human Immunodeficiency Virus Cases on the Rise in Pakistan. National Journal of Health Sciences, 4(3), pp.91-92.

142. Sharp, P.M. and Hahn, B.H., 2011. Origins of HIV and the AIDS pandemic. Cold Spring Harbor perspectives in medicine, 1(1), p.a006841.

143. Sharp, P.M., Bailes, E., Chaudhuri, R.R., Rodenburg, C.M., Santiago, M.O. and Hahn, B.H., 2001. The origins of acquired immune deficiency syndrome viruses: where and when? Philosophical Transactions of the Royal Society of London. Series B: Biological Sciences, 356(1410), pp.867-876.

144. Shcherbatova, O., Grebennikov, D., Sazonov, I., Meyerhans, A. and Bocharov, G., 2020. Modelling of the HIV-1 life cycle in productively infected cells to predict novel therapeutic targets. Pathogens, 9(4), p.255.

145. Shearer, W.T., 1998. HIV infection and AIDS. Primary Care: Clinics in Office Practice, 25(4), pp.759-774.

146. Singh, D., Cho, W.C. and Upadhyay, G., 2016. Drug-induced liver toxicity and prevention by herbal antioxidants: an overview. Frontiers in physiology, 6, p.363.

147. Smiley, C.L., Rebeiro, P.F., Cesar, C., Belaunzaran-Zamudio, P.F., Crabtree-Ramirez, B., Padgett, D., Gotuzzo, E., Cortes, C.P., Pape, J., Veloso, V.G. and McGowan, C.C., 2021. Estimated life expectancy gains with antiretroviral therapy among adults with HIV in Latin America and the Caribbean: a multisite retrospective cohort study. The Lancet HIV, 8(5), pp. 266- 273.

148. Smith, R.L., Tan, J.M., Jonker, M.J., Jongejan, A., Buissink, T., Veldhuijzen, S., van Kampen, A.H., Brul, S. and van der Spek, H., 2017. Beyond the polymerase-γ theory: Production of ROS as a mode of NRTI-induced mitochondrial toxicity. PLoS One, 12(11), p.e0187424.

149. Sohrabi, M.R. and Zarkesh, M.T., 2014. Spectra resolution for simultaneous spectrophotometric determination of lamivudine and zidovudine components in a pharmaceutical formulation of human immunodeficiency virus drug based on using continuous wavelet transform and derivative transform techniques. Talanta, 122, pp.223-228.

150. Southern African HIV Clinicians Society., 2012. Southern African guidelines for the safe use of pre-exposure prophylaxis in men who have sex with men who are at risk for HIV infection. Southern African Journal of HIV Medicine, 13, pp. 40–55.

151. Sperber, H.S., 2021. CD73: A Key Player in HIV Persistence (Doctoral dissertation, Freie Universitaet Berlin (Germany)).

152. Spinelli, J.B. and Haigis, M.C., 2018. The multifaceted contributions of mitochondria to cellular metabolism. Nature cell biology, 20(7), pp.745-754.

153. Suthiram, K.T., 2020. An investigation into the biochemical effects of Kojic acid (KA) on human hepatocellular carcinoma ($HepG_2$) cells (Doctoral dissertation). Available from. https://researchspace.ukzn.ac.za/handle/10413/19671, Accessed: 11 January 2022].

154. Spira, S., Wainberg, M.A., Loemba, H., Turner, D., and Brenner, B.G., 2003. Impact of clade diversity on HIV-1 virulence, antiretroviral drug sensitivity and drug resistance. Journal of Antimicrobial Chemotherapy, 51(2), pp.229-240.

155. Stevenson, K.A., Podewils, L.J., Zishiri, V.K., Castro, K.G. and Charalambous, S., 2020. HIV prevalence and the cascade of care in five South African correctional facilities. Plos one, 15(7), p.e0235178.

156. Szafranska, K., Kruse, L.D., Holte, C.F., McCourt, P. and Zapotoczny, B., 2021. The Whole Story About Fenestrations in LSEC. Frontiers in Physiology, p.1468.

157. Taqaddas, A., 2020. Effective and simple methods of preventing the transmission of viral diseases. Journal of Advancement in Medical and Life Sciences, 7(4), pp.1-9.

158. Taylor, K., Fritz, K. and Parmar, M., 2020. Lamivudine. [Updated 2023 Jan 17]. In: StatPearls [Internet]. Treasure Island (FL): StatPearls Publishing; 2023 Jan-. Available from: https://www.ncbi.nlm.nih.gov/books/NBK559252/

159. Tayyeb, J.Z., Popeijus, H.E., Mensink, R.P., Konings, M.C., Mokhtar, F.B. and Plat, J., 2020. Short-chain fatty acids (except hexanoic acid) lower NF-kB transactivation, which rescues inflammation-induced decreased apolipoprotein AI transcription in HepG2 cells. International journal of molecular sciences, 21(14), p.5088.

160. Thet, D. and Siritientong, T., 2020. Antiretroviral Therapy-Associated Metabolic Complications: Review of the Recent Studies. HIV/AIDS (Auckland, NZ), 12, p.507.

161. Trickey, A., May, M.T., Vehreschild, J.J., Obel, N., Gill, M.J., Crane, H.M., 2017. Survival of HIV-positive patients starting Antiretroviral therapy between 1996 and 2013: a collaborative analysis of cohort studies. The Lancet HIV, 4(8), pp. e349-e356.

162. Tourret, J., Deray, G. and Isnard-Bagnis, C., 2013. Tenofovir effect on the kidneys of HIV-infected patients: a double-edged sword. Journal of the American Society of Nephrology, 24(10), pp.1519-1527.

163. Umar, D., Waziri, B., Ndagi, U., Mohammed, S., Usman, N. and Abubakar-Muhammad, H., 2020. Impact of Tenofovir/Lamivudine/Dolutegravir (Tld) on the health-Related Quality of Life and Clinical Outcomes of HIV/AIDS Patients at a Tertiary Health Facility in Niger State.

164. United Nations Programme on HIV/AIDS (UNAIDS). UNAIDS Data 2021. Accessed: 26 November 2021.

165. Ustianowski, A. and Arends, J.E., 2015. Tenofovir: What we have learnt after 7.5 million person-years of use. Infectious diseases and therapy, 4(2), pp.145-157.

166. Van den Berg, R., Haenen, G.R.M.M., Van den Berg, H. and Bast, A., 2001. Transcription factor NF-κB as a potential biomarker for oxidative stress. British Journal of Nutrition, 86(S1), pp. S121-S127.

167. van Welzen, B.J., Mudrikova, T., El Idrissi, A., Hoepelman, A.I. and Arends, J.E., 2019. A review of non-alcoholic fatty liver disease in HIV-infected patients: the next big thing. Infectious diseases and therapy, 8(1), pp.33-50.

168. Venhoff, N., Setzer, B., Melkaoui, K. and Walker, U.A., 2007. Mitochondrial toxicity of tenofovir, emtricitabine and abacavir alone and in combination with additional nucleoside reverse transcriptase inhibitors. Antiviral therapy, 12(7), pp.1075-1086.

169. Venter, W.D., Moorhouse, M., Sokhela, S., Fairlie, L., Mashabane, N., Masenya, M., Serenata, C., Akpomiemie, G., Qavi, A., Chandiwana, N. and Norris, S., 2019. Dolutegravir plus two different prodrugs of tenofovir to treat HIV. New England Journal of Medicine, 381(9), pp.803-815.

170. Vidal, F., Domingo, J.C., Guallar, J., Saumoy, M., Cordobilla, B., Sanchez de la Rosa, R., Giralt, M., et al., 2006. In vitro cytotoxicity and mitochondrial toxicity of tenofovir alone and in combination with other antiretrovirals in human renal proximal tubule cells. Antimicrobial agents and chemotherapy, 50(11), pp.3824-3832.

171. Volberding, P.A., Levine, A.M., Dieterich, D., Mildvan, D., Mitsuyasu, R., Saag, M. and Anemia in HIV Working Group, 2004. Anaemia in HIV infection: clinical impact and evidence-based management strategies. Clinical infectious diseases, 38(10), pp.1454-1463.

172. Walker, J. M. 1996. The Bicinchoninic Acid (BCA) Assay for Protein Quantitation. In: Walker, J. M. (ed.) The Protein Protocols Handbook. Totowa, NJ: Humana Press, 11-14.

173. Walker, U.A., Setzer, B. and Venhoff, N., 2002. Increased long-term mitochondrial toxicity in combinations of nucleoside analogue reverse-transcriptase inhibitors. Aids, 16(16), pp.2165-2173.

174. Wassner, C., Bradley, N. and Lee, Y., 2020. A review and clinical understanding of tenofovir: tenofovir disoproxil fumarate versus tenofovir alafenamide. Journal of the International Association of Providers of AIDS Care (JIAPAC), 19, p.2325958220919231.

175. Williams, B.G., Karim, S.S.A., Karim, Q.A. and Gouws, E., 2011. Epidemiological impact of Tenofovir gel on the HIV epidemic in South Africa. Journal of acquired immune deficiency syndromes (1999), 58(2), pp.207.

176. World Health Organisation, 2018. Dolutegravir (DTG) and the fixed-dose combination (FDC) of tenofovir/lamivudine/dolutegravir (TLD). Accessed: 30 April 2021. https://www.researchgate.net/profile/Mondli_Alfred/post/With_the_introduction_of_the_new_HIV_drug_it_would_make_the_immune_system_to_be_stronger_Wouldnt_it_trigger_other_hidden_infections_to_it_patients/attachment/5e8d010ff155db0001f37906/AS%3A877816417640448%401586299151110/download/DTG-TLD-arv_briefing_2018.pdf

177. World Health Organization, 2014. Access to antiretroviral drugs in low-and middle-income countries: technical report July 2014. https://iris.who.int/handle/10665/128150

178. Xiao, Y., Wang, Y., Tang, Q., Wei, L., Zhang, X. and Jia, G., 2018. An elongation-and ligation-based qPCR amplification method for the radiolabeling-free detection of locus-specific N6-methyladenosine modification. Angewandte Chemie International Edition, 57(49), pp.15995-16000.

179. Xuan, J., Chen, S., Ning, B., Tolleson, W.H. and Guo, L., 2016. Development of HepG2-derived cells expressing cytochrome P450s for assessing metabolism-associated drug-induced liver toxicity. Chemical-biological interactions, 255, pp.63-73.

180. Xuan, W., Song, D., Yan, Y., Yang, M. and Sun, Y., 2020. A potential role for mitochondrial DNA in the activation of oxidative stress and inflammation in liver disease. Oxidative Medicine and Cellular Longevity, 2020.

181. Yang, L.L., 2021. Anatomy and Physiology of the Liver. In Anesthesia for Hepatico-Pancreatic-Biliary Surgery and Transplantation (pp. 15-40). Springer, Cham

182. Yi, B., Hu, X., Zhang, H., Huang, J., Liu, J., Hu, J., et al., 2014. Nuclear NF-κB p65 in peripheral blood mononuclear cells correlates with urinary MCP-1, RANTES, and the severity of type 2 diabetic nephropathy. PLoS One, 9(6), pp. e99633.

183. Zamora, F.J., Dowers, E., Yasin, F. and Ogbuagu, O., 2019. Dolutegravir and lamivudine combination for the treatment of HIV-1 infection. HIV/AIDS (Auckland, NZ), 11, p.255.

184. Zanger, U.M. and Schwab, M., 2013. Cytochrome P450 enzymes in drug metabolism: regulation of gene expression, enzyme activities, and impact of genetic variation. Pharmacology & Therapeutics, 138(1), pp.103-141.

185. Zhang, H. and Sun, S.C., 2015. NF-κB in inflammation and renal diseases. Cell & bioscience, 5(1), pp.1-12.

186. Zhang, H.G.Y., Li, L., Wang, Y., Kawamoto, S., Pénisson, S., Fouladi, D.F., Shayesteh, S., Blanco, A., Ghandili, S., Zinreich, E. and Graves, J.S., 2020. Organ size increases with obesity and correlates with cancer risk. arXiv preprint arXiv:2005.13112.

187. Zhang, L., and Bansal, M.B., 2020. Role of Kupffer cells in Driving Hepatic Inflammation and Fibrosis in HIV infection. Frontiers in Immunology, 2020(11), pp.1086.

188. Zhang, T., Ma, C., Zhang, Z., Zhang, H. and Hu, H., 2021. NF-κB signaling in inflammation and cancer. MedComm, 2(4), pp.618-653.

189. Zhang, X., Wang, R., Piotrowski, M., Zhang, H., and Leach, K.L., 2015. Intracellular concentrations determine the cytotoxicity of adefovir, cidofovir and tenofovir. Toxicology in Vitro, 29(1), pp.251-258.

190. Zhang, X., Wu, X., Hu, Q., Wu, J., Wang, G., Hong, Z., Ren, J. and for Trauma, L., 2019. Mitochondrial DNA in liver inflammation and oxidative stress. Life Sciences, 236, p.116464.

191. Zhao, R.Z., Jiang, S., Zhang, L., and Yu, Z.B., 2019. Mitochondrial electron transport chain, ROS generation and uncoupling. International Journal of molecular medicine, 44(1), pp.3-15.

192. Zídek, Z., Franková, D. and Holý, A., 2001. Activation by 9-(R)-[2-(phosphonomethoxy) propyl] adenine of chemokine (RANTES, macrophage inflammatory protein 1α) and cytokine (tumor necrosis factor alpha, interleukin-10 [IL-10], IL-1β) production. Antimicrobial agents and chemotherapy, 45(12), pp.3381-3386.

193. Zulu, S.S., Simola, N., Mabandla, M.V. and Daniels, W.M., 2018. Effect of long-term administration of antiretroviral drugs (tenofovir and nevirapine) on neuroinflammation and neuroplasticity in mouse hippocampi. Journal of chemical neuroanatomy, 94, pp.86-92.

APPENDICES

APPENDIX A: LITERATURE REVIEW PUBLICATION

Inflammatory properties of tenofovir in human liver cells

Songezo Vazi[1], Sanet van Zyl[1], Roné Vorster -de Wet[1], Charlette Tiloke[1#]

[1]Department of Basic Medical Sciences, Faculty of Health Sciences, University of the Free State, Bloemfontein, South Africa

Corresponding author:

[1#]Dr Charlette Tiloke: Department of Basic Medical Sciences, Faculty of Health Sciences, University of the Free state, Bloemfontein, South Africa

Email: TilokeC@ufs.ac.za

Received 2 March 2023, Revised 25 August 2023, Accepted 29 August 2023, Available online 3 September 2023, Version of Record 11 September 2023.

Health Sciences Review, Volume 8, September 2023, 100114

https://doi.org/10.1016/j.hsr.2023.100114

APPENDIX B: IL-6 standard curve

This standard curve was used to determine the IL-6 concentration at different time exposures by comparing it with a standard known concentration sample. Figure 1 illustrates the IL-6 standard curve.

Table 1: IL-6 standards raw data

Standards pg/ml	OD1	OD2	Average	Average-Blank	STDEV
0	0,083251626	0,079677493	0,081	0,000	0,003
7,8	0,077116834	0,0855747	0,081	0,000	0,006
15,6	0,137316347	0,139275912	0,138	0,057	0,001
31,3	0,196302596	0,231905953	0,214	0,133	0,025
62,5	0,296705643	0,309823952	0,303	0,222	0,009
125	0,47443833	0,580276637	0,527	0,446	0,075
250	0,859616884	0,92449294	0,892	0,811	0,046
500	1,15560575	1,747777737	1,452	1,370	0,419

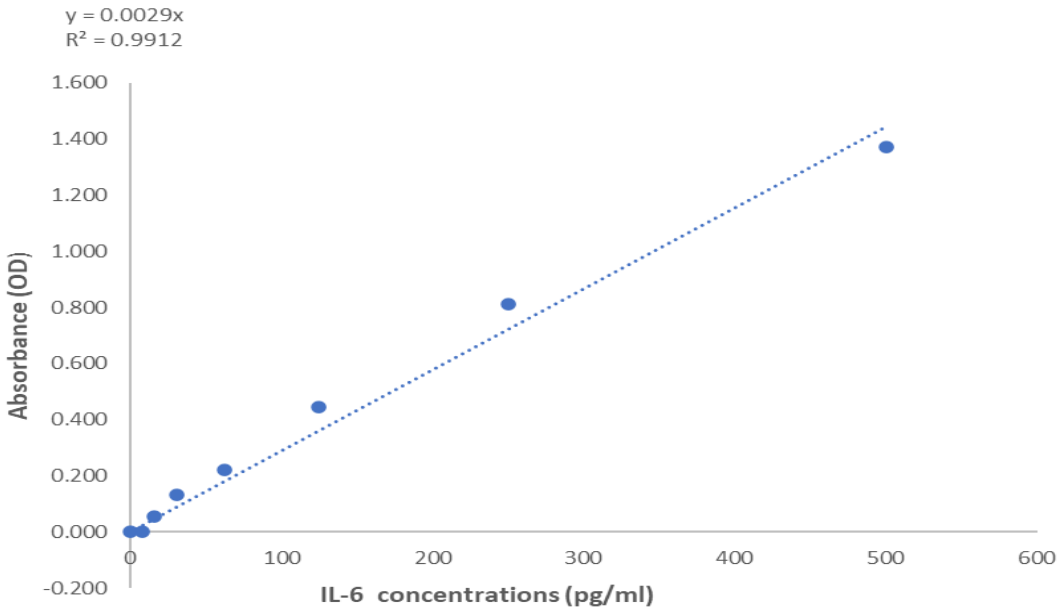

Figure 1: Standard curve of IL-6.

Table 2: IL-6 sample concentrations

$HepG_2$ Samples	**OD1**	**OD2**	**OD3**	**AVERAGE**
24 hrs control	0,089612596	0,094620061	0,067986406	0,084
24 hrs treatment	0,126794417	0,108118292	0,081076496	0,105
120 hrs control	0,141228011	0,133119727	0,122866414	0,132
120 hrs treatment	0,067318855	0,05198905	0,08087806	0,067

Table 3: IL-6 sample concentrations calculations

$HepG_2$ Samples	**Concentration (pg/ml)**	**Concentration (pg/ml)2**	**Concentration (pg/ml)3**	**Average**	**STDEV**
24 hrs control	30,901	32,628	23,444	28,991	4,881
24 hrs treatment	43,722	37,282	27,957	36,321	7,926
120 hrs control	83,07530056	78,30572202	72,27436137	77,88512798	5,412739262
120 hrs treatment	39,59932629	30,5817942	47,57532958	39,25215002	8,50208561

APPENDIX C: IL-1β standard curve

A standard curve was constructed by plotting the absorbance value against concentrations of IL-1β. The standard curve was used to determine the IL-1β concentration at different time exposures by comparing it with a standard known concentration sample. Figure 2 illustrates the IL-1β standard curve.

Table 4: IL-1β standards raw data

Standards pg/ml	OD1	OD2	Average	Average-Blank	STDEV
0	0,442397974	0,498244874	0,470	0,000	0,039
14,06	0,360898178	0,370535492	0,366	-0,105	0,007
28,13	0,040832902	0,514876038	0,278	-0,192	0,335
56,25	0,870332111	0,808523394	0,839	0,369	0,044
112,5	1,133582677	1,145334437	1,139	0,669	0,008
225	1,438112736	1,109382131	1,274	0,803	0,232
450	2,927900112	1,923628169	2,426	1,955	0,710
900	4,226085851	3,959169404	4,093	3,622	0,189

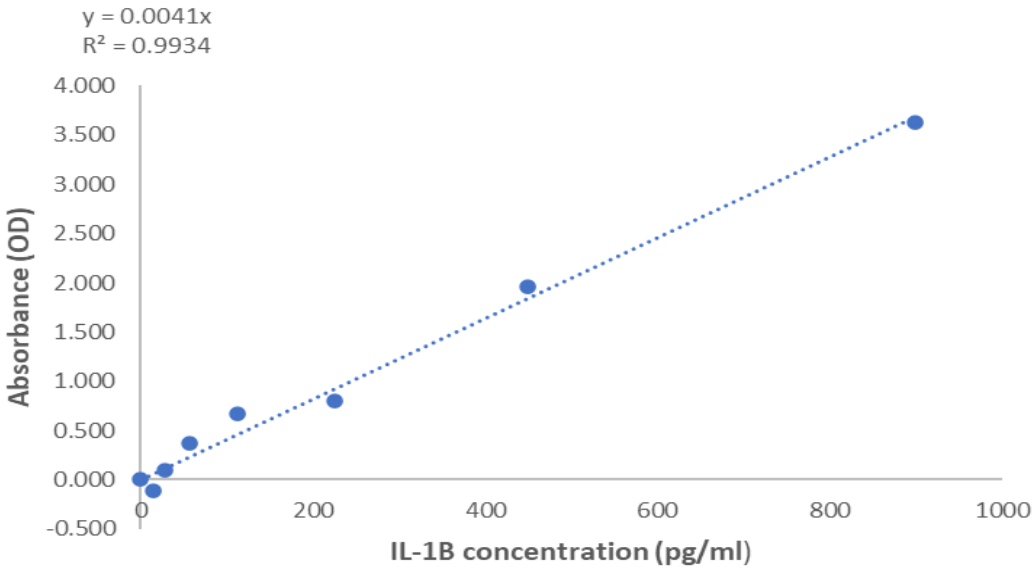

Figure 2: Standard curve of IL-1β.

Table 5: IL-1β sample concentrations

$HepG_2$ Samples	**OD1**	**OD2**	**OD3**	**AVERAGE**
24 hrs control	0,288135235	0,222512302	0,19323487	0,234627469
24 hrs treatment	0,089575538	0,089857783	0,087710287	0,089047869
120 hrs control	0,078997752	0,079933861	0,088998615	0,082643409
120 hrs treatment	0,095132592	0,086362292	0,080294006	0,087262964

Table 6: IL-1β sample concentrations calculations

$HepG_2$ Samples	**Concentration (pg/ml)**	**Concentration (pg/ml)**	**Concentration (pg/ml)**	**Average**	**STDEV**
24 hrs control	205,8108819	158,9373583	138,0249071	167,550491	94,22037989
24 hrs treatment	63,98252737	64,18413087	62,65020484	63,320562103	10.680157898
120 hrs control	56,42696584	57,09561514	63,57043919	59,03100672	3,45024356
120 hrs treatment	67,95185177	61,68735163	57,35286167	62,33068835	9.630356778

APPENDIX D: TNF-α standard curve.

A standard curve is a graphical relationship between the amount of cytokine and absorbance. This standard curve was used to determine the TNF-α concentration at different time exposures by comparing it with a standard known concentration sample. Figure 3 illustrates the TNF-α standard curve.

Table 7: TNF-α standards raw data

Standards pg/ml	OD1	OD2	Average	Average-Blank	STDEV
0	0,296635692	0,191045272	0,244	0,000	0,075
15,63	0,265676401	0,265676401	0,266	0,022	0,000
31,25	0,237350232	0,23342332	0,235	-0,008	0,003
62,5	0,37176782	0,414463905	0,393	0,149	0,030
125	0,462780978	0,617138048	0,540	0,296	0,109
250	0,774209527	0,80600859	0,790	0,546	0,022
500	1,85932567	1,65387433	1,757	1,513	0,145
1000	2,875090689	3,062110178	2,969	2,725	0,132

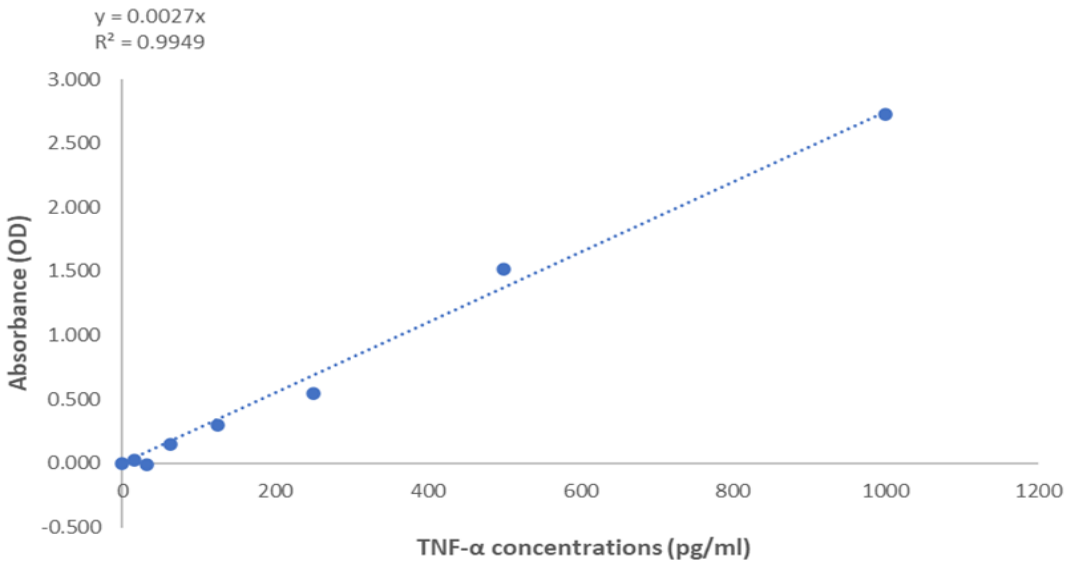

Figure 3: Standard curve of TNF-α.

Table 8: TNF-α sample concentrations

$HepG_2$ Samples	**OD1**	**OD2**	**OD3**	**Average**
24 hrs control	0,12376167	0,621523081	0,432462002	0,392582251
24 hrs treatment	0,229850691	0,37505563	0,340932361	0,315279561
120 hrs control	0,147902603	0,177385183	0,31428455	0,213190778
120 hrs treatment	0,208956286	0,336189362	0,457098301	0,334081317

Table 9: TNF-α concentrations calculations

$HepG_2$ Samples	**Concentration (pg/ml)**	**Concentration (pg/ml)**	**Concentration (pg/ml)**	**Average**	**STDEV**
24 hrs control	44,20059653	221,9725291	154,4507151	140,2079469	89,73771412
24 hrs treatment	82,08953262	133,9484392	121,7615576	112,5998431	27,1162185
120 hrs control	52,82235809	63,35185111	112,2444821	76,13956375	31,70790753
120 hrs treatment	74,62724507	120,0676294	163,2493933	119,3147559	44,31587077

APPENDIX E: IL-10 standard curve

This standard curve was used to determine the IL-10 concentration at different time exposures by comparing it with a standard known concentration sample. Figure 4 illustrates the IL-10 standard curve.

Table 10: IL-10 standards raw data

Standards pg/ml	OD1	OD2	Average	Average-Blank	STDEV
0	0,060202413	0,064017637	0,062	0,000	0,003
15,63	0,086473473	0,094574492	0,091	0,028	0,006
31,25	0,130908063	0,144273665	0,138	0,075	0,009
62,5	0,205269123	0,21758452	0,211	0,149	0,009
125	0,356032555	0,370275933	0,363	0,301	0,010
250	0,759393113	0,648723782	0,704	0,642	0,078
500	1,484519594	1,438296273	1,461	1,399	0,033
1000	2,809380188	2,900214763	2,855	2,793	0,064

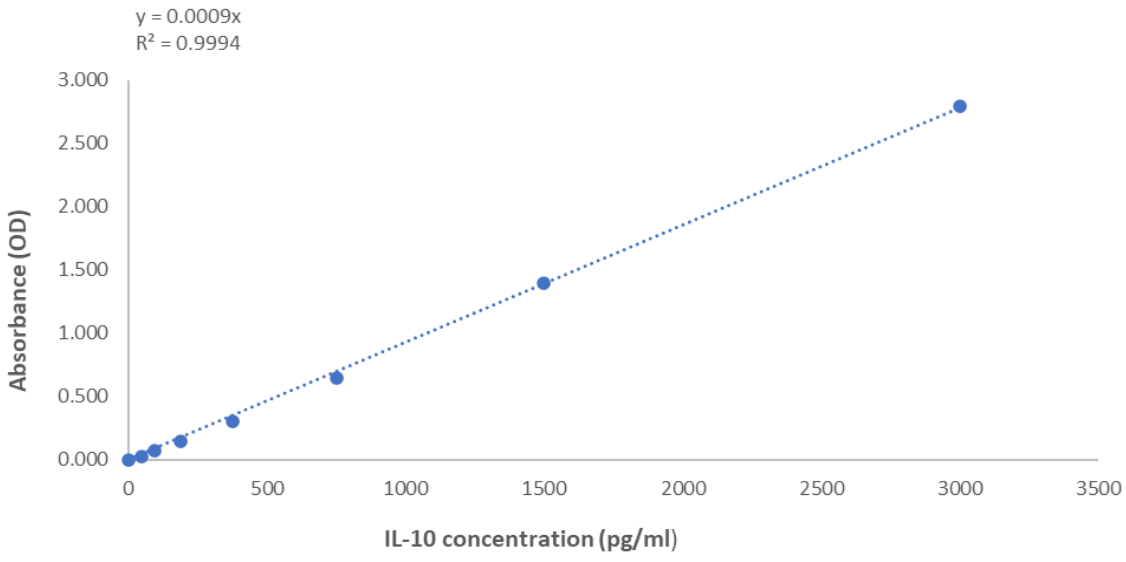

Figure 4: Standard curve of IL-10.

Table 11: IL-10 sample concentrations

$HepG_2$ Samples	**OD1**	**OD2**	**OD3**	**Average**
24 hrs control	0,045268099	0,047721759	0,050189362	0,048
24 hrs treatment	0,048953808	0,061047349	0,060202413	0,057
120 hrs control	0,072617857	0,062317843	0,060624675	0,065
120 hrs treatment	0,065296863	0,082501148	0,059359118	0,069
24 hrs control	0,045268099	0,047721759	0,050189362	0,048

Table 12: IL-10 concentrations calculations

$HepG_2$ Samples	**Concentration (pg/ml)**	**Concentration (pg/ml)**	**Concentration (pg/ml)**	**Average**	**STDEV**
24 hrs control	50,2978873	53,0241771	55,76595735	53,02934058	2,734038682
24 hrs treatment	54,39311992	67,83038738	66,89156978	63,03835903	7,501697409
120 hrs control	80,68650805	69,2420474	67,36075027	72,42976857	7,212151539
120 hrs treatment	72,55206999	91,66794232	65,95457513	76,72486248	13,354904

APPENDIX F: BCA standard curve

This standard curve was used to determine the extracted protein concentration at different time exposures by comparing it with a known concentration sample. Figure 5 illustrates the BCA protein standard curve.

Table 1: BCA Standards raw data

Protein concentration (µg/ml)	OD 1	OD2	OD3	Average	Average - blank
0	0,100926344	0,092590754	0,095178481	0,09623186	0
25	0,116636614	0,114460546	0,110723298	0,113940153	0,017708293
125	0,289518736	0,283804468	0,282737199	0,285353468	0,189121608
250	0,45258625	0,415773548	0,449641033	0,43933361	0,34310175
500	0,714030052	0,709201018	0,70689494	0,710042003	0,613810143
750	0,954591816	0,986061064	0,96697165	0,969208177	0,872976317
1000	1,171875997	1,186787169	1,195527914	1,18473036	1,0884985
1500	1,609417984	1,628636807	1,630265078	1,62277329	1,52654143

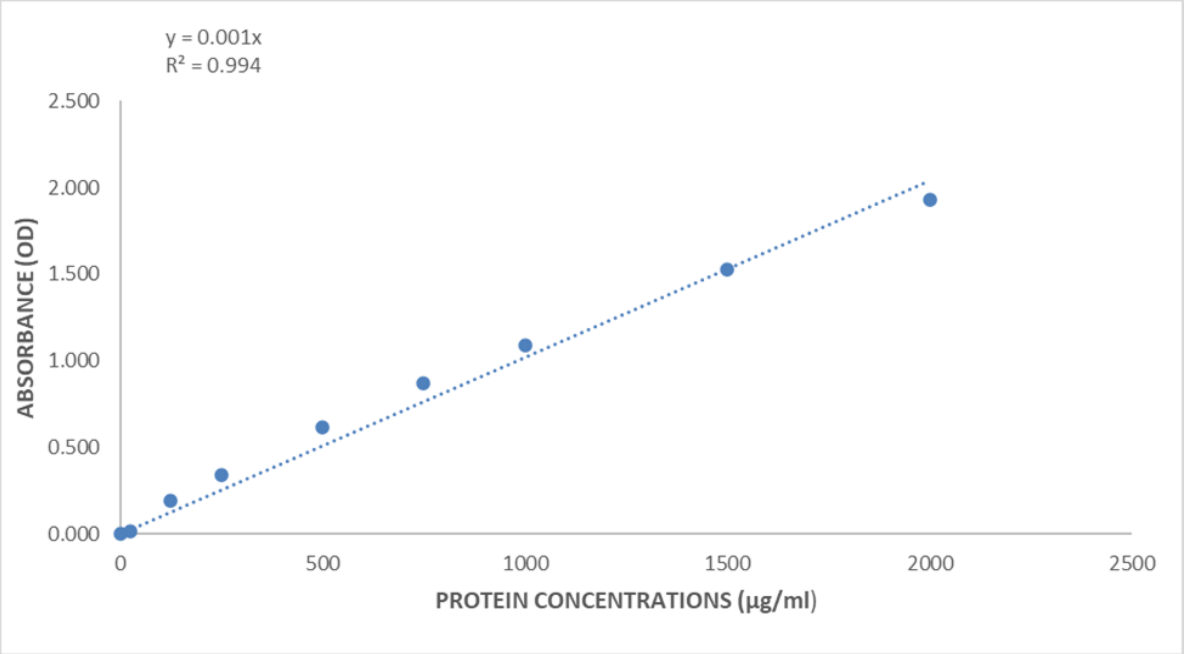

Figure 5: BCA standard curve.

APPENDIX G: qPCR raw data and calculations

Well Position	Sample Name	Target Name	CT
A1	Control 24 h	NFkB p65	26,10396
A2	Control 24 h	NFkB p65	26,65625
A3	Control 24 h	NFkB p65	26,67489
A4	Control 120 h	NFkB p65	28,36516
A5	Control 120 h	NFkB p65	29,54764
A6	Control 120 h	NFkB p65	29,30599
B1	Tenofovir 24 h	NFkB p65	26,45846
B2	Tenofovir 24 h	NFkB p65	26,26063
B3	Tenofovir 24 h	NFkB p65	26,72662
B4	Tenofovir 120 h	NFkB p65	31,47262
B5	Tenofovir 120 h	NFkB p65	32,64674
B6	Tenofovir 120 h	NFkB p65	32,40599

Well Position	Sample Name	Target Name	CT
C1	Control 24 h	IkBa	34,61397
C2	Control 24 h	IkBa	36,23128
C3	Control 24 h	IkBa	34,52875
C4	Control 120 h	IkBa	36,11857
C5	Control 120 h	IkBa	36,31857
C6	Control 120 h	IkBa	36,21857
D1	Tenofovir 24 h	IkBa	37,47887
D2	Tenofovir 24 h	IkBa	37,53554
D3	Tenofovir 24 h	IkBa	37,47887
D4	Tenofovir 120 h	IkBa	38,47262
D5	Tenofovir 120 h	IkBa	37,64674
D6	Tenofovir 120 h	IkBa	38,40599

Well Position	Sample Name	Target Name	CT
E1	Control 24 h	GAPDH	19,137
E2	Control 24 h	GAPDH	19,950
E3	Control 24 h	GAPDH	19,960
E4	Control 120 h	GAPDH	27,448
E5	Control 120 h	GAPDH	27,346
E6	Control 120 h	GAPDH	26,999
F1	Tenofovir 24 h	GAPDH	20,468
F2	Tenofovir 24 h	GAPDH	20,410
F3	Tenofovir 24 h	GAPDH	20,428
F4	Tenofovir 120 h	GAPDH	28,580
F5	Tenofovir 120 h	GAPDH	28,102
F6	Tenofovir 120 h	GAPDH	28,072

	NFkB p65				GAPDH			
	Control- 24 h	Tenofovir- 24 h	Control- 120 h	Tenofovir- 12	Control- 24 h	Tenofovir- 24 h	Control- 120 h	Tenofovir- 120 h
	26,104	26,458	28,365	31,473	19,137	20,468	27,448	28,580
	26,656	26,261	29,548	32,647	19,950	20,410	27,346	29,102
	26,675	26,727	29,306	32,406	19,960	20,428	26,999	28,072
Averages	**26,478**	**26,482**	**29,073**	**32,175**	**19,682**	**20,435**	**27,264**	**28,584**

Delta (Ct)				Delta-delta (Ct)				
Control- 24 h	Tenofovir- 24 h	Control- 120 h	Tenofovir- 120 h	Control- 24 h	Tenofovir- 24	Control- 120 h	Tenofovir- 120 h	
6,967	5,990	0,917	2,893		-0,976		1,976	
6,706	5,850	2,202	3,545		-0,856		1,343	
6,715	6,298	2,307	4,334		-0,417		2,027	
6,796	**6,046**	**1,809**	**3,591**		**-0,750**		**1,782**	**Averages**

Relative fold-change							
Control- 24 h	Tenofovir- 24 h	Control- 120 h	Tenofovir- 120 h				
1,000	1,967	1,000	0,254			NFkB p65	Relative fold-chang	STDEV
1,000	1,810	1,000	0,394			Control 24 h	1	
1,000	1,335	1,000	0,245			Tenofovir 24 h	1,703992728	0,329204058
						Control 120 h	1	
1,000	**1,704**	**1,000**	**0,298**	**Averages**		Tenofovir 120 h	0,297940895	0,083462278
	0,329		**0,083**	**Stdev**				

EXCEL SPREADSHEET:

	IkBa				GAPDH			
	Control- 24 h	Tenofovir- 24 h	Control- 120 h	Tenofovir- 120 h	Control- 24 h	Tenofovir- 24 h	Control- 120 h	Tenofovir- 120 h
	34,614	37,479	36,119	38,473	19,137	20,468	27,448	28,580
	34,231	37,536	36,319	37,647	19,950	20,410	27,346	28,102
	34,529	37,479	36,219	38,406	19,960	20,428	26,999	28,072
Average	**34,458**	**37,498**	**36,219**	**38,175**	**19,682**	**20,435**	**27,264**	**28,251**

	Delta (Ct)				Delta-delta (Ct)			
	Control- 24	Tenofovir- 24 h	Control- 120 h	Tenofovir- 120 h	Control- 24 h	Tenofovir- 24 h	Control- 120 h	Tenofovir- 120 h
	15,477	17,011	8,671	9,893		1,534		1,222
	14,281	17,125	8,973	9,545		2,844		0,572
	14,569	17,051	9,220	10,334		2,982		1,114
Average	**14,609**	**17,062**	**8,954**	**9,924**		**2,453**		**0,970**

	Relative fold-change				
	Control- 24	Tenofovir- 24 h	Control- 120 h	Tenofovir- 120 h	
	1,000	0,345	1,000	0,429	
	1,000	0,139	1,000	0,673	
	1,000	0,127	1,000	0,462	
	1,000	0,204	1,000	0,521	**Average**
		0,123		0,132	**Stdev**

IkBa	Relative fold-change	STDEV
Control 24 h	1,000	
Tenofovir 24 h	0,204	0,123
Control 120 h	1,000	
Tenofovir 120 h	0,521	0,132

EXCEL SPREADSHEET:

APPENDIX H: Western blot raw data

NF-κBp65 protein

Treatment groups	NF-KBp65 volume	Beta-actin volume	Nf-kbp65/beta-actin	Relative band density (RBD)
24 h Control	1240935	9851650	0,125962148	1
24 h Tenofovir	8323596	26822772	0,310318262	2,463583435
120 h Control	27186456	28077552	0,968263045	1
120 h Tenofovir	18328246	22461552	0,815983063	0,842728706

p-NF-κBp65 protein

Treatment groups	p-NF-kB-p65 volume	Beta-actin volume	p-NF-kB-p65/beta-actin	Relative band density
24 h Control	286747	9851650	0,029106495	1
24 h Tenofovir	2045505	26822772	0,076260015	2,620034311
120 h Control	786156	28077552	0,02799945	1
120 h Tenofovir	3918864	22461552	0,174469867	6,231189199

IκBα protein

Treatment groups	IkBa volume	Beta-actin volume	IkBa/beta-actin	Relative band density
24 h Control	13790790	9851650	1,399845711	1
24 h Tenofovir	10950480	26822772	0,408253107	0,291641503
120 h Control	4063387	28077552	0,144720131	1
120 h Tenofovir	14358970	22461552	0,639268827	4,417276457

p-IκBα protein

Treatment groups	phospho-IkBa volum	Beta-actin volum	phospho-IkBa/beta-actin	Relative band density
24 h Control	2330385	9851650	0,236547685	1
24 h Tenofovir	8184604	26822772	0,305136397	1,289957232
120 h Control	10147441	28077552	0,361407611	1
120 h Tenofovir	4649117	22461552	0,206981112	0,572708225

APPENDIX I: $HepG_2$ cell images

Following 24h treatment period, $HepG_2$ cell microscopic images were taken from the control and tenofovir-treated group. These images allowed the researcher to determine tenofovir's effect on the cell morphology of the tenofovir-treated cells when compared with the control group. These images show that tenofovir doesn't affect the morphology of $HepG_2$ cells, as the cell membranes are intact.

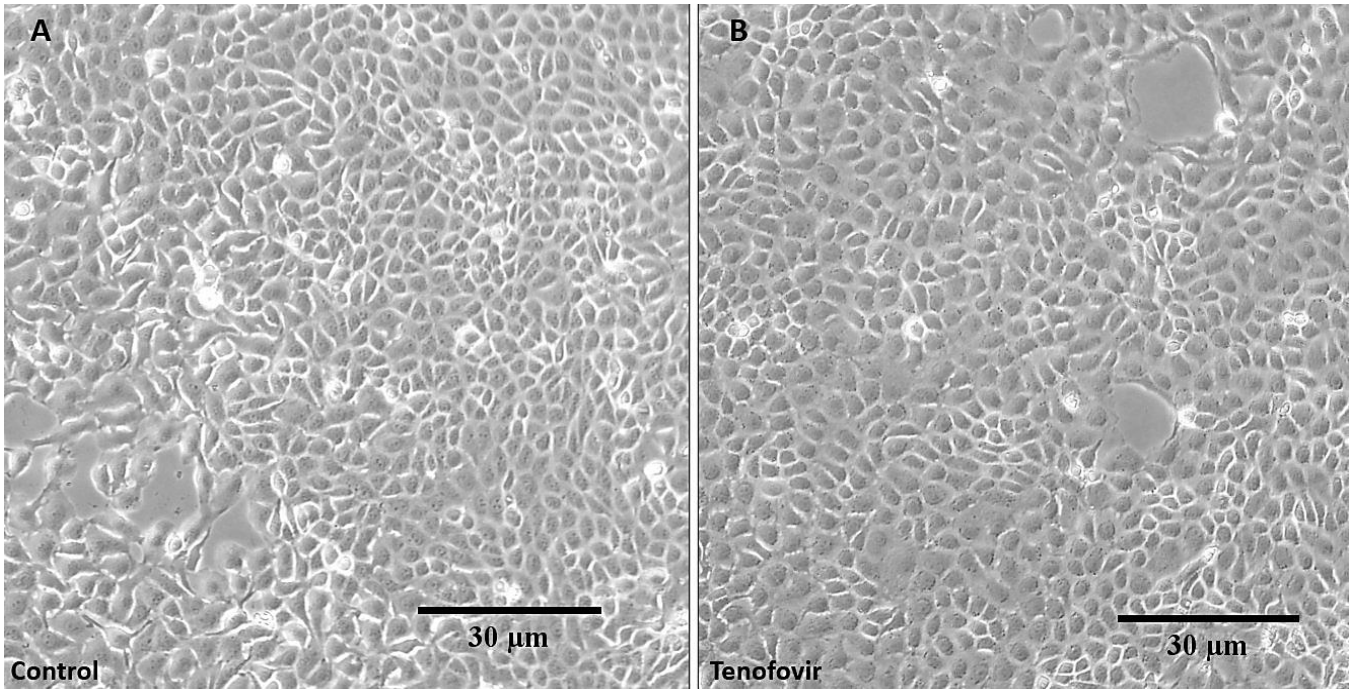

Figure 6: Morphological comparison between control and tenofovir-treated $HepG_2$ cells at 24h exposure. A) Morphological changes in control group. **B)** Morphological changes in tenofovir-treated group. Images were acquired using light inverted microscope at 100X magnification.

APPENDIX J: HepG2 cell images

Representative microscopic images of HepG2 cells at chronic exposure are shown in Figure 7 After 120h, HepG2 cell images were taken from the control and tenofovir-treated group. These images allowed the researcher to determine tenofovir's effect on the cell morphology of the tenofovir-treated cells when compared with the control group. These images show that tenofovir did not alter the morphology of HepG2 cells.

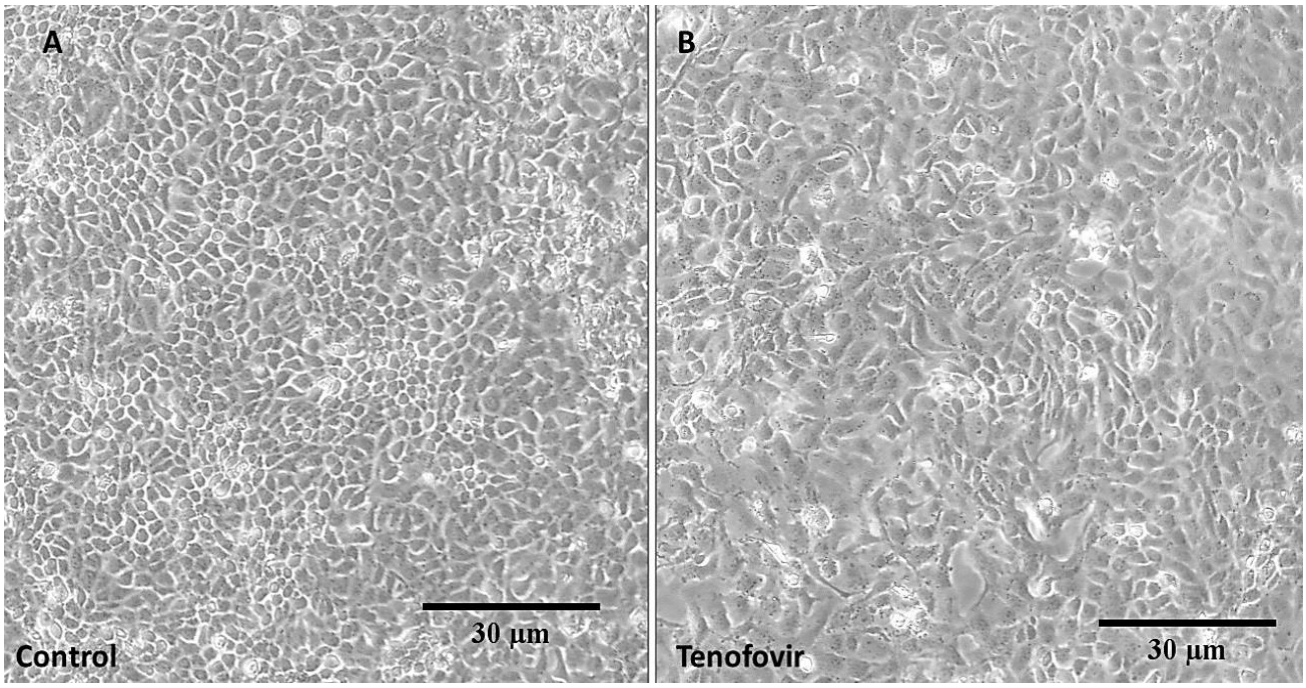

Figure 7: Morphological comparison between control and tenofovir-treated HepG2 cells at 120h exposure. A) Morphological changes in the control group. **B)** Morphological changes in the tenofovir-treated group. Images were acquired using a light inverted microscope at 100X magnification.

APPENDIX K: Hoechst stain 33342

INTRODUCTION

Hoechst 33342 is utilized for staining fixed and live cells. Hoechst stains the cellular nuclei through penetrating cellular membranes and binds to DNA. Upon binding, the dye emits blue fluorescence. Therefore, the Hoechst stain was used to analyse the overall health vitality of $HepG_2$ cells used in the study. The following image shows that the $HepG_2$ cells were not infected with mycoplasma contamination.

Fluorescent microscopy imaging

The $HepG_2$ cells were imaged using Axio Observer 7 for LSM 900 confocal microscope (Carl Zeiss, Germany) following manufactures guidelines. The following Figure 8 illustrates fluorescence confocal microscopy results after Hoechst 33342 staining in $HepG_2$ human liver cells.

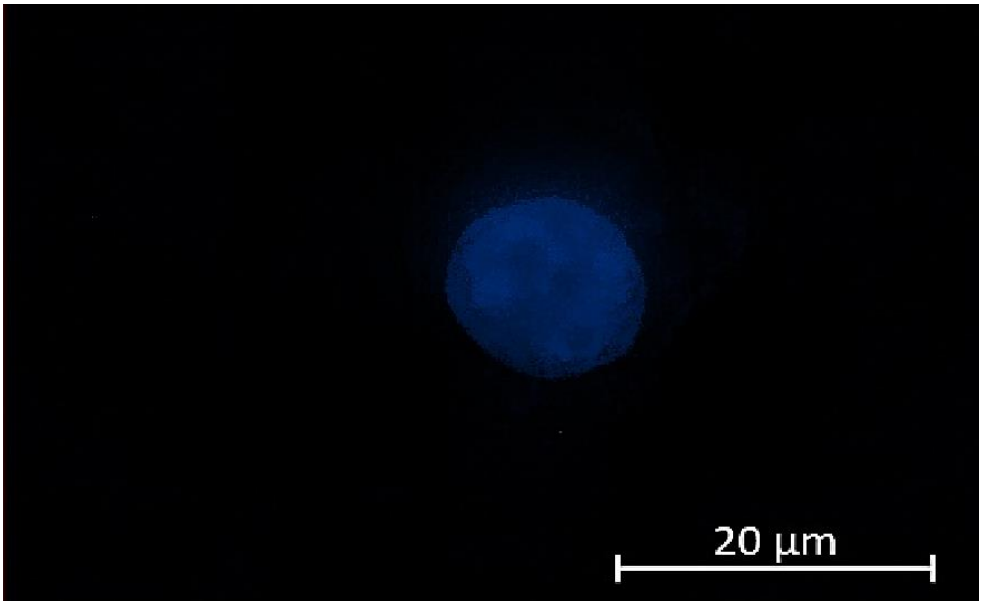

Figure 8: Hoechst 33342–stained $HepG_2$ human liver cells. The cells were viewed at 400x magnification and acquired with Zen Blue Imaging software.

APPENDIX L: Health Sciences Research Ethics Committee (HSREC) Initial approval letter.

UNIVERSITY OF THE FREE STATE
UNIVERSITEIT VAN DIE VRYSTAAT
YUNIVESITHI YA FREISTATA

UFS·UV
HEALTH SCIENCES
GESONDHEIDSWETENSKAPPE

Health Sciences Research Ethics Committee

09-Dec-2021

Dear **Mr Songezo Vazi**

Ethics Clearance: **An investigation into the inflammatory properties of Tenofovir in HepG2 human liver cells**

Principal Investigator: **Mr Songezo Vazi**

Department: **Basic Medical Sciences Department (Bloemfontein Campus)**

Submission Page

APPLICATION APPROVED

Please ensure that you read the whole document

With reference to your application for ethical clearance with the Faculty of Health Sciences, I am pleased to inform you on behalf of the Health Sciences Research Ethics Committee that you have been granted ethical clearance for your project.

Your ethical clearance number, to be used in all correspondence is:**UFS-HSD2021/1624/2501**

The ethical clearance number is valid for research conducted for one year from issuance. Should you require more time to complete this research, please apply for an extension.

We request that any changes that may take place during the course of your research project be submitted to the HSREC for approval to ensure we are kept up to date with your progress and any ethical implications that may arise. This includes any serious adverse events and/or termination of the study.

A progress report should be submitted within one year of approval, and annually for long term studies. A final report should be submitted at the completion of the study.

Research conducted in any Department of Health facility: Researchers are required to sign and return the HSREC approval letters to the provincial Department of Health where they applied. It is also a requirement for researchers to submit electronic copies of their final research findings, and/or make a presentation of their findings and recommendations at departmental research days when and where indicated.

The HSREC functions in compliance with, but not limited to, the following documents and guidelines: The SA National Health Act. No. 61 of 2003; Ethics in Health Research: Principles, Structures and Processes (2015); SA GCP(2006); Declaration of Helsinki; The Belmont Report; The US Office of Human Research Protections 45 CFR 461 (for non-exempt research with human participants conducted or supported by the US Department of Health and Human Services- (HHS), 21 CFR 50, 21 CFR 56; CIOMS; ICH-GCP-E6 Sections 1-4; International Council for Harmonisation (ICH) Harmonised Guideline, Integrated Addendum to ICH E6(R1), Guideline for Good Clinical Practice (GCP) E6(R2), 2016, SAHPRA Guidelines as well as Laws and Regulations with regard to the Control of Medicines, Constitution of the HSREC of the Faculty of Health Sciences.

For any questions or concerns, please feel free to contact HSREC Administration: 051-4017794/5 or email EthicsFHS@ufs.ac.za.

Thank you for submitting this proposal for ethical clearance and we wish you every success with your research.

Yours Sincerely

Prof. A. Sherriff
Chairperson: Health Sciences Research Ethics Committee

Health Sciences Research Ethics Committee
Office of the Dean: Health Sciences
T: +27 (0)51 401 7795/7794 | E: ethicsfhs@ufs.ac.za
IRB 00011992; REC 230408-011; IORG 0010096; FWA 00027947
Block D, Dean's Division, Room D104 | P.O. Box/Posbus 339 (Internal Post Box G40) | Bloemfontein 9300 | South Africa
www.ufs.ac.za

APPENDIX M: Health Sciences Research Ethics Committee (HSREC) Sub approval

UNIVERSITY OF THE FREE STATE
UNIVERSITEIT VAN DIE VRYSTAAT
YUNIVESITHI YA FREISTATA

UFS·UV
HEALTH SCIENCES
GESONDHEIDSWETENSKAPPE

Health Sciences Research Ethics Committee

28-Mar-2022

Dear **Mr Songezo Vazi**

Ethics Number: UFS-HSD2021/1624-0002

Ethics Clearance: **An investigation into the inflammatory properties of tenofovir in HepG2 human liver cells**

Principal Investigator: **Mr Songezo Vazi**

Department: **Basic Medical Sciences Department (Bloemfontein Campus)**

Submission Page

SUBSEQUENT SUBMISSION APPROVED

With reference to your recent submission for ethical clearance from the Health Sciences Research Ethics Committee. I am pleased to inform you on behalf of the HSREC that you have been granted ethical clearance for your request as stipulated below:

- The department has acquired the HepG2 cell line via Merck/Sigma. Unfortunately, there is a delay in permit approval from the Department of Health Sciences as well as a delay in stock availability and stock of the cell line. Please refer to the attachments for details on permit application and order delay.
- To prevent a delay in the project commencement, the Department of Medical Biochemistry and Chemical Pathology of the University of KwaZulu-Natal has kindly agreed to assists with providing the HepG2 cell line. Please find the attached letter for more information. The research protocol methodology remains the same as originally approved by the HSREC, However, we would like to inform you, the committee of this minor amendment.

The HSREC functions in compliance with, but not limited to, the following documents and guidelines: The SA National Health Act. No. 61 of 2003; Ethics in Health Research: Principles, Structures and Processes (2015); SA GCP(2020); Declaration of Helsinki; The Belmont Report; The US Office of Human Research Protections 45 CFR 461 (for non-exempt research with human participants conducted or supported by the US Department of Health and Human Services- (HHS), 21 CFR 50, 21 CFR 56; CIOMS; ICH-GCP-E6 Sections 1-4; International Council for Harmonisation (ICH) Harmonised Guideline, Integrated Addendum to ICH E6(R1), Guideline for Good Clinical Practice (GCP) E6(R2), 2016, SAHPRA Guidelines as well as Laws and Regulations with regard to the Control of Medicines, Constitution of the HSREC of the Faculty of Health Sciences.

For any questions or concerns, please feel free to contact HSREC Administration: 051-4017794/5 or email EthicsFHS@ufs.ac.za.

Thank you for submitting this request for ethical clearance and we wish you continued success with your research.

Yours Sincerely

Prof. A. Sherriff
Chairperson : Health Sciences Research Ethics Committee

Health Sciences Research Ethics Committee
Office of the Dean: Health Sciences
T: +27 (0)51 401 7795/7794 | E: ethicsfhs@ufs.ac.za
IRB 00011992; REC 230408-011; IORG 0010096; FWA 00027947
Block D, Dean's Division, Room D104 | P.O. Box/Posbus 339 (Internal Post Box G40) | Bloemfontein 9300 | South Africa
www.ufs.ac.za

APPENDIX N: Language editing declaration

LANGUAGE PRACTITIONER: Anneke-Jean Diesel

BA Communication Science (Corporate and Marketing Communications)*
BA Hons Communication Science (Corporate and Marketing Communications)*
* Cum Laude

17A Innes Avenue
Waverley, Bloemfontein

Tel: 084 244 8961
annekedenobili@gmail.com

July 2023

DECLARATION

I, Anneke-Jean Diesel, hereby declare that I did the language editing of the research of Songezo Vazi (title: *An investigation into the inflammatory properties of tenofovir in HepG2 human liver cells*). This research is submitted in fulfilment of the requirements of the degree Master of Medical Science (Physiology) in the Department of Basic Medical Sciences, School of Biomedical Sciences, Faculty of Health Sciences at the University of the Free State. All the suggested changes, including the implementation thereof, were left to the discretion of the student.

Please note:

The language editing did not include reference editing/checking or formatting. Also, the editor will not be held accountable for any later additions or changes to the document that the editor did not edit, nor if the student rejects/ignores any of the changes, suggestions or queries, which he/she is free to do. It remains the student's responsibility to ensure that the similarity index is according to the University's regulations. The editor can also not be held responsible for errors in the content of the document or whether or not the student passes or fails. It is the student's responsibility to review the edited document before submitting it for evaluation.

Sincerely

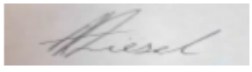

SATI Registration #: 1003466